

GENETIC SCREENS FOR P53 PATHWAY GENES IN ZEBRAFISH: THE
IDENTIFICATION AND CHARACTERIZATION OF NOVEL GENE WDR43

by

Stephen Alexander George

A dissertation submitted to the faculty of
The University of Utah
in partial fulfillment of the requirements for the degree of

Doctor of Philosophy

Department of Neurobiology and Anatomy

The University of Utah

May 2011

Copyright © Stephen Alexander George 2011

All Rights Reserved

The University of Utah Graduate School

STATEMENT OF DISSERTATION APPROVAL

The dissertation of Stephen Alexander George
has been approved by the following supervisory committee members:

<u>H. Joseph Yost</u>	, Chair	<u>March 7, 2011</u> Date Approved
<u>Alejandro Sanchez Alvarado</u>	, Member	<u>March 7, 2011</u> Date Approved
<u>Andrew Weyrich</u>	, Member	<u>March 7, 2011</u> Date Approved
<u>Jerry Kaplan</u>	, Member	<u>March 7, 2011</u> Date Approved
<u>Stephen Lessnick</u>	, Member	<u>March 7, 2011</u> Date Approved

and by Monica Vetter, Chair of
the Department of Neurobiology and Anatomy

and by Charles A. Wight, Dean of The Graduate School.

ABSTRACT

Zebrafish are vertebrate organisms offering many distinct advantages to study both genetics and development. The body of this dissertation describes research establishing and using zebrafish to model the p53 pathway.

The gene p53 is implicated in the vast majority of human tumors. It is known as, “the Guardian of the Genome” because of its functions of monitoring and maintaining the fidelity of the genome. The first resulting manuscript from our research centered on developing a zebrafish model for the human syndrome Li-Fraumeni. Dysfunction of the p53 pathway has been shown to be the primary cause of their propensity toward tumorigenesis. We first showed the p53 pathway is conserved in zebrafish. An F3 screen was devised and carried out using a reproducible apoptotic phenotype seen in p53 deficient fish. This led to the discovery of a viable zebrafish with no functional p53. These fish develop tumors that closely mimic Li-Fraumeni patients providing a zebrafish model to study human disease.

The next resulting manuscript describes a highly efficient method of genotyping zebrafish using high resolution melting analysis (HRMA). The sheer number of zebrafish used in laboratories necessitates a technique that is efficient, cost effective and accurate. HRMA was used to genotype zebrafish mutant embryos with 100 percent accuracy, removing the need for restriction

enzymes and agarose gel electrophoresis. This technique worked consistently well with three different types of mutations: point mutations, deletions, and insertions and is applicable to other model organisms.

The third manuscript results from a secondary screen of a known collection of insertional mutant zebrafish. A novel gene *wdr43* was recovered in the screen using a phenotype of p53 pathway activation. This gene was shown to activate downstream targets of p53. The mutant exhibited specific p53 dependent phenotypes, including apoptosis. Mutants displayed aberrant mitotic spindle formation which appeared to result in chromosomal instability.

The *wdr43* mutant also displayed p53 independent developmental phenotypes. Specifically the gut and eyes appeared to halt differentiation at particular stages of development, while other organs of the fish continued to develop appropriately. This ongoing project helps to elucidate the p53 independent role of *wdr43* in development.

TABLE OF CONTENTS

ABSTRACT	iii
LIST OF FIGURES	vii
ACKNOWLEDGEMENTS	ix
CHAPTERS	
1. INTRODUCTION	1
Genetics in Cancer.....	3
DNA Damage	9
Oncogenic Activation	9
Chromosomal Instability	10
References.....	12
2. GENETIC MODELING OF LI-FRAUMENI SYNDROME IN ZEBRAFISH.....	16
Summary.....	17
Introduction	17
Results	22
Discussion.....	31
Methods	39
References.....	43
Supplemental Experimental Procedures	63
Supplemental Results	63
Supplemental References	66

3. A RAPID AND EFFICIENT METHOD OF GENOTYPING ZEBRAFISH MUTANTS	70
Abstract.....	71
Introduction	71
Results	75
Discussion.....	79
Experimental Procedures.....	81
References.....	83
4. MITOTIC CATASTROPHE AND P53-DEPENDENT APOPTOSIS IN WDR43 MUTANT ZEBRAFISH	90
Abstract.....	91
Introduction	91
Results	95
Discussion.....	103
Material and Methods.....	106
References.....	109
5. P53-INDEPENDENT ROLE OF WDR43 IN DEVELOPMENT	120
6. CONCLUSIONS AND FUTURE DIRECTIONS.....	130
Overview	131
Li-Fraumeni Model	131
High Resolution Melting Analysis to Genotype Animal Models	133
Identification of Novel Gene wdr43	134
P53 Independent Role of wdr43 in Development	135

LIST OF FIGURES

<u>Figure</u>	<u>Page</u>
2.1 Identification of the p53 I166T mutation	48
2.2 Expression data from WT and p53 mutant embryos following irradiation	51
2.3 p53 mutant survival curves	52
2.4 Gross and histological analysis of tumors	53
2.5 p53 heterozygotes develop tumors and display loss of heterozygosity	54
2.6 mdm2 knockdown embryonic lethality is rescued in p53 morphants and p53 ^{I166T/I166T} mutants.....	55
2.7 p53 ^{I166T/+} dominant negative phenotypes	59
Supplemental 2.1 Induction of p53 target genes.....	67
Supplemental 2.2 IR induced apoptosis in zebrafish embryos.....	68
Supplemental 2.3 Rescue of IR induced apoptosis by p53 knockdown or bcl2 overexpression	69
3.1 Point mutation genotyping of p53 ^{I166T} and APC ^{mcr} by HRMA	86
3.2 Genotyping a small deletion in the BAP28 mutant by melting curve analysis.....	88
3.3 Genotyping of the retroviral insertion mutant wdr43 by melting curve analysis.....	89
4.1 Identification of novel gene wdr43 in a zebrafish screen.....	112

4.2	Loss of wdr43 activates p53 target genes and apoptosis	113
4.3	wdr43 Mutant embryos are partially rescued by bcl2 mRNA and CHK2 morpholino.....	114
4.4	Cell cycle analysis showed decrease of S-phase cells in wdr43 mutant.....	115
4.5	Immunohistochemistry shows mitotic spindle at 24hpf	116
4.6	Localization of His-wdr43.....	117
4.7	Activation of p53 pathway model	118
	Supplemental 4.1 RT-PCR of embryos injected with wdr43 morpholino.....	119
5.1	Expression pattern of wdr43 in wild type embryos	125
5.2	Gross morphology of wild type, wdr43 mutant and wdr43;p53 double mutant embryos	126
5.3	FKD2, iFABP and Histology of wild type, wdr43 mutant, and wdr43; p53 double mutant embryos	127
5.4	Expression of eye markers in wild type and wdr43 MO embryos.....	128
5.5	In situ hybridization of tropoelastin in wild type, wdr43 mutant and wdr43;p53 double mutant embryos.....	129

ACKNOWLEDGEMENTS

My graduate school experience has encompassed a broad range of characteristics, from euphoria to perseverance and discipline. Because graduate school is not meant to be experienced alone, I am grateful to my boss, Joseph Yost for his guidance throughout my time in his lab. He provided direction when it was necessary, but I am most thankful his desire that each of his students direct their own project. It was a memorable moment not long after joining the lab, when he told me that I would be in the driver's seat of my project. The fact that he encouraged complete ownership of a project led to an excellent education.

Thank you to my entire thesis committee, including: Joseph Yost, Alejandro Sanchez Alvarado, Jerry Kaplan, Stephen Lessnick and Andrew Weyrich. Each of these faculty members provided excellent advice and support. I am particularly thankful for Alejandro. He spent many additional hours discussing my project with me and his ideas led to several advancements in my project. His thoughts and positive attitude were always welcome.

The MD/PhD program has provided a wonderful support network. Jerry Kaplan has served to guide me through the entire process. His thoughts on my research were always helpful, but even more important was his continued

guidance in this career path. Janet Bassett makes it easy to be a MudPhud in Utah.

The entire Yost Lab provided an excellent and diverse working atmosphere. The diversity of the people and projects always provided multiple helpful perspectives. John Parant, in particular, was always helpful. He helped train me from the beginning, and for this I am appreciative.

Because not every experiment works as planned and not every moment proceeds as expected, it was necessary to commiserate with friends in the program. Reid Phelps and Leah Owen turned from my friends to my family during this time. The therapy sessions we had in the coffee shop and over lunch not only made this experience more productive, but helped turn tough times into good times, and good times into great times.

Perhaps most importantly, I thank my family. Mom, Dad and Andrew have always been supportive no matter what the circumstance. They have experienced the same feelings and emotions that I have during this time. Because their support never wavered, they provided the foundation for me to succeed. Ευχαριστώ!

CHAPTER 1

INTRODUCTION

Zebrafish offer many unique characteristics and distinct advantages which make them excellent model organisms for the study of genetics and development. The ability to study genetics in zebrafish stems from the fact that zebrafish have many offspring compared to other vertebrate organisms. In mouse, it can be unclear whether genes are functioning as dominant or recessive genes based on the small number of pups available from a breeding cross. Compared to other model organisms, such as *Drosophila* or *C. elegans*, zebrafish have the distinct advantage of being vertebrates that live long enough to develop diseases similar to humans, such as cancer. Therefore fish allow the opportunity to examine these diseases from a unique genetic standpoint. The large number of offspring from zebrafish also allows the expansion into other experimental research approaches such as drug discovery. Sheer numbers of embryos that are attainable from fish allow the possibility of testing many thousands of drugs in order to find lead compounds that either activate or inhibit specific genetic targets. Therefore, once genes are identified in fish, the tools are in place to take the research to the next level of potential pharmacological intervention.

Zebrafish reach reproductive maturity in approximately two to three months. This length of time allows forward genetics screens to be carried out. In order to carry out a forward genetics screen for recessive genes, it is necessary to look at the F3 generation. Considering the relatively small size of fish and

ease of housing large numbers, compared to mice, fish have become an important vertebrate model organism for screens.

Genetics in Cancer

Cancer is often due to the malfunction of multiple genes. However, there are single gene deficiencies that result in hereditary or familial cancer. Some of the early genes involved in cancer were discovered using linkage analysis in human families (e.g., BRCA1 and APC) (King et al., 2003; Spirio et al., 1998). The Rb gene provided the basis for proposing the two-hit model in humans (Knudson, 1971, 1986). In this scenario, one copy of the gene is already mutated (an inherited mutation) and once the other allele is mutated (a somatic mutation, or second hit), there is increased potential for tumor formation. This is in contrast to an individual with two wild type copies of the gene. Having two de novo hits in the same genome would be an extremely rare occurrence. Knowledge of genetics and how single gene defects lead to hereditary cancer has been extremely important to understanding human disease as well as cellular biology.

P53 was originally discovered due to its increased levels in cells transformed with the SV40 virus (Lane and Crawford, 1979; Linzer and Levine, 1979). Studies of this protein revealed its role as a tumor suppressor and it was coined the “guardian of the genome” (Lane, 1993). P53 appears to be located at the intersection of several important signal transduction pathways, including DNA damage, oncogenic activation, apoptosis and growth arrest. P53’s role as a

transcription factor explains its importance. When an upstream signal is transduced to activate or stabilize p53, it has the ability to activate a large cohort of downstream target genes that drive apoptotic (programmed cell death), growth arrest, and autoregulatory pathways (Pietsch et al., 2008).

The importance of p53 as a tumor suppressor is revealed by evidence of p53 mutations in approximately 70% of human tumors (Cadwell and Zambetti, 2001). In humans, Li-Fraumeni Syndrome is an autosomal dominant disease with affected individuals developing tumors with approximately 85% penetrance, and approximately 50-70% percent of these families carry mutations in p53 (Birch, 1994; Frebourg et al., 1995; Kleihues et al., 1997; Li and Fraumeni, 1969; MacGeoch et al., 1995; Varley, 2003). The working model for this syndrome is that p53's normal ability to activate apoptosis ensures that deleterious or tumorigenic mutations are not propagated to daughter cells. In the absence of functional p53, tumorigenic mutations are allowed to propagate. This syndrome, along with mouse models and our recently discovered zebrafish model for the disease are discussed in depth in Chapter 2.

Although mutations in p53 exist in the majority of human cancers, it is important to learn what happens in the remaining cancers where p53 is still functional. This is based on the assumption that evading apoptosis is a necessity of tumorigenesis. To propagate mutations, cells must find some mechanism to inactivate the pathway that would normally repair mutations or cause cell death. This highlights the importance of using zebrafish to find new

genes that potentially function in the same pathway. It is possible that mutations in other genes could allow inactivation of this pathway in cases where p53 is not mutated.

To set up forward genetic screens to find new genes in the p53 pathway, we needed to find phenotypes that were indicative of modulation of this pathway in zebrafish embryos. Morpholino technology enables rapid and reproducible knock down of specific genes (Nasevicius and Ekker, 2000). Morpholinos are highly stable antisense oligonucleotides that inactivate genes in one of two ways. Start site morpholinos are designed to be complementary to the ATG region of a gene and prevent translation of the mRNA. Splice blocking morpholinos bind to the splice donor or splice acceptor sites in a gene and either include an intron into the spliced product, or delete an exon. In either case, an optimal morpholino will inhibit protein synthesis, effectively abrogating the function of the targeted gene. Although there are distinct benefits of such a rapid method of knocking down a gene in vivo, there are also disadvantages. Morpholinos can have off-target effects, binding to other genes for which they were not intended. They can bind with weaker efficacy, so the knock down of a gene is incomplete (Robu et al., 2007). In spite of these issues, and with proper controls, multiple morpholinos can be used effectively to obtain highly useful information.

Using a splice blocking morpholino, we were able to identify some p53-dependent phenotypes that we could use for subsequent genetic screens. Upon irradiation of a zebrafish 28hpf (hours postfertilization) embryo, we see

reproducible apoptosis in the neural region as well as a tail phenotype. If we inject p53 morpholino into a single cell embryo and irradiate them at the same time point, we rescue these phenotypes. The apoptosis that is visible along the CNS, via acridine orange staining, was the basis for the screen described in Chapter 2. The goal of this screen was to find genes that could potentially inhibit the irradiation response, or decrease apoptosis in the embryo. The first gene recovered was p53, which served as a proof of principle of our screen, and also provided a new animal model of Li-Fraumeni syndrome.

The screen described above utilized *N*-ethyl-*N*-nitrosourea (ENU) treated fish. ENU mutagenesis most often results in single base pair changes and some small deletions. The advantages of ENU mutagenesis is the random, unbiased whole genome coverage that results. In theory, every base pair has the same probability of being mutated. The main disadvantages of ENU mutagenesis are the necessity of mapping the causative mutation, and genotyping affected animals. After we discovered the causative mutation in the p53 mutant, I166T, in the DNA binding region of the gene, we needed reliable, efficient methods of genotyping fish. With a single base pair change, and no gross embryonic phenotype, sequencing these fish was the only reliable genotyping method. Other methods to genotype include PCR based Restriction Fragment Length Polymorphism (RFLP), derived Cleaved Amplified Polymorphic Sequence (dCAPS), and Allele Specific Amplification (ASA) (Botstein et al., 1980; Kwok et al., 1990; Neff et al., 1998; Newton et al., 1989). These techniques are

described in depth in Chapter 3. In short, RFLP and dCAPS involve a restriction enzyme digest of an amplified sequence, where the mutation either creates or eliminates the restriction site. Therefore, different products represent the different alleles present in an embryo. ASA utilizes different PCR primers such that the 3' end binds either mutant or wild type allele. All of these methods are plagued with problems, such as incomplete digestion, or non-specific amplification. Also, DNA gels are necessary in every case.

We devised a technique for genotyping fish that utilizes a rapid cycle PCR (entire reaction in less than 1 hour), followed by a melting curve analysis of the products. Neither agarose gels nor rare restriction enzymes are required. The theory behind this technique is that DNA duplexes will melt at different temperatures (Lyon and Wittwer, 2009). Melting temperature is measured by the fluorescence emitted by a stain only when DNA is bound in a duplex. Upon dissociation, fluorescence ceases. Even a single nucleotide change will result in a small difference in T_m . If the equipment is sensitive enough to detect small differences, products could be differentiated, and fish could be genotyped. Specific causes of melting temperature elevation and depression are described in depth in Chapter 3. This technique has proven efficacious in multiple types of mutations, including SNPs, small deletions, and retroviral insertions.

Retroviral insertion mutagenesis has become a very useful way of disrupting genes in zebrafish. The next screen described in this thesis takes advantage of a collection of embryonic lethal zebrafish mutants acquired via

retroviral insertional mutagenesis (Amsterdam et al., 2004; Golling et al., 2002). The Hopkins lab devised this technique by injecting single cell embryos with retroviruses, to obtain their G0 fish (the original adult fish that will be mated to form mutant lines). They collected and maintained approximately 350 embryonic lethal mutant lines.

Like any other mutagenesis, retroviral insertion has both advantages and disadvantages. The most notable advantage is the ability for rapid mapping of the mutation. Inverse PCR is performed on mutants, with the primers annealing to the retrovirus. A disadvantage of this technique is the biased insertion of retroviruses into the genome. Retroviruses tend to insert into particular regions; therefore, whole genome coverage is not possible.

The next forward genetic screen utilized the Hopkins collection of mutants (Amsterdam et al., 2004), and again was focused on finding new genes that function in the p53 pathway. This screen was carried out in multiple steps. First, the mutant collection was examined for fish that exhibited phenotypes indicative of the p53 pathway. As described above, these phenotypes include brain necrosis/apoptosis and the curled tail phenotype. Next, the p53 morpholino was injected into mutant lines to see if any of the embryonic phenotypes were rescued by the loss of p53.

It is important to consider the type of genes that would be expected from this type of screen. In essence, we are looking for genes, that when lost, activated the p53 pathway. This activation most likely results in p53 dependent

apoptosis and growth arrest, resulting in the embryonic phenotype. The p53 pathway can be activated in multiple ways, including DNA damage, oncogenic activation and chromosomal instability. Importantly, genes involved in these pathways are likely to be recovered in our screen

DNA Damage

When DNA damage is sensed by many different genes, the p53 pathway is activated. Double strand breaks in the DNA result from stresses such as irradiation, and cause foci of damage where proteins such as ATM and BRCA1 are localized and involved in repair (Deng and Brodie, 2000; Lavin, 2007). CHK2, a kinase, is activated in this case, and in turn activates p53 via phosphorylation. P53 is also activated in single strand breaks in the DNA involving a signal transduction with ATR and CHK1 (Chen et al., 2003).

Oncogenic Activation

This pathway broadly encompasses genes that are involved in oncogenic transformations within cells. The gene often thought to be immediately upstream of p53 is the inhibitor mdm2. Mdm2 is an E3 ubiquitin ligase that targets p53 to be degraded. It also is target of p53, so it functions in an autoregulatory loop . Data suggest the sole function of mdm2 is to regulate p53 (Lozano and Montes de Oca Luna, 1998; Reinke and Lozano, 1997). This has been suggested because the early embryonic lethal phenotype of an mdm2 knockout is completely rescued in a p53 mutant background (Montes de Oca Luna et al., 1995). In fact, these mice develop completely normally, except for an increased

tumor incidence in adulthood. Genes upstream of mdm2 are p19 ARF as well as growth signals, such as Ras (Humbey et al., 2008).

Chromosomal Instability

Mutations in genes that cause chromosomal instability also lead to the activation of p53. One of the best described cases is that of Aurora A. Aurora A is a kinase that functions during mitosis and localizes to the centrosome of the mitotic spindle. Mutants in mice deficient in Aurora A have exhibited defects in the mitotic spindle, leading to chromosomal abnormalities (Lu et al., 2008). Interestingly, an overexpression of Aurora A also leads to chromosomal abnormalities. In both cases, p53 is activated (Cowley et al., 2009).

Of the 350 mutants, we were able to inject approximately 60 lines that displayed either of these embryonic phenotypes. Of the injected lines, we recovered mutants with retroviral insertions disrupting 10 genes. These mutants included known genes in the pathways described above, including Topoisomerase II (Topo II) and Replication Protein A1 (RPA1). Both of these genes have been implicated in the DNA damage pathway. In the absence of Topo II, DNA is unable to be unwound appropriately, and double strand breaks result (McClendon and Osheroff, 2007). RPA1 has been noted as having roles in DNA replication, DNA repair and homologous recombination (Osman et al., 2009). Another gene recovered was Aurora B. This kinase functions in the midzone of the mitotic spindle and phosphorylates several proteins necessary to the progression of mitosis. In the absence of Aurora B, mitotic spindle

abnormalities exist (Andrews et al., 2003). This leads to chromosomal instability and an activation of p53. These known genes fall into the categories described above, and provide proof of principle that our screen will recover genes of interest. A main component of this thesis is the study of one of the novel genes recovered. The characterization of the p53-dependent roles of this gene, *wdr43*, is described in Chapter 4. *wdr43* appears to play a role in ensuring the normal formation of the mitotic spindle in order to correctly segregate the chromosomes. Spindle aberrations were apparent in mitotic cells in the mutant.

Zebrafish mutants have been recovered with documented spindle aberrations. Denticleless, another Hopkins insertional mutant, was identified in a screen for mutants that had defective G2/M checkpoints. Immunohistochemistry showed these mutants had aberrant spindle formation due to multiple spindle poles (Sansam, GD 2006). Mechanistically, DTL1 associates with an E3 ubiquitin ligase, and is responsible for the destruction of CDT1. Interestingly, unpublished data from our lab indicates this mutant is rescued by loss of p53.

Another mitotic spindle mutant is Casseopia, which possesses in SIL (SCL Interrupting Locus). It was recovered from a screen looking for mutants with cell cycle defects. The fish show spindle abnormalities in a large portion of M-phase cells. Additionally, the mutants display developmental defects (Pfaff, MCB 2007).

Although we saw a rescue of the *wdr43* mutant with the concurrent knock down of p53, this did not result in a viable fish. The *wdr43* mutant also had some developmental abnormalities that were p53 independent. The transparent nature

of zebrafish embryos is a distinct advantage when studying development. In fact, many mutants have been described with many different types of developmental anomalies. Examination of APC and Retinoic Acid (RA) deficient fish reveals a similar phenotype. Hallmarks of developmental abnormalities in the APC mutant fish are the inability to differentiate gut, retina defect, and the inability to form a pectoral fin (Nadauld et al., 2004; Nadauld et al., 2005). The cellular mechanism for why this phenotype occurs is unknown, but is explored in Chapter 5.

The body of this thesis centers on using zebrafish as a genetic model to study the p53 pathway. Forward genetic screens have helped us to recover a p53 mutant that serves as a new model of the genetic syndrome Li-Fraumeni. Next, we will describe a novel method of genotyping zebrafish using High Resolution Melting Analysis (HRMA). This method is applicable in a variety of mutations and should be applicable to all model organisms. Also, we recovered a mutant line with a retroviral insertion into novel gene *wdr43*. Characterization of this mutant reveals a role for *wdr43* in the mitotic spindle as well as a p53 independent role in development.

References

- Amsterdam, A., Nissen, R.M., Sun, Z., Swindell, E.C., Farrington, S., and Hopkins, N. (2004). Identification of 315 genes essential for early zebrafish development. *Proc Natl Acad Sci U S A* *101*, 12792-12797.
- Andrews, P.D., Knatko, E., Moore, W.J., and Swedlow, J.R. (2003). Mitotic mechanics: the auroras come into view. *Curr Opin Cell Biol* *15*, 672-683.
- Birch, J.M. (1994). Li-Fraumeni syndrome. *Eur J Cancer* *30A*, 1935-1941.

Botstein, D., White, R.L., Skolnick, M., and Davis, R.W. (1980). Construction of a genetic linkage map in man using restriction fragment length polymorphisms. *Am J Hum Genet* 32, 314-331.

Cadwell, C., and Zambetti, G.P. (2001). The effects of wild-type p53 tumor suppressor activity and mutant p53 gain-of-function on cell growth. *Gene* 277, 15-30.

Chen, Z., Xiao, Z., Chen, J., Ng, S.C., Sowin, T., Sham, H., Rosenberg, S., Fesik, S., and Zhang, H. (2003). Human Chk1 expression is dispensable for somatic cell death and critical for sustaining G2 DNA damage checkpoint. *Mol Cancer Ther* 2, 543-548.

Cowley, D.O., Rivera-Perez, J.A., Schliekelman, M., He, Y.J., Oliver, T.G., Lu, L., O'Quinn, R., Salmon, E.D., Magnuson, T., and Van Dyke, T. (2009). Aurora-A kinase is essential for bipolar spindle formation and early development. *Mol Cell Biol* 29, 1059-1071.

Deng, C.X., and Brodie, S.G. (2000). Roles of BRCA1 and its interacting proteins. *Bioessays* 22, 728-737.

Frebourg, T., Barbier, N., Yan, Y.X., Garber, J.E., Dreyfus, M., Fraumeni, J., Jr., Li, F.P., and Friend, S.H. (1995). Germ-line p53 mutations in 15 families with Li-Fraumeni syndrome. *Am J Hum Genet* 56, 608-615.

Golling, G., Amsterdam, A., Sun, Z., Antonelli, M., Maldonado, E., Chen, W., Burgess, S., Haldi, M., Artzt, K., Farrington, S., *et al.* (2002). Insertional mutagenesis in zebrafish rapidly identifies genes essential for early vertebrate development. *Nat Genet* 31, 135-140.

Humbey, O., Pimkina, J., Zilfou, J.T., Jarnik, M., Dominguez-Brauer, C., Burgess, D.J., Eischen, C.M., and Murphy, M.E. (2008). The ARF tumor suppressor can promote the progression of some tumors. *Cancer Res* 68, 9608-9613.

King, M.C., Marks, J.H., and Mandell, J.B. (2003). Breast and ovarian cancer risks due to inherited mutations in BRCA1 and BRCA2. *Science* 302, 643-646.

Kleihues, P., Schauble, B., zur Hausen, A., Esteve, J., and Ohgaki, H. (1997). Tumors associated with p53 germline mutations: a synopsis of 91 families. *Am J Pathol* 150, 1-13.

Knudson, A.G., Jr. (1971). Mutation and cancer: statistical study of retinoblastoma. *Proc Natl Acad Sci U S A* 68, 820-823.

Knudson, A.G., Jr. (1986). Genetics of human cancer. *Annu Rev Genet* 20, 231-251.

Kwok, S., Kellogg, D.E., McKinney, N., Spasic, D., Goda, L., Levenson, C., and Sninsky, J.J. (1990). Effects of primer-template mismatches on the polymerase chain reaction: human immunodeficiency virus type 1 model studies. *Nucleic Acids Res* 18, 999-1005.

Lane, D.P. (1993). Cancer. A death in the life of p53. *Nature* 362, 786-787.

Lane, D.P., and Crawford, L.V. (1979). T antigen is bound to a host protein in SV40-transformed cells. *Nature* 278, 261-263.

Lavin, M.F. (2007). ATM and the Mre11 complex combine to recognize and signal DNA double-strand breaks. *Oncogene* 26, 7749-7758.

Li, F.P., and Fraumeni, J.F., Jr. (1969). Rhabdomyosarcoma in children: epidemiologic study and identification of a familial cancer syndrome. *J Natl Cancer Inst* 43, 1365-1373.

Linzer, D.I., and Levine, A.J. (1979). Characterization of a 54K dalton cellular SV40 tumor antigen present in SV40-transformed cells and uninfected embryonal carcinoma cells. *Cell* 17, 43-52.

Lozano, G., and Montes de Oca Luna, R. (1998). MDM2 function. *Biochim Biophys Acta* 1377, M55-59.

Lu, L.Y., Wood, J.L., Ye, L., Minter-Dykhouse, K., Saunders, T.L., Yu, X., and Chen, J. (2008). Aurora A is essential for early embryonic development and tumor suppression. *J Biol Chem* 283, 31785-31790.

Lyon, E., and Wittwer, C.T. (2009). LightCycler technology in molecular diagnostics. *J Mol Diagn* 11, 93-101.

MacGeoch, C., Turner, G., Bobrow, L.G., Barnes, D.M., Bishop, D.T., and Spurr, N.K. (1995). Heterogeneity in Li-Fraumeni families: p53 mutation analysis and immunohistochemical staining. *J Med Genet* 32, 186-190.

McClendon, A.K., and Osheroff, N. (2007). DNA topoisomerase II, genotoxicity, and cancer. *Mutat Res* 623, 83-97.

Montes de Oca Luna, R., Wagner, D.S., and Lozano, G. (1995). Rescue of early embryonic lethality in mdm2-deficient mice by deletion of p53. *Nature* 378, 203-206.

Nadauld, L.D., Sandoval, I.T., Chidester, S., Yost, H.J., and Jones, D.A. (2004). Adenomatous polyposis coli control of retinoic acid biosynthesis is critical for

zebrafish intestinal development and differentiation. *J Biol Chem* 279, 51581-51589.

Nadauld, L.D., Shelton, D.N., Chidester, S., Yost, H.J., and Jones, D.A. (2005). The zebrafish retinol dehydrogenase, *rdh11*, is essential for intestinal development and is regulated by the tumor suppressor adenomatous polyposis coli. *J Biol Chem* 280, 30490-30495.

Nasevicius, A., and Ekker, S.C. (2000). Effective targeted gene 'knockdown' in zebrafish. *Nat Genet* 26, 216-220.

Neff, M.M., Neff, J.D., Chory, J., and Pepper, A.E. (1998). dCAPS, a simple technique for the genetic analysis of single nucleotide polymorphisms: experimental applications in *Arabidopsis thaliana* genetics. *Plant J* 14, 387-392.

Newton, C.R., Graham, A., Heptinstall, L.E., Powell, S.J., Summers, C., Kalsheker, N., Smith, J.C., and Markham, A.F. (1989). Analysis of any point mutation in DNA. The amplification refractory mutation system (ARMS). *Nucleic Acids Res* 17, 2503-2516.

Osman, K., Sanchez-Moran, E., Mann, S.C., Jones, G.H., and Franklin, F.C. (2009). Replication protein A (AtRPA1a) is required for class I crossover formation but is dispensable for meiotic DNA break repair. *EMBO J* 28, 394-404.

Pietsch, E.C., Sykes, S.M., McMahon, S.B., and Murphy, M.E. (2008). The p53 family and programmed cell death. *Oncogene* 27, 6507-6521.

Reinke, V., and Lozano, G. (1997). The p53 targets *mdm2* and *Fas* are not required as mediators of apoptosis in vivo. *Oncogene* 15, 1527-1534.

Robu, M.E., Larson, J.D., Nasevicius, A., Beiraghi, S., Brenner, C., Farber, S.A., and Ekker, S.C. (2007). p53 activation by knockdown technologies. *PLoS Genet* 3, e78.

Spirio, L.N., Samowitz, W., Robertson, J., Robertson, M., Burt, R.W., Leppert, M., and White, R. (1998). Alleles of APC modulate the frequency and classes of mutations that lead to colon polyps. *Nat Genet* 20, 385-388.

Varley, J.M. (2003). Germline TP53 mutations and Li-Fraumeni syndrome. *Hum Mutat* 21, 313-320.

CHAPTER 2

GENETIC MODELING OF LI-FRAUMENI SYNDROME IN ZEBRAFISH

Summary

Li-Fraumeni syndrome (LFS) is a highly penetrant autosomal dominant human familial cancer predisposition. Although a key role for the tumor suppressor p53 has been described in LFS, the genetic and cellular mechanisms underpinning this disease remain unknown. Therefore, modeling LFS in a vertebrate system accessible to both large-scale genetic screens and *in vivo* cell biological studies will facilitate the *in vivo* dissection of disease mechanisms, help identify candidate genes and spur the discovery of therapeutic compounds. Here, we describe a forward genetic screen in zebrafish embryos to identify LFS candidate genes, which yielded a p53 mutant that as an adult develops tumors, predominantly sarcomas, with 100% penetrance. As in humans with LFS, tumors arise in heterozygotes and display loss of heterozygosity (LOH). This first report of LOH in a zebrafish cancer model indicates that the Knudson's two hit hypothesis, a hallmark of human autosomal dominant cancer syndromes, can be modeled in zebrafish. Further, like some LFS mutations, the zebrafish p53^{I166T} allele is a loss-of-function allele with dominant-negative activity *in vivo*. Additionally, we demonstrate that the p53 regulatory pathway, including mdm2 regulation, is evolutionarily conserved in zebrafish, providing a *bona fide* biological context in which to systematically uncover novel modifier genes and therapeutic agents for human LFS.

Introduction

Familial cancers, although rare in the general population, represent important starting points to understanding the genetic components and

mechanisms of cancer. Much of our knowledge of key cancer-causing genes has been gained by studying familial cancers, such as RB in retinoblastoma, APC in Familial Adenomatous Polyposis (FAP), WT1 in Wilms Tumor, VHL in Von Hippel-Lindau disease, and others (Field et al., 2007; Ganjavi and Malkin, 2002). These familial syndromes often model sporadic cancer in the general population and help in devising strategies for cancers treatment.

Li-Fraumeni syndrome (LFS) is an autosomal dominant, highly penetrant cancer predisposition that presents with a wide variety of tumors types at an early age (Kleihues et al., 1997; Varley, 2003). Even though a wide variety of tumors occur, sarcomas are the hallmarks of the disease. The criteria for diagnosis of LFS are the presenting individual has a sarcoma before the age of 45, and has two 1st degree relatives who develop cancer before age 45 or a sarcoma at any age. Li-Fraumeni-like syndrome (LFL) and incomplete LFS (LFI) are similar to LFS, but with slightly different diagnostic criteria. Germ-line mutations in p53 have been identified in 50-70% of LFS, 40% of LFL, and 6% of LFI families (Birch et al., 1994; Chompret et al., 2000; Frebourg et al., 1995; Li and Fraumeni, 1969; MacGeoch et al., 1995). Chk2 has been suggested to be responsible for 5% of LFS families (Bell et al., 1999); however, this has been questioned since *chk2* ^{-/-} mice do not develop tumors (Takai et al., 2002). None the less, the genes responsible for the remaining 25-45% of LFS families, 60% of LFL families and 94% of LFI are unknown. In four families in which a p53 mutation was excluded, linkage mapping implicated chromosome 1q23 and at least one additional locus (Bachinski et al., 2005), indicating that multiple loci

contribute to LFS. However, due to the small size of the families, mapping to a single gene on 1q23 and other loci has been difficult.

Among LFS families there appears to be a genotype-phenotype correlation, with a subset of missense p53 alleles conferring more severe cancer predisposition (Birch et al., 1998). The idea that specific mutant p53 proteins have increased tumorigenic potential not found in null alleles is supported by the observation that a disproportionate number of missense, as compared to nonsense, mutations are found in Li-Fraumeni families. *In vitro* studies have demonstrated mutant p53 proteins have loss-of-function (LOF) activity (Sigal and Rotter, 2000), dominant-negative (DN) activity (Milner and Medcalf, 1991), and/or gain-of-function (GOF) activity (Dittmer et al., 1993), perhaps conferring advantages for tumor progression (Cadwell and Zambetti, 2001; Varley, 2003).

In addition to LFS, p53 is mutated in 50-70% of sporadic cancers, making it one of the most widely implicated genes in cancer biology (Cadwell and Zambetti, 2001). The tumor suppressor p53 is a transcription factor known to induce many targets following DNA damage. The outcome of p53 activation is predominantly apoptosis (through Puma, Noxa, and Bax) and cell cycle arrest (p21 and Cyclin G); both have been shown to be important in cancer prevention.

While p53 null mice display some of the dominant phenotypes seen in LFS, such as autosomal dominance and loss of heterozygosity (LOH) (Clarke et al., 1993; Donehower et al., 1992; Jacks et al., 1994), mice with missense mutations analogous to those found in LFS (LFS mice) are a better model in that they display dominant negative (DN) and gain-of-function (GOF) activity (Lang et

al., 2004; Olive et al., 2004). However, the difficulty of forward genetic screens in mice and the challenges of mapping in humans, hampered by the small size of some LFS families, emphasize the importance of designing genetic approaches in other organisms to unravel the p53 pathway and identify new Li-Fraumeni cancer genes.

P53-related genes have been identified in a variety of genetically useful invertebrates, including *D. melanogaster* (Brodsky et al., 2000; Ollmann et al., 2000), and *C. elegans* (Derry et al., 2001; Schumacher et al., 2001). However, they lack the p53-like genes p63 and p73, as well as the p53 regulators mdm2 and mdm4 (Lu and Abrams, 2006). In *Drosophila*, the p53 pathway appears to be simplified; DNA damage activates CHK2, which phosphorylates and activates p53 to transcribe apoptotic target genes such as *reaper* and *hid*, thereby resulting in cell death. Unlike the mammalian system, *Drosophila* p53 does not induce growth arrest and phosphorylation does not stabilize the p53 protein (Lu and Abrams, 2006). This lack of modulated p53 protein stability concurs with *Drosophila's* lack of the negative regulators mdm2 or mdm4. Therefore, although genetically powerful, these invertebrate systems do not recapitulate the complexity of the p53 regulatory pathways in mammalian systems.

Zebrafish are becoming a powerful tool for cancer research (Feitsma and Cuppen, 2008; Goessling et al., 2007), in part due to ease of *in vivo* manipulation and the ability to perform both genetic and *in vivo* drug screens. Zebrafish have p53, p63 and p73 genes, as well as the regulatory mdm2 and mdm4 genes (Lu and Abrams, 2006). A zebrafish p53^{M214K} mutant was recently identified in a

TILLing project (Berghmans et al., 2005). This mutant develops tumors, suggesting zebrafish might be a good model for cancer studies. However, these tumors were seen with low penetrance and no tumors were found in heterozygous fish, indicating this mutant line does not recapitulate LFS.

Most human familial cancer predispositions are autosomal dominant and loss of the functional wildtype allele, referred to as Loss of Heterozygosity (LOH), is an important mechanism of the Knudsen two-hit hypothesis for cancer progression (Field et al., 2007; Ganjavi and Malkin, 2002). Surprisingly, none of the autosomal dominant cancer models in zebrafish undergo LOH, including RP mutants (Amsterdam et al., 2004) and an APC mutant (Haramis et al., 2006), raising significant concerns that zebrafish does not serve as a genetic model for LOH and human tumor formation.

In this study, we characterized a p53-dependent IR-sensitivity phenotype in zebrafish embryos and used this embryonic phenotype to genetically screen for novel mutations in LFS genes that give rise to tumors in adults. As proof of principle, this screen identified an isoleucine to threonine mutation at codon 166, analogous to codon 195 in human, in the highly conserved DNA-binding domain of p53. The resulting p53^{I166T} mutant displayed highly penetrant tumorigenesis in both the heterozygous and homozygous states, and displayed a high rate of LOH, demonstrating for the first time in zebrafish a fundamental mechanism that contributes to human cancer. This mutant has the dominant phenotypes of human LFS: sarcomas, autosomal dominant tumor formation, and dominant negative functional activity. Utilizing the mdm2 knock-down lethal phenotype, we

show this p53 mutant is a loss-of-function allele with dominant-negative activities. This LFS zebrafish mutant will serve to uncover novel modifier genes and drugs capable of modulating the evolutionarily conserved LFS pathway.

Results

Genetic Screen for Li-Fraumeni Syndrome in Zebrafish

Genetic screens in nonvertebrates eukaryotes have been utilized to identify components of cancer pathways. However, not all pathway components are conserved between simpler eukaryotes and humans. The p53 gene is only found in metazoans, and functions as a tumor suppressor only in vertebrates (Goessling et al., 2007; Lu and Abrams, 2006). Thus a genetic screen in vertebrates would be necessary to identify genes responsible for tumor susceptibility in Li-Fraumeni syndrome.

We designed an F3 recessive genetic screen in zebrafish to identify components of the LFS/p53 pathway, using phenotypic response in embryos to ionizing (gamma) irradiation (IR) as an assay (Figure 2.1A). Northern blot analyses of putative p53 target genes (Supplemental Figure 2.1) and whole embryo apoptotic staining at various doses and times were performed to determine both the optimal IR conditions (Supplemental Figure 2.2) and p53-dependence both of target gene induction and apoptotic response (Supplemental Figures 2.1 & 2.3). The resulting screen scored for loss of neural tube (NT) apoptosis in zebrafish embryos irradiated at 30hpf with 30Gy and assessed 8 hours postirradiation (hpi). Approximately 1800 F3 clutches from 300 F2 (F1 x F1) families, approximately 489 genomic equivalences, were screened, yielding

one mutant with IR-resistant phenotype (Figure 2.1A) that segregated with Mendelian inheritance. Homozygous mutants were completely viable and fertile.

Sequencing of p53 cDNA and genomic DNA from mutant embryos revealed a T to C transition at codon 166 (Figure 2.1B), causing an isoleucine to threonine change in the DNA binding domain of p53. This mutation occurs at a conserved amino acid position in p53 among vertebrates (Figure 2.1C) and this exact mutation, in analogous codon 195 (Figure 2.1C), has been found in many human sporadic cancers. We modified a PCR-based mutation detection technique (Zhou et al., 2005) to develop a novel differential melting curve assay to efficiently genotype embryos and adult p53 mutant fish (Figure 2.1D, further details in Supplemental Materials).

P53^{I166T} Protein Is Stabilized Following DNA Damage but Does Not Transactivate p53 Target Genes

Stabilization of p53 protein is important in the regulation of p53 activity in mammals. In wildtype zebrafish, strong induction of p53 protein accumulation was observed at 2hpi, which continued through 20hpi (Figure 2.2A). Thus, p53 protein stabilization in response to irradiation-induced DNA damage is conserved in zebrafish. Therefore we tested whether p53^{I166T} mutant protein was stabilized with kinetics similar to wildtype p53 protein. Strikingly, mutant p53 protein was induced by IR and accumulated with similar kinetics as wildtype p53 protein (Figure 2.2A), suggesting the mutant phenotype is not due to altered p53 protein stabilization.

To determine whether the mutant protein can induce p53 target genes, the expression of the cell cycle genes p21 and Cyclin G, the p53 regulatory gene mdm2, and the apoptotic genes Bax, Puma, and Noxa were assessed in non-irradiated or irradiated p53^{+/+}, p53^{I166T/I166T} and p53 morpholino (MO)-injected embryos (p53 morphants) (Figure 2.2B). The p53 target genes were induced in wildtype samples following irradiation, but were not induced in p53 mutant or p53 morphants. The p53 morphant results indicate that induction of this battery of genes is dependent on the presence of functional p53 protein. Although mutant p53 protein is stabilized with normal kinetics following IR, it has lost the functional ability to induce transcription of p53 target genes in the cell cycle, autoregulatory and apoptotic pathways.

p53^{I166T/I166T} Mutants Have High Rates of Tumorigenesis

In LFS families, 85% of individuals carrying a p53 mutation will develop cancer, and 50% will do so by age 30 yrs (Field et al., 2007). In contrast, previously described zebrafish cancer models, p53^{M214K}, ribosomal protein (RP) or APC mutations, display only low penetrance tumorigenic phenotypes. To determine whether p53^{I166T} mutant fish, like Li-Fraumeni patients, are susceptible to increased tumor incidence and penetrance, genotyped cohorts of p53^{I166T/I166T} adult fish (n=144) were raised and compared to p53^{+/+} adult siblings (n=60), generated from a heterozygous-heterozygous mutant cross. The first incidence of tumor formation in p53^{I166T/I166T} fish occurred at 269 days (8.8 months), and the last 679 days (22.3 months) with a 50% survival at 465 days (15.2 months) (Figure 2.3A), indicating that the p53^{I166T} allele results in a fully penetrant tumor

phenotype. One advantage of this zebrafish model is that every fish developed a tumor that was grossly observable in the tank, in contrast to other zebrafish cancer models.

Tumors predominantly occurred in three locations: abdomen (64 of 134), eye (26 of 134) or flank (22 of 134), with less frequent occurrences in the gills (4 of 134), rectum (6 of 134) and skin (2 of 134). There was no difference in the onset of abdominal and flank tumors, but significantly later onset of eye tumors (Figure 2.3B). Histological analyses of $p53^{l166T/l166T}$ tumors from abdomen (Figure 2.4A,E,I), eye (Figure 2.4B,F,J), flank (Figure 2.4 C,G,K), or gills (Figure 2.4D,H,L) indicate they are predominantly soft tissue sarcomas (27/29 were STS), like the majority of sarcomas in LFS (Varley, 2003).

$p53^{l166T/+}$ Heterozygotes Are Tumor Prone and Exhibit Loss of Heterozygosity (LOH)

LFS and most familial cancer diseases are autosomal dominant diseases. In contrast, previously reported zebrafish heterozygous $p53^{M214K}$ mutants do not develop tumors (Berghmans et al., 2005). To determine whether the $p53^{l166T}$ heterozygous mutants develop tumors, cohorts of heterozygous (n=190) and wild-type (n=60) siblings were monitored for tumor burden. Similar to Li-Fraumeni patients, heterozygous mutant zebrafish developed tumors at significantly increased rates compared to wildtype siblings (Figure 2.5A). As in $p53^{l166T/l166T}$ homozygotes, tumors in $p53^{l166T/+}$ heterozygotes were predominantly in the abdomen (15 of 33), eye (2 of 33), flank (4 of 33), gills (3 of 33), rectum (5 of 33) and skin (1 of 33).

A central hallmark of LFS tumorigenesis and Knudson's two-hit hypothesis is Loss of Heterozygosity (LOH), i.e., loss of the wildtype allele in tumorigenic tissue. Interestingly, LOH has not been detected in tumors in RP heterozygous mutants or APC heterozygous mutant zebrafish (Amsterdam et al., 2004; Haramis et al., 2006), raising the significant concern that LOH does not occur in zebrafish. To determine whether LOH occurred in tumors in p53^{I166T/+} fish, pair-matched tumor and nontumorigenic genomic DNA samples were obtained from individual fish and PCR products containing codon 166 were amplified and sequenced. In 87.5% of cases there was clear LOH, with loss of the wildtype allele in tumors but not in other tissue from the same individual fish (Figure 2.5B). This is the first example of LOH in zebrafish, indicating that the p53^{I166T} recapitulates human LFS and opening the possibility of applying genetics to elucidate the regulatory mechanisms of LOH.

p53^{I166T/I166T} Is a Loss of Function Allele that Rescues mdm2

Knockdown Lethality

Mdm2 is a transcriptional target of p53 and an E3 ubiquitin ligase that binds to p53 and promotes its degradation, thereby providing a negative feedback loop in the p53 response pathway. In mouse, mdm2 null is embryonic lethal but is viable in the context of p53 null. In contrast to the irradiation response in which p53 maintains its feedback regulatory control mechanism, loss of mdm2 results in unrestrained activation of p53. Thus, loss of mdm2 provides a stringent assay for testing whether there are remnants of functionality in mutant p53 proteins in multiple tissues and many pathways, including apoptosis, cell cycle

arrest, and others. For example, mouse p53 loss-of-function (LOF) alleles (p53^{null} and p53^{R172H}) are able to completely rescue mdm2 null lethality. In contrast, p53 hypomorphic alleles (p53^{Δpro}, p53^{S389A} and p53^{R172P}) do not restore viability to mdm2 null mutants (Iwakuma et al., 2004; Jones et al., 1995; Lang et al., 2004; Liu et al., 2007; Montes de Oca Luna et al., 1995; Toledo et al., 2006).

We have shown (Figure 2.2B) that IR induction of mdm2 expression is dependent on p53 and is abrogated in p53^{I166T/I166T} embryos. To assess whether the other arm of the mdm2-p53 feedback regulatory pathway functions in zebrafish, an mdm2 splice-blocking MO that effectively knocks-down mdm2 mRNA accumulation (data not shown) was used to induce mdm2-dependent embryonic lethality. The earliest gross observable mdm2 MO phenotypes occur at 14hpf, but are more apparent at 26hpf and 50hpf (Figure 2.6B, H). In mouse, loss of mdm2 results in increased apoptosis at the blastocyst stage, but cell cycle arrest could not be determined (Chavez-Reyes et al., 2003). Due to accessibility of zebrafish embryos, we were able to determine that mdm2 knockdown lethality is due to both increased apoptosis (Figure 2.6D) and cell cycle arrest (Figure 2.6F). Complete rescue by injection of mdm2 mRNA (Figure 2.6J) demonstrates this phenotype is not due to MO off-target effects. Rescue of the mdm2 knockdown lethality by co-injection with p53 MO (Figure 2.6I) indicates that the p53-mdm2 regulatory loop described in mammals is conserved in zebrafish.

Within the context of this epistatic approach, a p53 LOF mutant would be predicted to rescue mdm2 knockdown lethality, whereas a p53 hypomorphic allele would be predicted to have residual p53 function that would be sufficient to

confer lethality in mdm2 deficient embryos. To test whether the p53^{I166T} mutant is a LOF or hypomorphic allele, p53^{I166T/I166T} embryos were injected with mdm2 MO, and found to be completely viable, providing functional evidence that p53^{I166T} is a LOF mutation (Figure 2.6N). In mammalian tissue culture, loss of mdm2 results in stabilization (or lack of degradation) of the p53 protein (Iwakuma and Lozano, 2003). Western blot analysis revealed that wildtype and mutant p53 protein accumulated to comparable levels in wildtype and p53^{I166T/I166T} mutant embryos, respectively, following mdm2 MO injection (Figure 2.6O), indicating there is no *in vivo* defect in the mdm2-dependent arm of the regulation of p53^{I166T} mutant protein stability.

The p53^{I166T} Allele Has Dominant Negative (DN) Activity

Among LFS families there appears to be a genotype-phenotype correlation with a subset of missense p53 alleles conferring more severe cancer predisposition (Birch et al., 1998). One possibility is that increased tumor potential is due to dominant negative (DN) activity, since some, but not all, human missense mutations have DN activity when overexpressed in cell culture (Milner and Medcalf, 1991), and heterozygous p53^{R172H} murine models respond differently to IR compared to heterozygous p53^{null}. If mutant p53 protein has dominant negative activity, it would be capable of reducing the functional activity of co-expressed wild-type p53 protein. In order to test this, we designed several sensitized assays of p53 function in p53^{I166T/+} heterozygotes. The prediction is that the heterozygotes would have a phenotype similar to the homozygous mutants if the p53 mutant protein had strong dominant negative activity, or have

an intermediate phenotype if the p53 mutant protein had partial/weak dominant negative activity. Conversely, if a p53 mutant protein did not have dominant negative activity, the heterozygotes would display a wildtype phenotype.

Our results from multiple *in vivo* assays indicate that p53^{I166T} protein has DN activity. In the first assay, embryos were treated with low dose (5Gy) IR that was sufficient to cause mild apoptosis in wildtype embryos (Figure 2.7B) but no apoptosis in p53^{I166T/I166T} homozygotes (Figure 2.7D). There was also no increased apoptosis in p53^{I166T/+} embryos, indicating the heterozygous phenotype (Figure 2.7C) was similar to the homozygous mutant phenotype. In the second assay, we observed that p53 mutants were resistant to the curled tail phenotype normally induced by 100Gy irradiation (Figure 2.7E,G). Irradiated p53^{I166T/+} heterozygotes (Figure 2.7F) also did not have a curled tail phenotype, again a similar phenotypic response in heterozygotes and homozygous mutants indicative of a dominant negative activity in the heterozygotes. In a third assay, to assess whether DN activity also occurs in late stage fry, we developed an *in vivo* radiation resistance thymocyte paradigm using transgenic fish that express EGFP in mature T cells, under the regulation of the Lck promoter Tg(lck:lck-GFP) (Langenau et al., 2004). Eight day old p53^{+/+}; Tg(lck:lck-GFP)/+ and p53^{I166T/I166T}; Tg(lck:lck-GFP)/+ fry were irradiated with 0 or 30Gy and imaged the following day for EGFP expression. Untreated p53^{+/+}; Tg(lck:lck-gfp)/+ and p53^{I166T/I166T}; Tg(lck:lck-gfp)/+ fry were identical in their EGFP expression (data not shown), indicating that the p53^{I166T} allele did not alter T cell development or Lck-GFP expression. When irradiated, p53^{+/+}; Tg(lck:lck-gfp)/+ fry had severely reduced

EGFP expression (Figure 2.7H). In contrast, $p53^{I166T/I166T}$; Tg(lck:lck-gfp)/+ fry retained EGFP expression (Figure 2.7J) similar to nonirradiated controls, indicating that the IR induced T-cell apoptosis is p53 dependent. To test dominant negative activity the thymocyte assay was repeated with $p53^{I166T/+}$; Tg(lck:lck-gfp)/+ fry. When irradiated, $p53^{I166T/+}$; Tg(lck:lck-gfp)/+ fry retained some EGFP expression (Figure 2.7I), indicating that IR-induced apoptosis in thymocytes was at least partially abrogated in $p53^{I166T}$ heterozygotes, suggesting the mutant allele has DN activity at older stages as well. Thus, in each of these three IR-response assays, the mutant $p53^{I166T}$ protein appeared to have DN activity sufficient to block the function of wildtype p53 protein.

To assess whether $p53^{I166T}$ has dominant negative activity in other cellular processes besides the response to irradiation, we used mdm2 knockdown lethality as an assay for p53 function. Injection of mdm2 MO into embryos from a $p53^{I166T/+}$ intercross resulted in three phenotypes distributed in a Mendelian ratio (Figure 2.7K,L,M), suggesting that the p53 wild-type, heterozygous and homozygous mutants each had a distinct phenotype. Embryos were segregated into each of these three phenotypic categories, and then individually genotyped. Mdm2 morphant embryos with a lethal phenotype were wildtype for p53. Morphants with a partially rescued phenotype were heterozygous mutants ($p53^{I166T/+}$). Completely rescued embryos were homozygous mutants ($p53^{I166T/I166T}$) (Figure 2.7N).

The intermediate phenotype of the $p53^{I166T/+}$ heterozygotes injected with mdm2 MO is strikingly distinct from the p53 wildtype embryos injected with mdm2

MO. In $p53^{I166T/+}$ *mdm2* morphants, the opaque necrotic head phenotype is similar to phenotype in the $p53^{+/+}$ *mdm2* morphants or IR treated embryos, suggesting apoptosis contributes to the intermediate phenotype. However the phenotype could be due to delay in p53 dependent apoptosis. Alternatively, the eye, head, tail and somite appear to develop fairly normal in $p53^{I166T/+}$ *mdm2* morphants. These tissues also do not appear to undergo apoptosis following irradiation, suggesting p53 may have alternative effects, such as cell cycle arrest or other outcomes in these tissues and these p53 activities are inhibited by the p53 mutant DN activity, thereby making these tissues appear normal in $p53^{I166T/+}$ *mdm2* morphants but not $p53^{+/+}$ *mdm2* morphants. Together, this suggests that $p53^{I166T}$ has DN activity capable of rescuing some, but not all, aspects of the lethal *mdm2* knockdown phenotype. In addition, the fact that $p53^{I166T}$ heterozygous fish develop tumors, unlike $p53^{M214K}$ heterozygous fish, suggests tumor induction might occur in part through DN activity of the $p53^{I166T}$ allele.

Discussion

This study provides the first zebrafish mutant that recapitulates the dominant phenotype of human Li-Fraumeni Syndrome (LFS), derived from an unbiased forward genetic screen. Strikingly, this forward genetics screen utilizes a specific irradiation-induced embryonic phenotype to successfully identify mutations that give rise to tumors in adults. We show heterozygous $p53^{I166T}$ fish, like LFS patients, have a high rate of tumor development and follow Knudson's two-hit hypothesis in which the tumors display LOH at the p53 locus. These results demonstrate the evolutionary conservation of the vertebrate LFS pathway

and suggest zebrafish genetics will accelerate the discovery of other LFS genes. In addition, we have shown at a molecular level that regulation of the p53 pathway is conserved between zebrafish and mammals. Cell cycle target genes (p21, Cyclin G and Gadd45), a regulatory gene (mdm2), and apoptosis genes (Bax, Puma, and Noxa) are all induced in a p53-dependent manner in zebrafish. Loss of mdm2 in the mouse results in apoptosis (Chavez-Reyes et al., 2003); however, cell cycle arrest could not be tested in the blastocyst stage of mdm2 null embryos. In contrast, the accessibility of zebrafish embryos allowed us to demonstrate that the embryonic lethality in mdm2 morphants was due to both increased apoptosis and cell cycle arrest. As in mammalian systems, p53 wildtype and mutant protein are stabilized, and IR-induced apoptosis is p53 dependent in embryonic neural tube and in thymocytes.

Among LFS families there appears to be a genotype-phenotype correlation with distinct missense p53 alleles conferring a more severe cancer predisposition (Birch et al., 1998; Cadwell and Zambetti, 2001). Molecularly, some LFS missense mutations in p53 have been shown to be loss-of-function alleles, equivalent to truncation or null alleles, whereas other mutations are hypomorphic, dominant-negative (DN) and/or gain-of-function (GOF) alleles. In addition, LFS models in mouse demonstrated both DN and GOF activity. Here we use whole-animal studies to show that the zebrafish p53^{I166T} mutation is a loss-of-function allele with DN activity, analogous to the roles of mutant p53 in LFS patients.

Loss of Function

Within LFS families, 80% of p53 mutations are missense mutations. However, not all are complete loss of function (LOF) mutations; some mutations have been shown to lose apoptosis but preserve growth arrest function (Aurelio et al., 2000). In genetics, the formal definition of a full loss-of-function (LOF) in a missense allele is that the missense allele over a deficiency (deletion) mutation has the same phenotype as a homozygous deletion mutation. In mouse, p53 null and LFS mice were shown to be deficient in p53 dependent neural tube apoptosis *in vivo* and thymocyte apoptosis *ex vivo* following IR treatment. Determining if a p53 missense mutation results in complete loss of function is difficult in zebrafish in the absence of a deletion allele. However, we have performed multiple assays to assess the function of mutant p53 protein in zebrafish, and all results suggest that the p53^{I166T} is a loss-of-function allele.

First, similar to mutations found in LFS patients, our zebrafish mutant is deficient in induction of p53 target genes, including cell cycle, regulatory and apoptotic pathway genes (Figure 2.2B). This is in contrast to hypomorphic LFS human mutations and some mouse hypomorphic alleles (i.e. p53^{R172P}, p53^{S389A} and p53^{Δpro}). Second, we show that the induction defect is not due to altered stabilization of the mutant protein, but instead lies in its inability to transactivate target genes. Third, correlating with its failure to induce p53 apoptotic genes, the p53^{I166T} zebrafish is deficient in p53-dependent apoptosis in embryonic neural tissues and in thymocytes (Figure 2.1A and Figure 2.7J), similar to results from p53^{null} and p53^{R172H} mice.

Fourth, in a more global assay, mdm2 knock-down lethality is prevented in the p53^{I166T/I166T} background. Following irradiation, p53 continues to maintain its feedback regulatory control mechanism. In contrast, loss of mdm2 results in unrestrained activation of p53. Thus, loss of mdm2 provides a stringent assay for testing whether there are remnants of functionality in mutant p53 protein in multiple tissues and many pathways, including apoptosis, cell cycle arrest, and others. Mouse LOF mutants, p53^{Null} and p53^{R172H}, both completely rescue mdm2 loss. However, hypomorphic alleles, p53^{Δpro}, p53^{S389A} and p53^{R172P}, do not rescue the mdm2 null lethality. Fifth, in contrast to the low penetrance of the p53^{M214K} allele (Berghmans et al., 2005), the 100% penetrance of tumor formation in these mutants suggest p53^{I166T} is a LOF allele.

Dominant Negative Activity

Distinct LFS missense mutations in the DNA binding domain have earlier cancer onset compared to truncation mutations or LFS mutations lying outside the DNA binding domain (Birch et al., 1998). One possibility is that increased tumor potential is due to DN activity. Milner and Medcalf (Milner and Medcalf, 1991) showed that some, but not all, human missense mutations had DN activity in cell culture. DN activity was also observed in murine models of LFS, in both IR-induced neuronal apoptosis as well as IR-induced thymocyte apoptosis studies in heterozygous p53^{R172H} mice, but not in heterozygous p53^{null} mice. To assay DN activity in the p53^{I166T} mutant we developed multiple *in vivo* assays, and were able to show DN activity by several criteria. First, p53^{I166T} heterozygous fish were partially resistant to both IR-induced embryonic neural apoptosis and

thymocyte apoptosis, analogous to the DN activity seen in the p53^{R172H} LFS mouse. Second, p53^{I166T} heterozygous fish were able to partially rescue loss of mdm2. Third, p53^{I166T} heterozygous fish develop tumors, unlike p53^{M214K} heterozygous fish, suggesting this might occur in part through the DN activity of the p53^{I166T} allele.

Protein Stability

Human tumor and cell culture studies have shown that mutant p53 proteins are typically very stable. However, we show that in the absence of stress, the p53^{I166T} mutant protein is not abundant, and that following IR-induced DNA damage or mdm2 loss, the mutant protein becomes stable and more abundant, at levels comparable to wildtype p53 protein. This suggests that the higher levels of p53 protein in human tumor and cell culture studies may be due to constitutively active DNA damage signals in tumors and ongoing cell stress in culture, which provide signals that stabilize and activate the p53 protein. This difference may confound studies meant to address DN or GOF activities which might depend on high protein levels that are increased by DNA damage, lack of negative regulation (loss of mdm2), or tumorigenesis. This is consistent with the context in which we detect DN activity, and the circumstances in which the LFS mice display DN and GOF activities. Further, studies (Terzian et al., 2008) have shown that mdm2^{-/-}; p53^{R172H/R172H} mice develop tumors much faster than p53^{R172H/R172H} animals, and that mutant protein is stabilized in non-tumor tissues of mdm2^{-/-}; p53^{R172H/R172H} mice. Together, these observations suggest that additional activities and phenotypes may manifest when mutant p53 protein is

stabilized. The observation of similar p53 mutant protein stability in zebrafish implies zebrafish may be a useful model to explore mechanisms of p53 stability, either through genetic or pharmacological perturbation *in vivo*. Furthermore, this emphasizes the importance of careful evaluation of p53 mutations in cancer patients when considering treatment with p53-activating compounds. For example, the use of nutlin and nutlin-like compounds that work by inhibiting mdm2 and thereby stabilizing p53, might be therapeutic if wildtype p53 is present but could be detrimental if particular mutants in p53 are present. This same theme might be applicable to considerations of chemotherapeutics, such as doxorubicin or DNA damaging agents known to stabilize p53.

A Zebrafish Li-Fraumeni Syndrome Model

Tumors from LFS families are diverse; however sarcomas are the hallmark that defines the syndrome. Correspondingly, the p53^{L166T} fish develop primarily sarcomas. Due to the absence of a full set of diagnostic antibodies in zebrafish, the exact subtype of these sarcomas has not been determined, but they appear histologically to be soft tissue sarcomas (STS), like the majority of sarcomas in LFS (Varley, 2003). Do p53^{L166T} fish display the complete spectrum of tumors seen in LFS patients? The most prevalent tumor after sarcomas in LFS patients is breast carcinoma. Given the absence of mammary glands, it is not surprising that breast carcinoma was not observed in p53 mutant fish. However, in LFS patients, the 5th and 6th most common cancers are brain tumors or hematological tumors, which were not detected in p53 mutant fish. This could be due to the time of onset. In LFS patients the mean incidence of soft tissue

sarcomas is 15.5 years; however the mean age of brain or hematological tumors is 25 years (Kleihues et al., 1997). Therefore, with the high penetrance of STS seen in p53^{I166T} fish, it is likely the fish die (or are sacrificed) due to the onset of sarcomas before the onset of brain or hematological tumors. Similar observations were made for murine knockout of p53. The predominant tumors in these mice were lymphomas (not found in LFS patients) and sarcomas, with very few other tumors. Another possibility is that genetic background may influence the diversity of tumor types, as supported by studies of tumor spectrum changes in p53^{null} mice on different genetic backgrounds (Kuperwasser et al., 2000). Both mouse and zebrafish have been bred to isogenic or partial isogenic backgrounds, whereas human LFS patients are genetically diverse.

One of the hallmarks of LFS tumorigenesis and Knudson's two-hit hypothesis is loss of the wildtype allele (LOH). In this study we provide the first example of LOH in zebrafish, which further demonstrates the similarity of p53^{I166T} tumors to human LFS tumors. To date, other zebrafish cancer models have not exhibited LOH. The lack of LOH in RP mutants may not be surprising in that partial loss of translational efficiencies may be tolerated and tumorigenic, but complete loss is likely cell lethal. On the other hand, the fact that APC tumors do not exhibit LOH is surprising. Utilizing the p53^{I166T} mutant and the powerful genetics of zebrafish provides an opportunity to identify the regulatory mechanisms of LOH and their influence on cancer progression.

One confusing issue in all three LFS models, human, mouse and zebrafish, is that tumors from heterozygous individuals often display LOH even

though the mutant allele has been shown to have DN activity. There are at least three potential explanations for this: 1) DN activity is not against p53 but other interacting proteins (potential GOF activity), and in order for a cell to be tumorigenic, it still needs to lose the wildtype p53 allele; 2) the DN activity does not inhibit all p53 functions, hence the partial rescue of the mdm2 lethality; and 3) the DN activity depends on the mutant protein being stable, as discussed above, which does not occur until tumorigenesis has begun. Now that we have identified a LFS model in zebrafish, we can begin to address these questions using both molecular and genetic techniques.

Zebrafish: New Directions in Cancer Genetics

Zebrafish are proving to be a very useful model for studying tumorigenesis (Feitsma and Cuppen, 2008; Goessling et al., 2007). With the ability to do powerful genetics in zebrafish, future studies can use this mutant p53 allele to identify cooperative tumor suppressor genes, p53 modifiers, and modifiers of genomic stability. Since most familial tumor suppressors are autosomal dominant, and most homozygous mouse tumor suppressor knock-outs are embryonic lethal, a dominant/heterozygous screen would be particularly rewarding. For example, dominant screens for tumor enhancers in the $p53^{I166T/I166T}$ background may identify tumor suppressors as well as regulators of p53 protein stability and modulators of mutant p53 DN activity. In addition, since tumor onset in $p53^{I166T/+}$ is largely dependent on LOH, an enhancer screen in the $p53^{I166T/+}$ background could identify modifiers influencing the frequency or timing of LOH events.

Zebrafish provide an ideal organism for the discovery of novel cancer therapeutics. Drug screens can be performed on p53^{I166T/I166T} embryos to identify compounds that either specifically kill p53 mutant embryos or restore apoptosis in these mutant embryos following DNA damage. Identified compounds could conceivably be invaluable in fighting cancer since 70% of tumors have p53 mutations.

Methods

Zebrafish Maintenance, Lines and Mutagenesis

Zebrafish (*Danio rerio*) were maintained on an Aquatic Habitat system (Florida, USA). Embryos were collected from natural matings and raised as described (Westerfield, 1995). The Tubingen (TU) wildtype strain was used for morpholino oligonucleotides (MO) and mRNA injections. ENU mutagenesis was carried out in the AB wildtype background using standard protocols (Mullins et al., 1994). Adult male fish were exposed to 4 to 6 weekly treatments of 3.0mm ENU (sigma cat# n3385), allowed to recover for 1 month, bred to golden (Mullins et al., 1994; Streisinger et al., 1981) to determine mutation frequency and subsequently bred to wildtype females to generate F1 fish. F2 families were obtained from F1 intercrosses. For p53^{I166T} cancer studies, fry were raised at a density of n=30/3L tank until 8 months of age, then maintained at 16 fish/3liter tanks. Tg(lck:lck-gfp) (Langenau et al., 2004) fish were maintained on a WIK wildtype background.

Morpholino Knockdown and mRNA Injections

Morpholino antisense oligonucleotides (Gene Tools, Oregon) and mRNA synthesized with a mMessage machine SP6 transcription kit (Ambion) were injected into the yolk just under the nuclei of 1- to 2-cell stage embryos in a volume of 0.5 or 1.0 nl. p53 splice-blocking morpholino (p53 MO) overlaps to splice donor site of exon 2 and intron 2 effectively preventing splicing out of intron 2, (5'- cccttgcgaaacttacatcaaattct -3'); mdm2 splice-blocking morpholino (mdm2 MO) overlaps the splice donor site of exon 4 and intron 4, (5'- tgtaagagattcagtagcgaccgc -3'). Working concentrations of p53 MO was 0.35mM and mdm2 MO was 0.35mM. The Bcl2 and mdm2 ORFs were cloned by RT-PCR using primers Bcl2 cDNA f1: accatggctaacgaaatt with Bcl2 cDNA r1: cgcagaggctgtcacttc and Mdm2 cDNA f1: ccaaaatggcaacagaga with Mdm2 cDNA r1: atttcagtcctcagctc respectively, and subcloned into the CS2+ expression plasmid (Rupp et al., 1994; Turner and Weintraub, 1994). Capped RNAs were synthesized from these pCS2+ using the mMessage machine SP6 transcription kit (Ambion). The working mRNA concentration for both Bcl2 and mdm2 was 300 ng/ul.

Irradiation and Apoptotic Detection

Apoptosis was assayed following IR treatment (^{137}Cs source) or Morpholino injection by soaking embryos in 50 ug/ml Acridine Orange (Sigma) for 45 min and subsequently destaining for 15 minutes. Photographs were taken using a FITC filter.

Genotyping Using Melting Curve Analysis

Initially the I166T mutation was identified by RT-PCR of total RNA from pooled mutant embryos and pooled wildtype embryos using primers p53 cDNA f1: atggcgcaaaacgaca with p53 cDNA r1: tagcatcccatcacctta, followed by single embryo genomic PCR with the same primers. Genomic DNAs from embryos or fin clips were digested in 100ul ELB solution (0.01M TRIS pH 8.3, 0.05M KCl, 1.5mL 0.3% Tween 20, 0.3% NP40) and 5ul Proteinase K (Roche) at 55°C overnight, followed by 10min. at 95°C to inactivate the Proteinase K. Melting Curve analysis primers (gcgctgctggtca and ctgattgccctccactctt) were designed to produce a 40bp PCR product surrounding the point mutation. The PCR reactions were performed in 96 well plates (Biorad) with the following PCR conditions: 95°C for 10s, 30 cycles of 95°C for 2s, 60°C for 2s, 72°C for 2s, and a final cycle of 95°C for 2s, then 45°C for 10s. Each reaction contained 1ul genomic DNA, 1x Icgreen+, 1x ExTaq buffer, 1x dNTP, 0.5mm primer1, 0.5mm primer2, and 1u ExTAQ. The melting curve analysis is performed on a lightscanner (Idaho tech.).

Protein Analysis and Real-Time PCR

The quantity of protein loaded on western blots was assessed by hybridizing with α -tubulin primary antibody (Santa Cruz Biotechnologies) and subsequent gels adjusted based on α -tubulin results. P53 was detected by hybridizing with the ZFp53-9.1 antibody (Lee et al., 2008). For PH3 staining, embryos were incubated with rabbit polyclonal anti-phospho-Histone H3 (ser10) antibody (1:1,000 dilution) (Santa Cruz Biotechnology). monoclonal p53 specific

antibody (ZFp53-9.1) Real time RT-PCR was performed on a light cycler PCR machine (Roche). The following primer sets were used: for p21 (SG1:tgacatcagcgggtttacag and i102:ttctgctgcttttctgaca), for Cyclin G (C11:ccaccatgattgaccaggtgacc and C15:agcagcacagacccacac), for mdm2 (SG76:ctcggtgctgttcttgag and SG77:cactgcttctctctctctg), for Bax (SG66:acagggatgctgaagtgacc and SG67:gaaaagcgccacaactcttc), for Puma (i97:acgctgtcttcttcagagg and i98:cctgcagaaaattcccagag), for Noxa (i91:atggcgaagaaagagcaaac and i92:cgctcccctccattgtat), for p53 (SG72:accccggatggagataactt and SG73:cccagcaactgaccttctgag), and for β -actin (SG86:ggatgggacagaaagacag and SG87:agagtcacacgataccag). Experiments were done in triplicate and normalized to β -actin.

Tumor Analysis

Adult fish were screened weekly for tumors and/or missing/dead fish. Fish identified with tumor burden were fixed in 10% neutral buffer formalin (VWR). A portion of each tumor from abdomen burdened fish was flash frozen along with a fin clip for future DNA-RNA analysis. Kaplan Meijer analysis was performed using Graphpad Prism 5 analysis. Tumor burdened fish were sectioned and H&E stained for histological analysis. LOH analysis was performed by sequencing of PCR products (primers: gtgctgttaaagccaccaca and ggtctacaaaaaggctgtga) from genomic DNA of tumor and somatic tissues from the same heterozygous tumor burdened fish.

Imaging

Light and fluorescent dissection images were taken on an Olympus SZX12 with an Olympus S97809 color CCD camera. LCK-EGFP images were taken using an Olympus Fluoview FV300 laser-scanning confocal microscope. The fluorescent images presented represent the sum of multiple focal planes through the embryo (z-series) assembled using ImageJ (NIH) and Photoshop (Adobe) software.

References

- Amsterdam, A., Sadler, K.C., Lai, K., Farrington, S., Bronson, R.T., Lees, J.A., and Hopkins, N. (2004). Many ribosomal protein genes are cancer genes in zebrafish. *PLoS biology* 2, E139.
- Aurelio, O.N., Kong, X.T., Gupta, S., and Stanbridge, E.J. (2000). p53 mutants have selective dominant-negative effects on apoptosis but not growth arrest in human cancer cell lines. *Molecular and cellular biology* 20, 770-778.
- Bachinski, L.L., Olufemi, S.E., Zhou, X., Wu, C.C., Yip, L., Shete, S., Lozano, G., Amos, C.I., Strong, L.C., and Krahe, R. (2005). Genetic mapping of a third Li-Fraumeni syndrome predisposition locus to human chromosome 1q23. *Cancer research* 65, 427-431.
- Bell, D.W., Varley, J.M., Szydlo, T.E., Kang, D.H., Wahrer, D.C., Shannon, K.E., Lubratovich, M., Verselis, S.J., Isselbacher, K.J., Fraumeni, J.F., *et al.* (1999). Heterozygous germ line hCHK2 mutations in Li-Fraumeni syndrome. *Science* (New York, NY 286, 2528-2531.
- Berghmans, S., Murphey, R.D., Wienholds, E., Neuberg, D., Kutok, J.L., Fletcher, C.D., Morris, J.P., Liu, T.X., Schulte-Merker, S., Kanki, J.P., *et al.* (2005). tp53 mutant zebrafish develop malignant peripheral nerve sheath tumors. *Proceedings of the National Academy of Sciences of the United States of America* 102, 407-412.
- Birch, J.M., Blair, V., Kelsey, A.M., Evans, D.G., Harris, M., Tricker, K.J., and Varley, J.M. (1998). Cancer phenotype correlates with constitutional TP53 genotype in families with the Li-Fraumeni syndrome. *Oncogene* 17, 1061-1068.
- Birch, J.M., Hartley, A.L., Tricker, K.J., Prosser, J., Condie, A., Kelsey, A.M., Harris, M., Jones, P.H., Binchy, A., Crowther, D., *et al.* (1994). Prevalence and

diversity of constitutional mutations in the p53 gene among 21 Li-Fraumeni families. *Cancer research* 54, 1298-1304.

Brodsky, M.H., Nordstrom, W., Tsang, G., Kwan, E., Rubin, G.M., and Abrams, J.M. (2000). *Drosophila* p53 binds a damage response element at the reaper locus. *Cell* 101, 103-113.

Cadwell, C., and Zambetti, G.P. (2001). The effects of wild-type p53 tumor suppressor activity and mutant p53 gain-of-function on cell growth. *Gene* 277, 15-30.

Chavez-Reyes, A., Parant, J.M., Amelse, L.L., de Oca Luna, R.M., Korsmeyer, S.J., and Lozano, G. (2003). Switching mechanisms of cell death in mdm2- and mdm4-null mice by deletion of p53 downstream targets. *Cancer research* 63, 8664-8669.

Chompret, A., Brugieres, L., Ronsin, M., Gardes, M., Dessarps-Freichay, F., Abel, A., Hua, D., Ligot, L., Dondon, M.G., Bressac-de Paillerets, B., *et al.* (2000). P53 germline mutations in childhood cancers and cancer risk for carrier individuals. *British journal of cancer* 82, 1932-1937.

Clarke, A.R., Purdie, C.A., Harrison, D.J., Morris, R.G., Bird, C.C., Hooper, M.L., and Wyllie, A.H. (1993). Thymocyte apoptosis induced by p53-dependent and independent pathways. *Nature* 362, 849-852.

Derry, W.B., Putzke, A.P., and Rothman, J.H. (2001). *Caenorhabditis elegans* p53: role in apoptosis, meiosis, and stress resistance. *Science (New York, NY)* 294, 591-595.

Dittmer, D., Pati, S., Zambetti, G., Chu, S., Teresky, A.K., Moore, M., Finlay, C., and Levine, A.J. (1993). Gain of function mutations in p53. *Nature genetics* 4, 42-46.

Donehower, L.A., Harvey, M., Slagle, B.L., McArthur, M.J., Montgomery, C.A., Jr., Butel, J.S., and Bradley, A. (1992). Mice deficient for p53 are developmentally normal but susceptible to spontaneous tumours. *Nature* 356, 215-221.

Feitsma, H., and Cuppen, E. (2008). Zebrafish as a cancer model. *Mol Cancer Res* 6, 685-694.

Field, M., Shanley, S., and Kirk, J. (2007). Inherited cancer susceptibility syndromes in paediatric practice. *Journal of paediatrics and child health* 43, 219-229.

Frebourg, T., Barbier, N., Yan, Y.X., Garber, J.E., Dreyfus, M., Fraumeni, J., Jr., Li, F.P., and Friend, S.H. (1995). Germ-line p53 mutations in 15 families with Li-Fraumeni syndrome. *American journal of human genetics* 56, 608-615.

Ganjavi, H., and Malkin, D. (2002). Genetics of childhood cancer. *Clinical orthopaedics and related research*, 75-87.

Goessling, W., North, T.E., and Zon, L.I. (2007). New waves of discovery: modeling cancer in zebrafish. *J Clin Oncol* 25, 2473-2479.

Haramis, A.P., Hurlstone, A., van der Velden, Y., Begthel, H., van den Born, M., Offerhaus, G.J., and Clevers, H.C. (2006). Adenomatous polyposis coli-deficient zebrafish are susceptible to digestive tract neoplasia. *EMBO reports* 7, 444-449.

Iwakuma, T., and Lozano, G. (2003). MDM2, an introduction. *Mol Cancer Res* 1, 993-1000.

Iwakuma, T., Parant, J.M., Fasulo, M., Zwart, E., Jacks, T., de Vries, A., and Lozano, G. (2004). Mutation at p53 serine 389 does not rescue the embryonic lethality in mdm2 or mdm4 null mice. *Oncogene* 23, 7644-7650.

Jacks, T., Remington, L., Williams, B.O., Schmitt, E.M., Halachmi, S., Bronson, R.T., and Weinberg, R.A. (1994). Tumor spectrum analysis in p53-mutant mice. *Curr Biol* 4, 1-7.

Jones, S.N., Roe, A.E., Donehower, L.A., and Bradley, A. (1995). Rescue of embryonic lethality in Mdm2-deficient mice by absence of p53. *Nature* 378, 206-208.

Kleihues, P., Schauble, B., zur Hausen, A., Esteve, J., and Ohgaki, H. (1997). Tumors associated with p53 germline mutations: a synopsis of 91 families. *The American journal of pathology* 150, 1-13.

Kuperwasser, C., Hurlbut, G.D., Kittrell, F.S., Dickinson, E.S., Laucirica, R., Medina, D., Naber, S.P., and Jerry, D.J. (2000). Development of spontaneous mammary tumors in BALB/c p53 heterozygous mice. A model for Li-Fraumeni syndrome. *The American journal of pathology* 157, 2151-2159.

Lang, G.A., Iwakuma, T., Suh, Y.A., Liu, G., Rao, V.A., Parant, J.M., Valentin-Vega, Y.A., Terzian, T., Caldwell, L.C., Strong, L.C., *et al.* (2004). Gain of function of a p53 hot spot mutation in a mouse model of Li-Fraumeni syndrome. *Cell* 119, 861-872.

Langenau, D.M., Ferrando, A.A., Traver, D., Kutok, J.L., Hezel, J.P., Kanki, J.P., Zon, L.I., Look, A.T., and Trede, N.S. (2004). In vivo tracking of T cell development, ablation, and engraftment in transgenic zebrafish. *Proceedings of*

the National Academy of Sciences of the United States of America *101*, 7369-7374.

Lee, K.C., Goh, W.L., Xu, M., Kua, N., Lunny, D., Wong, J.S., Coomber, D., Vojtesek, B., Lane, E.B., and Lane, D.P. (2008). Detection of the p53 response in zebrafish embryos using new monoclonal antibodies. *Oncogene* *27*, 629-640.

Li, F.P., and Fraumeni, J.F., Jr. (1969). Rhabdomyosarcoma in children: epidemiologic study and identification of a familial cancer syndrome. *Journal of the National Cancer Institute* *43*, 1365-1373.

Liu, G., Terzian, T., Xiong, S., Van Pelt, C.S., Audiffred, A., Box, N.F., and Lozano, G. (2007). The p53-Mdm2 network in progenitor cell expansion during mouse postnatal development. *The Journal of pathology* *213*, 360-368.

Lu, W.J., and Abrams, J.M. (2006). Lessons from p53 in non-mammalian models. *Cell death and differentiation* *13*, 909-912.

MacGeoch, C., Turner, G., Bobrow, L.G., Barnes, D.M., Bishop, D.T., and Spurr, N.K. (1995). Heterogeneity in Li-Fraumeni families: p53 mutation analysis and immunohistochemical staining. *Journal of medical genetics* *32*, 186-190.

Milner, J., and Medcalf, E.A. (1991). Cotranslation of activated mutant p53 with wild type drives the wild-type p53 protein into the mutant conformation. *Cell* *65*, 765-774.

Montes de Oca Luna, R., Wagner, D.S., and Lozano, G. (1995). Rescue of early embryonic lethality in mdm2-deficient mice by deletion of p53. *Nature* *378*, 203-206.

Mullins, M.C., Hammerschmidt, M., Haffter, P., and Nusslein-Volhard, C. (1994). Large-scale mutagenesis in the zebrafish: in search of genes controlling development in a vertebrate. *Curr Biol* *4*, 189-202.

Olive, K.P., Tuveson, D.A., Ruhe, Z.C., Yin, B., Willis, N.A., Bronson, R.T., Crowley, D., and Jacks, T. (2004). Mutant p53 gain of function in two mouse models of Li-Fraumeni syndrome. *Cell* *119*, 847-860.

Ollmann, M., Young, L.M., Di Como, C.J., Karim, F., Belvin, M., Robertson, S., Whittaker, K., Demsky, M., Fisher, W.W., Buchman, A., *et al.* (2000). *Drosophila* p53 is a structural and functional homolog of the tumor suppressor p53. *Cell* *101*, 91-101.

Rupp, R.A., Snider, L., and Weintraub, H. (1994). *Xenopus* embryos regulate the nuclear localization of XMyoD. *Genes & development* *8*, 1311-1323.

Schumacher, B., Hofmann, K., Boulton, S., and Gartner, A. (2001). The *C. elegans* homolog of the p53 tumor suppressor is required for DNA damage-induced apoptosis. *Curr Biol* 11, 1722-1727.

Sigal, A., and Rotter, V. (2000). Oncogenic mutations of the p53 tumor suppressor: the demons of the guardian of the genome. *Cancer research* 60, 6788-6793.

Streisinger, G., Walker, C., Dower, N., Knauber, D., and Singer, F. (1981). Production of clones of homozygous diploid zebra fish (*Brachydanio rerio*). *Nature* 291, 293-296.

Takai, H., Naka, K., Okada, Y., Watanabe, M., Harada, N., Saito, S., Anderson, C.W., Appella, E., Nakanishi, M., Suzuki, H., *et al.* (2002). Chk2-deficient mice exhibit radioresistance and defective p53-mediated transcription. *The EMBO journal* 21, 5195-5205.

Terzian, T., Suh, Y.A., Iwakuma, T., Post, S.M., Neumann, M., Lang, G.A., Van Pelt, C.S., and Lozano, G. (2008). The inherent instability of mutant p53 is alleviated by Mdm2 or p16INK4a loss. *Genes & development* 22, 1337-1344.

Toledo, F., Krummel, K.A., Lee, C.J., Liu, C.W., Rodewald, L.W., Tang, M., and Wahl, G.M. (2006). A mouse p53 mutant lacking the proline-rich domain rescues Mdm4 deficiency and provides insight into the Mdm2-Mdm4-p53 regulatory network. *Cancer cell* 9, 273-285.

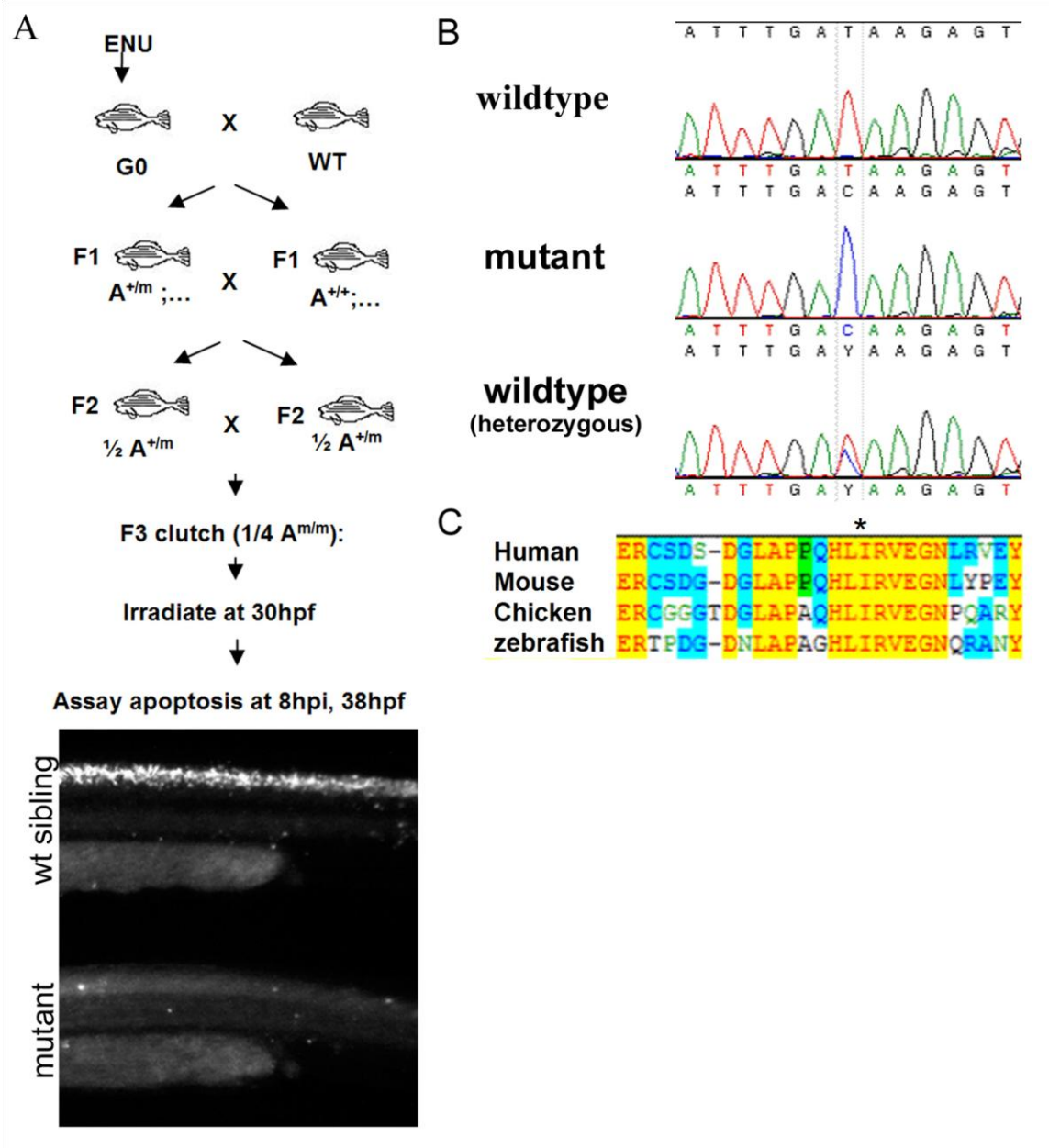
Turner, D.L., and Weintraub, H. (1994). Expression of achaete-scute homolog 3 in *Xenopus* embryos converts ectodermal cells to a neural fate. *Genes & development* 8, 1434-1447.

Varley, J.M. (2003). Germline TP53 mutations and Li-Fraumeni syndrome. *Human mutation* 21, 313-320.

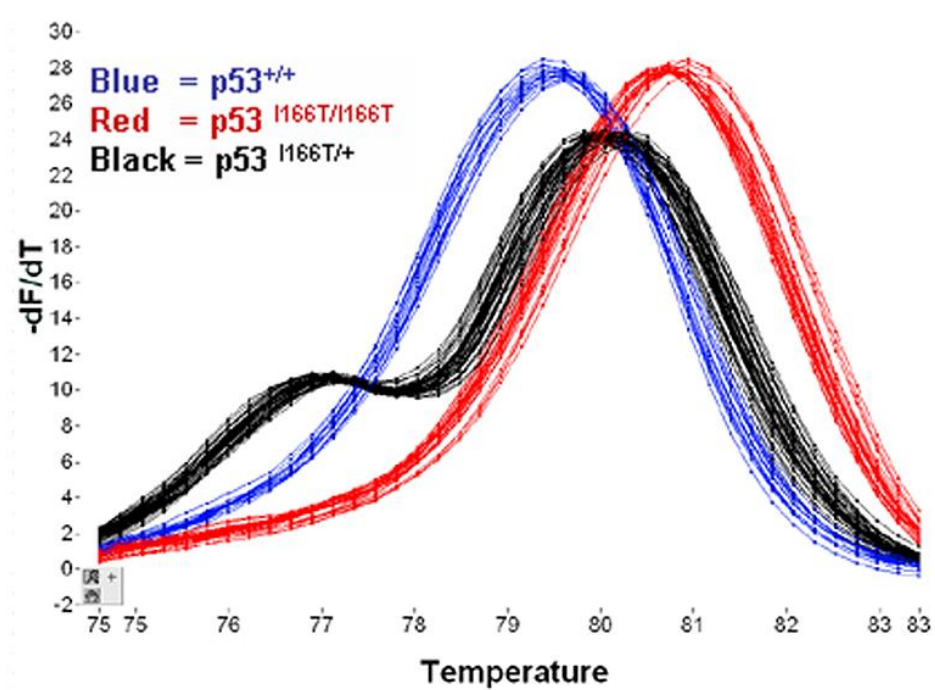
Westerfield, M. (1995). *The Zebrafish Book* (University of Oregon Press, Eugene, OR).

Zhou, L., Wang, L., Palais, R., Pryor, R., and Wittwer, C.T. (2005). High-resolution DNA melting analysis for simultaneous mutation scanning and genotyping in solution. *Clinical chemistry* 51, 1770-1777.

Figure 2.1: Identification of the p53 I166T mutation. (A) F3 screen for LFS mutants. Males were treated with ENU mutagen (G0) and bred to generate F1 fish, each of which is genetically unique and heterozygous for many mutations. To propagate heterozygotes, F1's were intercrossed to generate F2 fish which are also heterozygous for a particular mutation. F2's were intercrossed to generate F3 offspring, one-quarter of which are homozygous for a particular mutation. These F3 clutches were irradiated at 30hpf and scored for Acridine orange (AO) staining (50ug/ml) 8hpi. Approximately 1800 F3 clutches from 300 F2 (F1 x F1) families were screened, yielding a family in which one quarter of the embryos (33 of 130) embryos displayed resistance to IR-induced apoptosis. (B) Sequence analyses of genomic PCR products of two WT and one mutant embryo from F2 heterozygous crosses. Mutants were homozygous for a thymine to cytosine transition in codon 166. (C) Amino acid sequence comparison of the human, mouse, chicken, and zebrafish around codon 166 in zebrafish (codon 195 in human; * marks the mutated Ile codon). (D) Melting curve analysis of PCR products from p53^{+/+} (blue), p53^{I166T/+} (black) and p53^{I166T/I166T} (red) embryos.



D



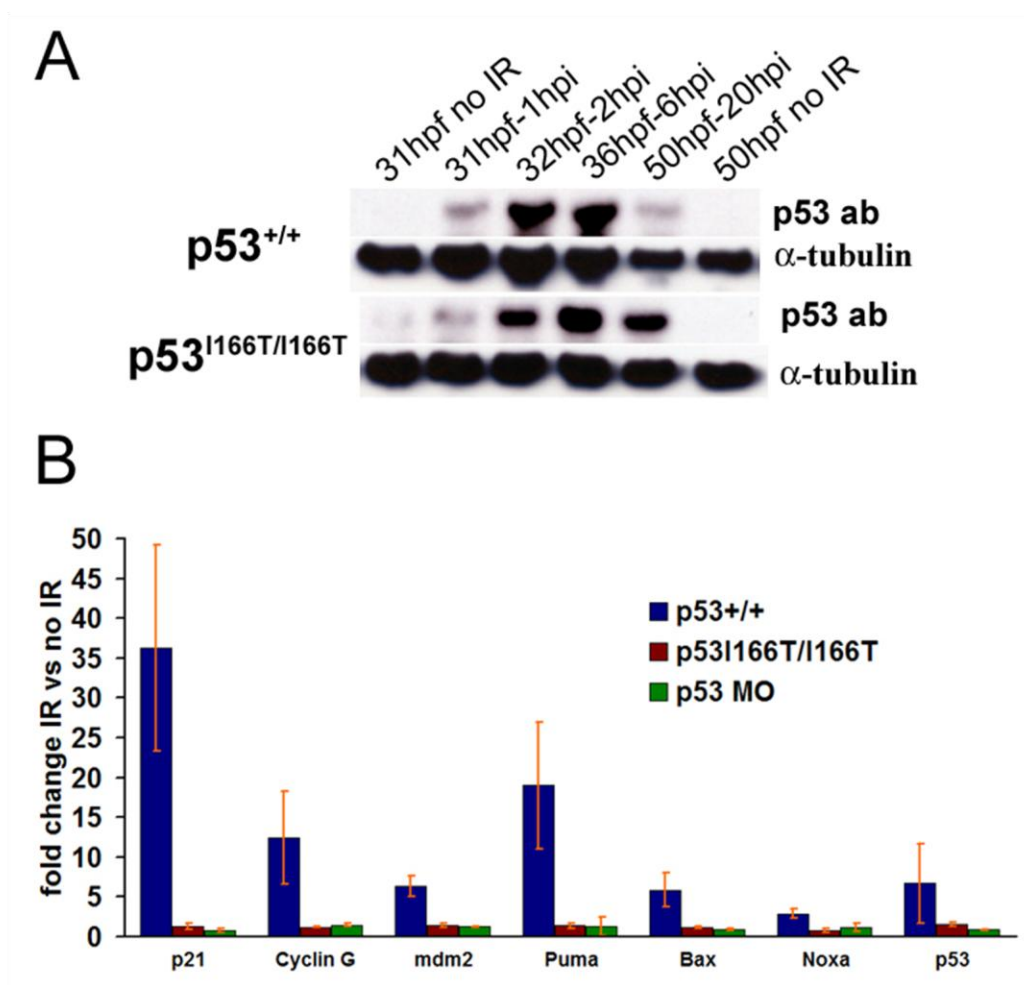


Figure 2.2: (A) Western blots of protein extracts from WT and p53^{I166T/I166T} mutant embryos collected 1, 2, 6, and 20 hours following 0Gy (mock irradiation) or 30Gy irradiation at 30hpf. Blots were probed with p53 ab and α -tubulin ab. Note p53^{+/+} 50hpf 20hpi is under-loaded. (B) Real time RT-PCR assays for p21, Cyclin G, mdm2, p53, Puma, Noxa and Bax were performed in triplicate on WT, p53^{I166T/I166T}, and p53 MO injected embryos. Fold induction reflects the comparison between IR-induced and no IR matched samples. Error bars are standard deviation.

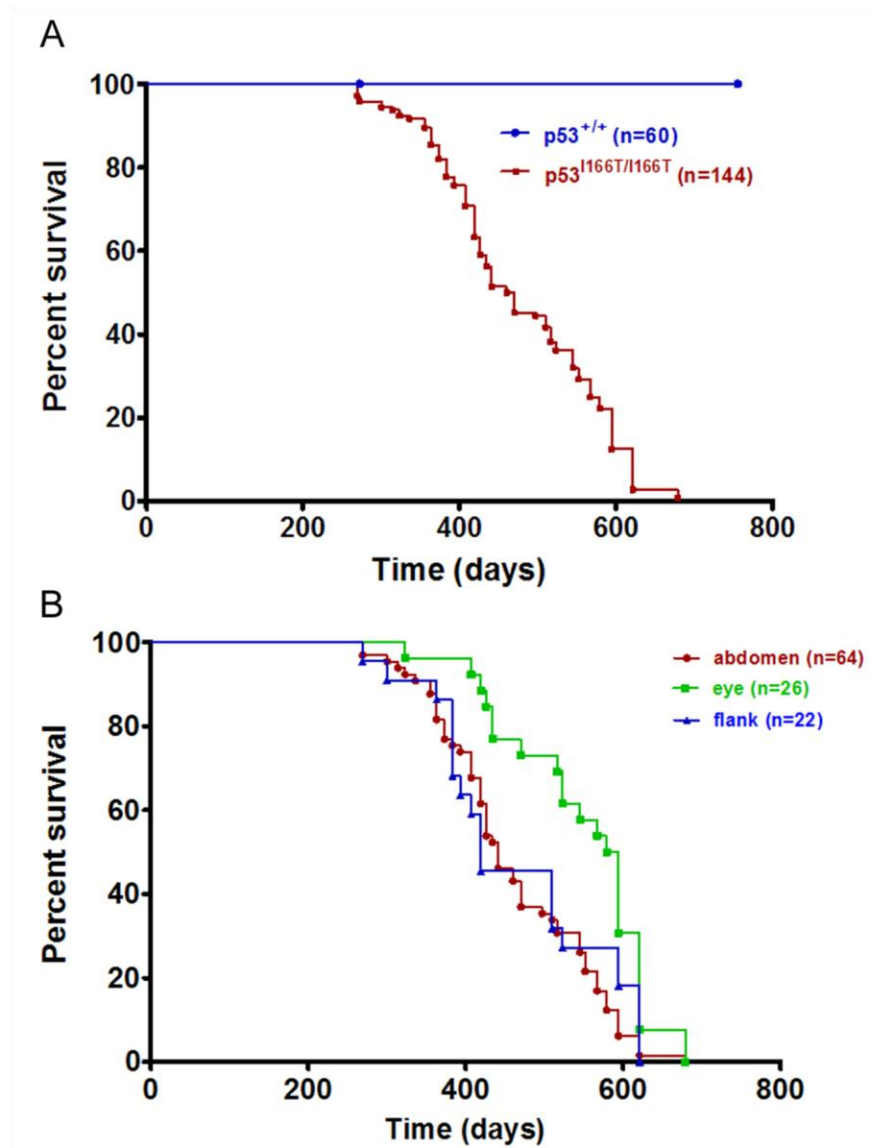


Figure 2.3: $p53^{I166T/I166T}$ survival curves. (A) Using Kaplan Meier analysis $p53^{I166T/I166T}$ (n=144) adult fish had significantly ($p < 0.0001$) increased tumor incidence compared to $p53^{+/+}$ (n=60). The first tumor was identified at 269 days (8.8 months) of age, and the last tumors were identified at 679 days (22.3 months) with 50% incidence at 465 days (15.2 months). (B) Tumors predominantly occurred in the abdomen, eye, or flank. There was a significant difference between the later onset of eye tumor development ($p < 0.0086$) versus flank or abdomen. (C) Population density influenced tumor formation in $p53^{I166T/I166T}$ fish. Blue triangles are the original cohort described above (n=144), green squares are the high density cohort separated at 2 months age into 30 fish per 3 liter tank (n=60), and red circles are the low density cohort separated at 2 months of age into 10 fish per 3 liter tank (n=90). The original cohort and the high density cohort did not have a significant difference. However, the low density cohort was significantly different ($p < 0.0001$) than either the original or high density cohort curves. Tumor initiation was 269, 271, and 224 days and 50% incidence was 465, 485, and 305 days, respectively.

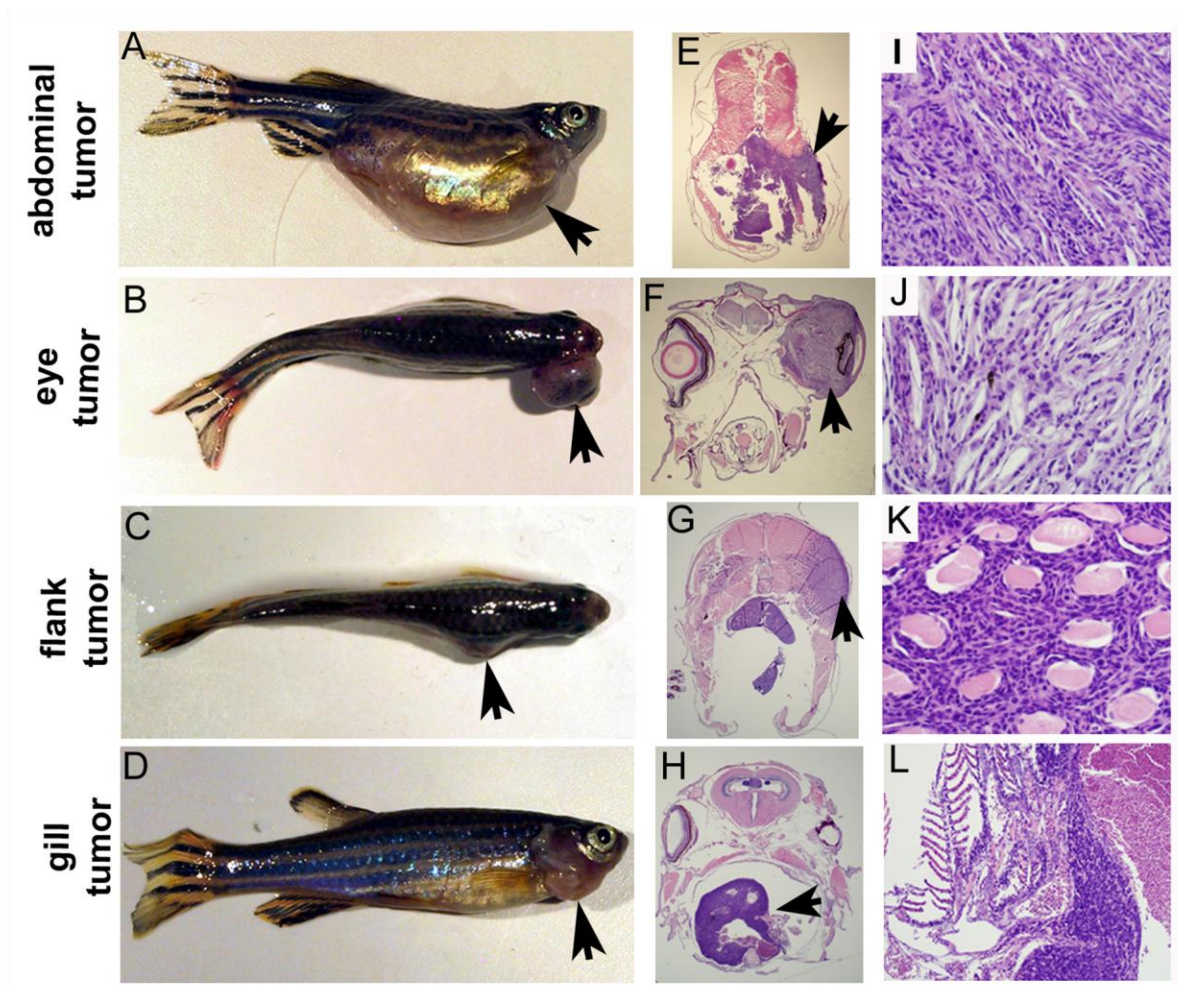
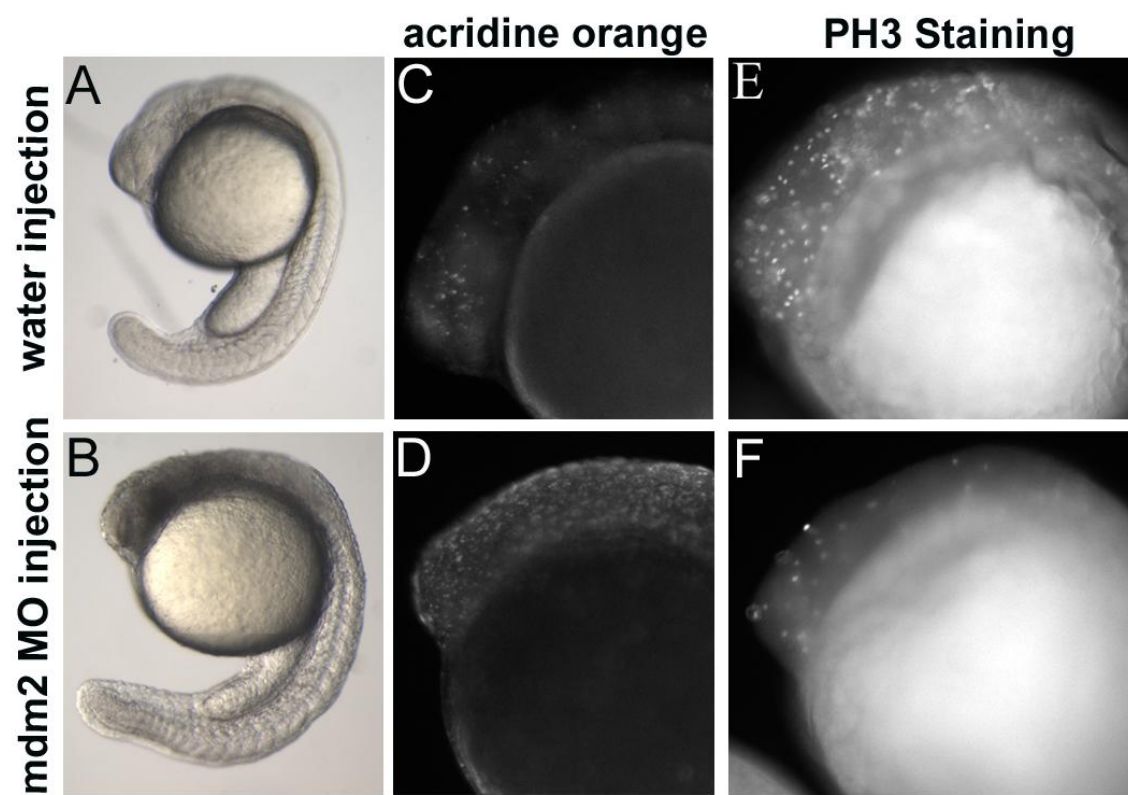
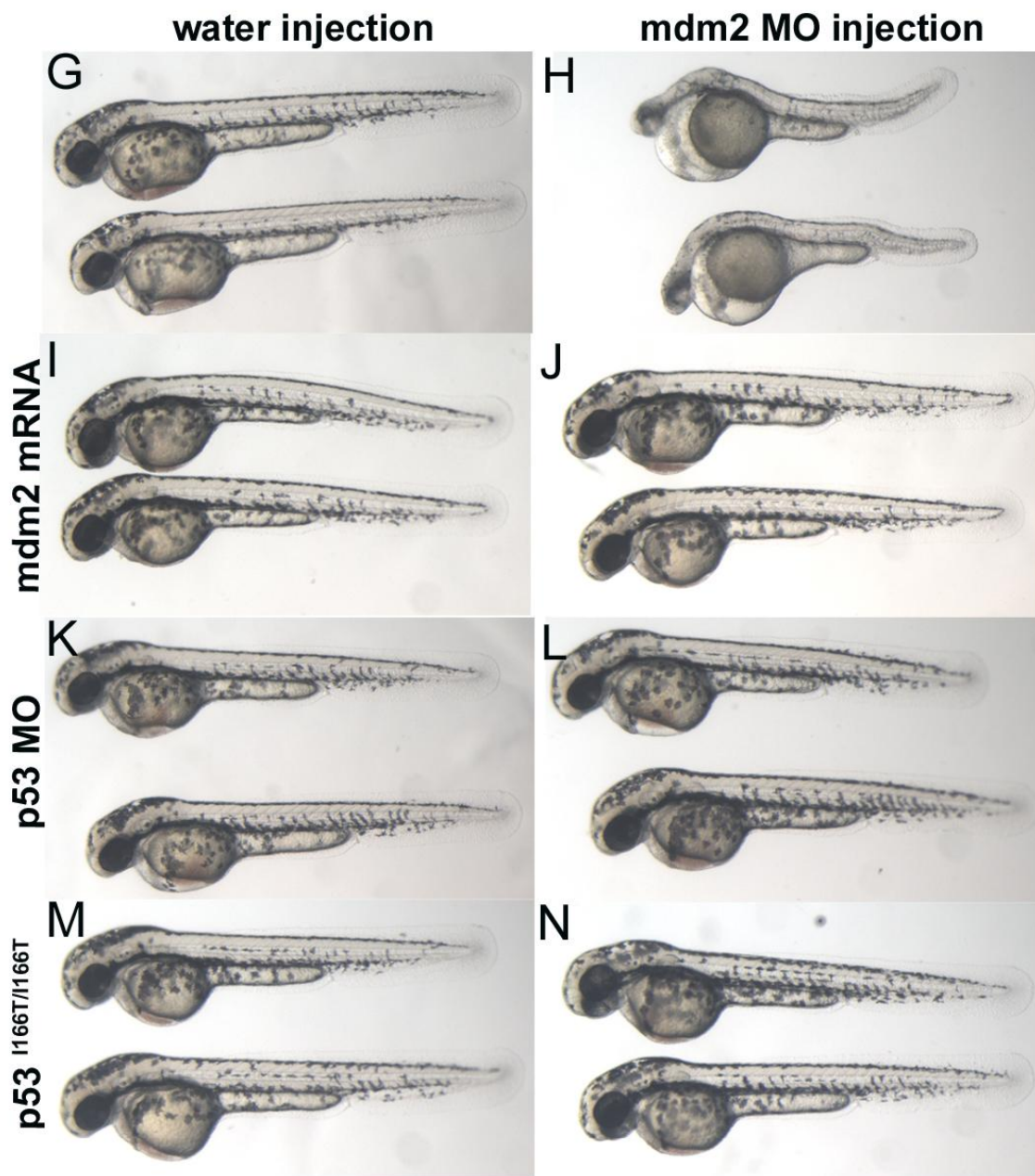


Figure 2.4: Gross and histological analysis of tumors. $p53^{I166T/I166T}$ fish with (A) abdominal, (B) eye, (C) flank and (D) gill tumors. Sections stained with H&E of tumors at low magnification and high magnification, respectively, of (E, I) abdominal, (F, J) eye, (G, K) flank and (H, L) gill tumors. Histologically, 7 of 9 abdominal tumors, 10 of 10 eye tumors, 7 of 7 flank, and 2 of 2 gill tumors (in total, 27 of 29 tumors) were spindle cell sarcomas.

Figure 2.5: p53^{166T/+} heterozygotes develop tumors and display loss of heterozygosity (LOH). (A) p53^{166T/+} fish show a significant increase ($p < 0.0006$) in tumor incidence compared to p53^{+/+} cohorts. By 23 months, 33 of 190 p53^{166T/+} fish had developed tumors. (B) Sequence analysis of PCR products from 7 of 8 matched tumor and normal (tail) genomic DNA samples. A compound red and blue trace indicates heterozygosity in normal genomic samples and a trace with blue only indicates LOH detected only in tumor tissue samples.

Figure 2.6: mdm2 knockdown embryonic lethality is rescued in p53 morphants and p53^{I166T/I166T} mutants. (A, C, E) Embryos injected with water or (B, D, F) with mdm2 MO were assessed at 26hpf by (A, B) Transmitted-light microscopy, (C, D) acridine orange staining for apoptotic cells and (E, F) phospho-Histone H3 (PH3) specific antibody staining (C, D). Mdm2 morphants displayed (B) embryonic lethality, likely due to both (D) increased apoptosis and (F) decreased cell cycling. With mock (water) injections as controls (G, I, K, M), mdm2 morpholino injections (H) yield a readily discernable lethal phenotype at 50hpf. (J) As a control for non-specific morpholino effects, co-injection of 150 pg mdm2 mRNA rescues the mdm2 MO phenotype. (L) Co-injection of p53 MO rescues mdm2 MO lethality, indicating that loss of p53 function abrogates loss of mdm2 phenotype. (N) Injection of mdm2 MO into p53^{I166T/I166T} embryos did not yield the mdm2 lethal phenotype, indicating that the p53 mutant has loss-of-function similar to p53 MO. (O) p53 protein levels were assessed using anti-p53 antibody (ZFp53-9.1) on western blots of extracts from p53^{+/+} and p53^{I166T/I166T} embryos that were un-irradiated (no IR), irradiated with 30Gy (IR), or injected with mdm2 MO (M2 MO). Extracts of wild-type embryos injected with p53 MO injected embryos are shown as controls for antibody specificity.





O

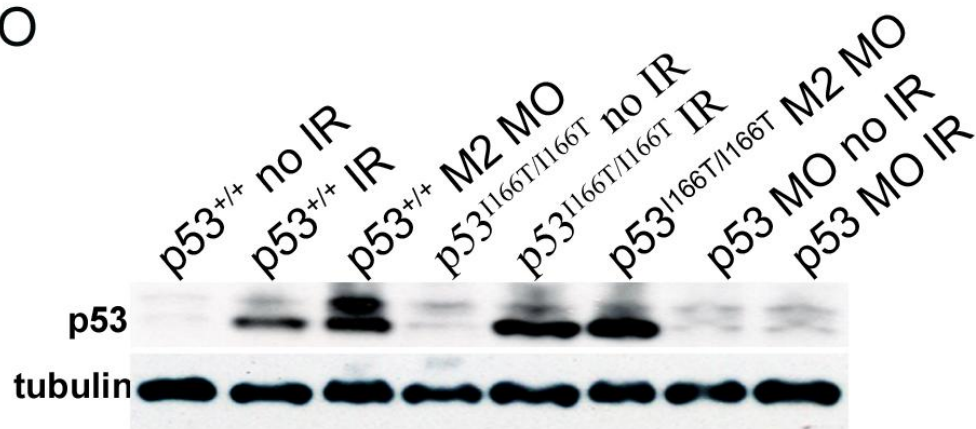
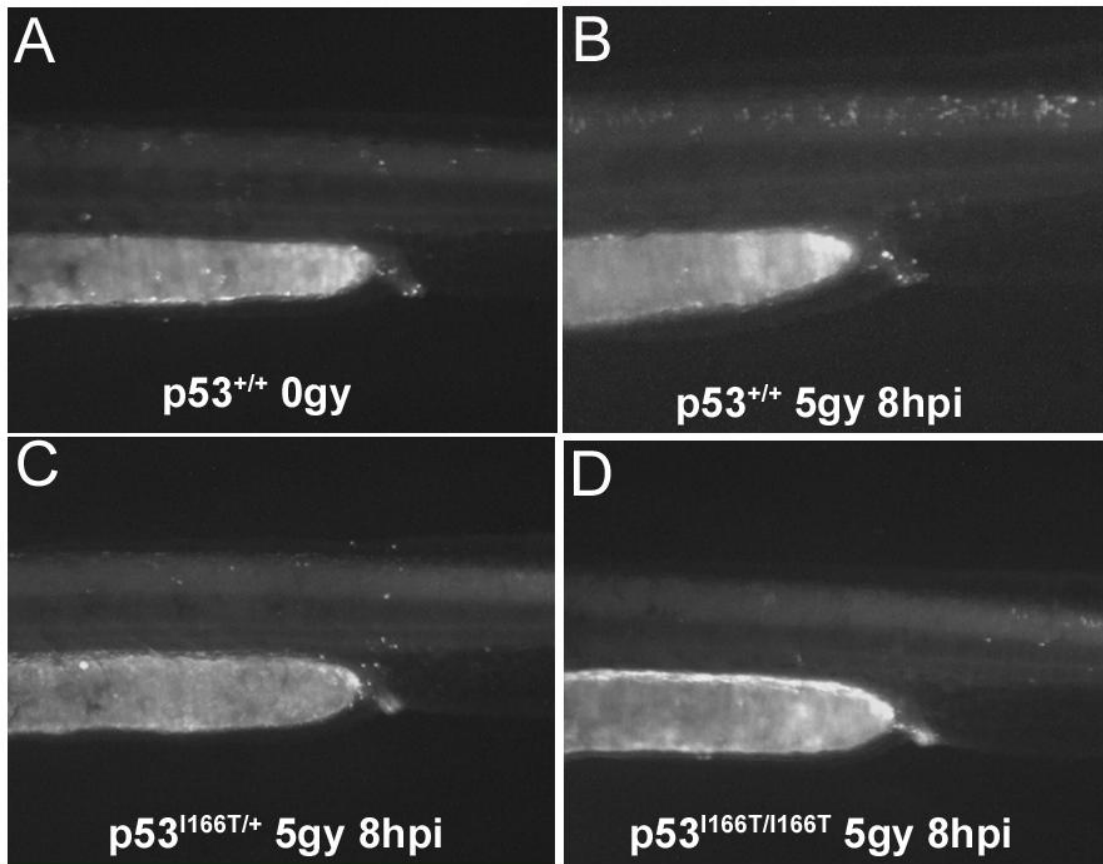
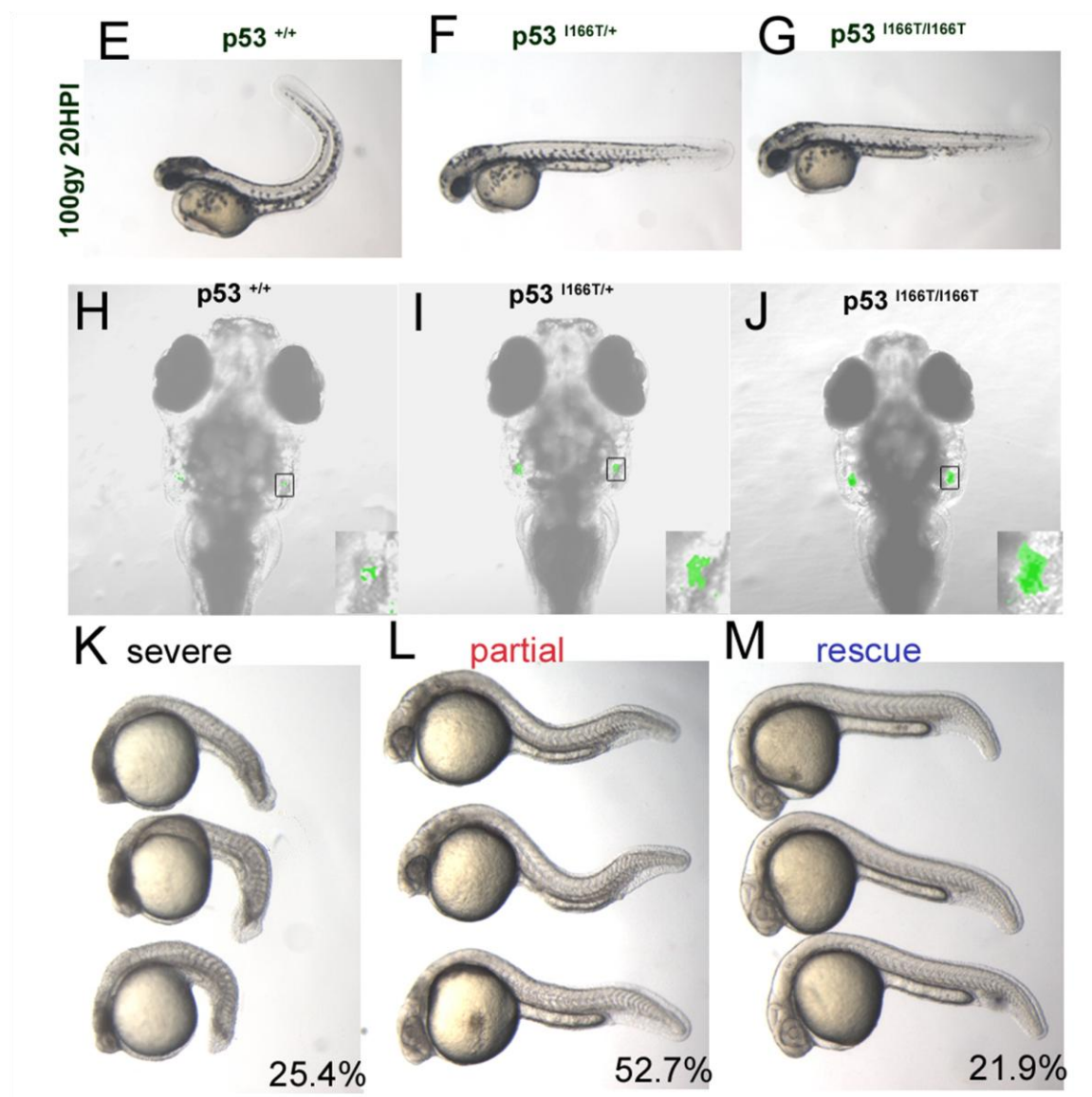
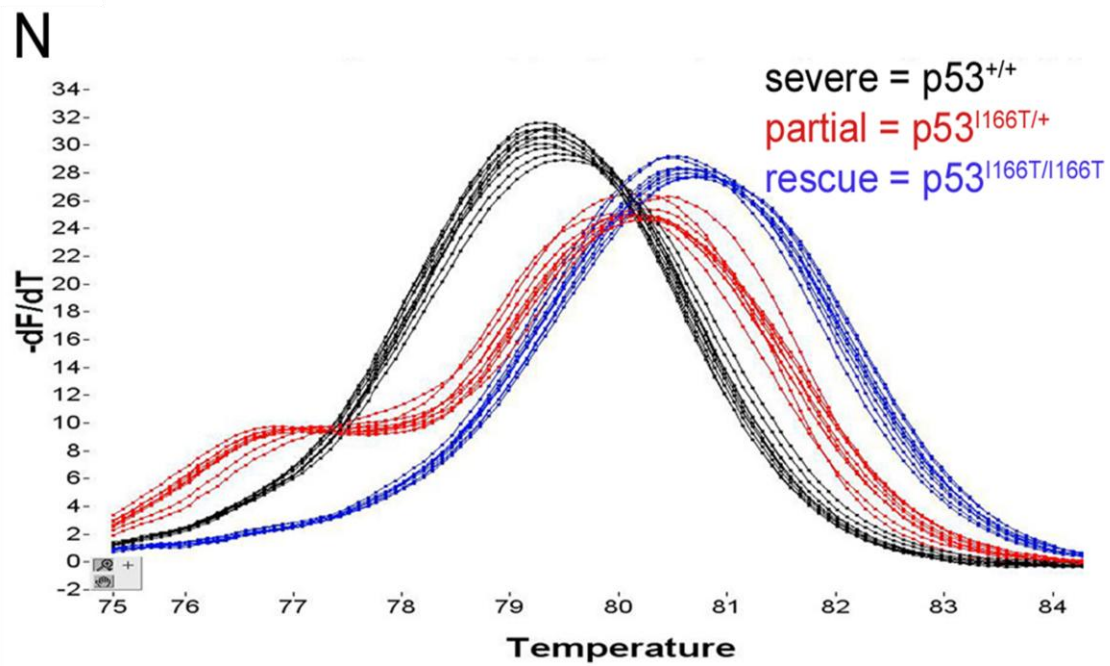


Figure 2.7: p53^{I166T/+} dominant negative phenotypes. (A) Neural tube in the trunk and tail of non-irradiated p53^{+/+} embryos have a low level of apoptosis, detected with acridine orange. (B) Apoptosis is increased in embryos 8 hours post 5Gy IR. In contrast, (C) p53^{I166T/+} and (D) p53^{I166T/I166T} did not display increased apoptosis at 8 hours post 5Gy IR. (E) Wildtype embryos have a curled tail phenotype at 20 hours post 100Gy IR, whereas both (F) p53^{I166T/+} and (G) p53^{I166T/I166T} did not display a curled tail phenotype. (H-J) Confocal analysis of EGFP expression at 9dpf in p53^{+/+}; Lck-EGFP/+ (l), p53^{I166T/+}; Lck-EGFP/+ (m), and p53^{I166T/I166T}; Lck-EGFP/+ (n) fish at 1 day post 30Gy IR. Insets are higher magnification of EGFP expression. As another test for DN phenotypes, embryos from a p53^{I166T/+} intercross were injected with mdm2 MO, and sorted by phenotype at 24 hpf: (K) 25.4% had a severe lethal phenotype, (L) 52.7% had a partially rescued phenotype, and (M) 21.9% had a rescued phenotype. (N) Melting curve analysis of PCR products from individual genomic DNA samples from embryos with severe (black), partial (red) and rescued (blue) phenotypes, which corresponded respectively with p53^{+/+}, p53^{I166T/+} and p53^{I166T/I166T} genotypes.







Supplemental Experimental Procedures

Northern Blot Analysis of p53 Target Genes

Total RNA was obtained from pools of approximately 30 zebrafish embryos using Trizol reagent (Invitrogen). Zebrafish p21 and Cyclin G were cloned by RT-PCR (Ambion) of irradiated embryos (30gy 6hpi), using primers p21 cDNA f1:atggcggcgcaacaagc with p21 cDNA r1: cactagacgcttcttggc, and cyclin G cDNA f1:ccaccatgattgaccaggtgacc with Cyclin G cDNA r1:tcttaacaagcatattcagg. Gadd45 was a gift from Dr. Majors. Probes were random labeled with γ -p³²-dCTP using primer-it II random primer kit (Stratagene). Northern blots and hybridization were performed as per instruction of NorthernMax[®]-Gly Kit (Ambion). Fifteen ug of total RNA were loaded per lane.

Supplemental Results

Conservation of the p53 Transcriptional Targets

We asked whether components of the p53-response pathway, including p21, Cyclin G, Gadd45, and Mdm2 are induced by irradiation. Northern blot analysis of total RNA collected 6hpi from 36hpf embryos treated with 100Gy indicated that all of these target genes were indeed induced (Supplemental Figure 2.1A). Embryos injected with the p53 MO were refractory to this induction, indicating these target genes are bona fide targets of the p53 pathway in zebrafish (Supplemental Figure 2.1A). The induction kinetics of p53 target genes with a low dose of 10Gy (Supplemental Figure 2.1B) or a high dose of 100Gy (Supplemental Figure 2.1C) were assayed. At either dose, p53 target genes

were induced within 2 hours, with higher induction levels in the 100Gy samples, and maintained through 24hpi. To determine the optimal dose for transcriptional induction, analysis was performed on embryos 36hpf and 6hpi at different doses (Supplemental Figure 2.1D). For p21 and mdm2, significant induction was detected at 20Gy, however maximal induction was at 60Gy.

p53-dependent Apoptosis in Zebrafish Embryos

Apoptosis is one of the key mechanisms by which p53 prevents cancer. *In-vivo* studies in the mouse have shown that p53 null embryos are deficient in irradiation-induced apoptosis in neural tissues (Lee et al., 2001). To determine whether similar apoptosis occurs in zebrafish, we irradiated embryos and then used Acridine Orange (AO) to stain apoptotic cells. Initially embryos were treated with 100 gray (Gy) of IR at 30 hours postfertilization (hpf), and strong apoptotic staining was found in the neural tube (NT) 6 hours postirradiation (hpi). Doses of irradiation and time post-IR were optimized for apoptosis detection. Very little apoptosis was seen in untreated embryos at 32, 36 and 50hpf (analogous to 2hpi, 6hpi and 20hpi; Supplemental Figure 2.2A-C) and at 2hpi in embryos treated with 5, 30 or 100Gy irradiation (Supplemental Figure 2.2 A,D,G, or J). 5Gy produced low levels of apoptosis at 6 and 20hpi (Supplemental Figure 2.2E, F). In contrast, 30 and 100Gy produced very strong AO staining at 6hpi that persists through 20hpi (Supplemental Figure 2.2H,I,K,L). Interestingly, a curled up tail phenotype was observed in 100% (n=50) of embryos treated with 100Gy (Supplemental Figure 2.2L inset) and 32% (n=50) of embryos treated with 30Gy (Supplemental Figure 2.2I inset).

To determine whether apoptosis in the NT and the curled tail phenotype are p53-dependent, a p53 splice-blocking morpholino oligonucleotide (MO) was utilized. RT-PCR and western blot analyses revealed the p53 MO effectively knocked down wildtype (WT) p53 mRNA (data not shown) and protein levels (Figure 2.2O). p53 MO-injected embryos irradiated at 30hpf with 30Gy or 100Gy were stained with AO at 6hpi, or scored for curly tail phenotype at 20hpi. Both phenotypes were rescued in p53 MO-injected embryos (Supplemental Figure 2.3E, H). In mammalian tissue culture, p53-dependent apoptosis can be inhibited by overexpression of Bcl2 (Cadwell and Zambetti, 2001). To test whether p53-dependent apoptosis can be inhibited by Bcl2 overexpression in zebrafish, embryos were injected with Bcl2 mRNA at 1-2 cell stage, and then treated with 30Gy or 100Gy IR at 30hpf. Unirradiated injected embryos had no gross morphological phenotypes (Supplemental Figure 2.3C), indicating that Bcl2 overexpression does not cause development defects. Embryos injected with Bcl2 mRNA were resistant to apoptosis normally induced by 30Gy (Supplemental Figure 2.3F), and the curly tail phenotype invariably induced by 100Gy (Supplemental Figure 2.3I). This demonstrates that the curly tail phenotype is a useful indicator of IR-induced p53-dependent apoptosis.

Differential Melting Curve Analysis to Genotype Zebrafish Mutants

Genotyping missense mutations are often difficult to do in a fast, efficient and inexpensive manner. Using a novel PCR-based genotyping technique of differential melting curve analysis, previously used to scan human samples for mutations in specific disease genes (Zhou et al., 2005), we have been able to

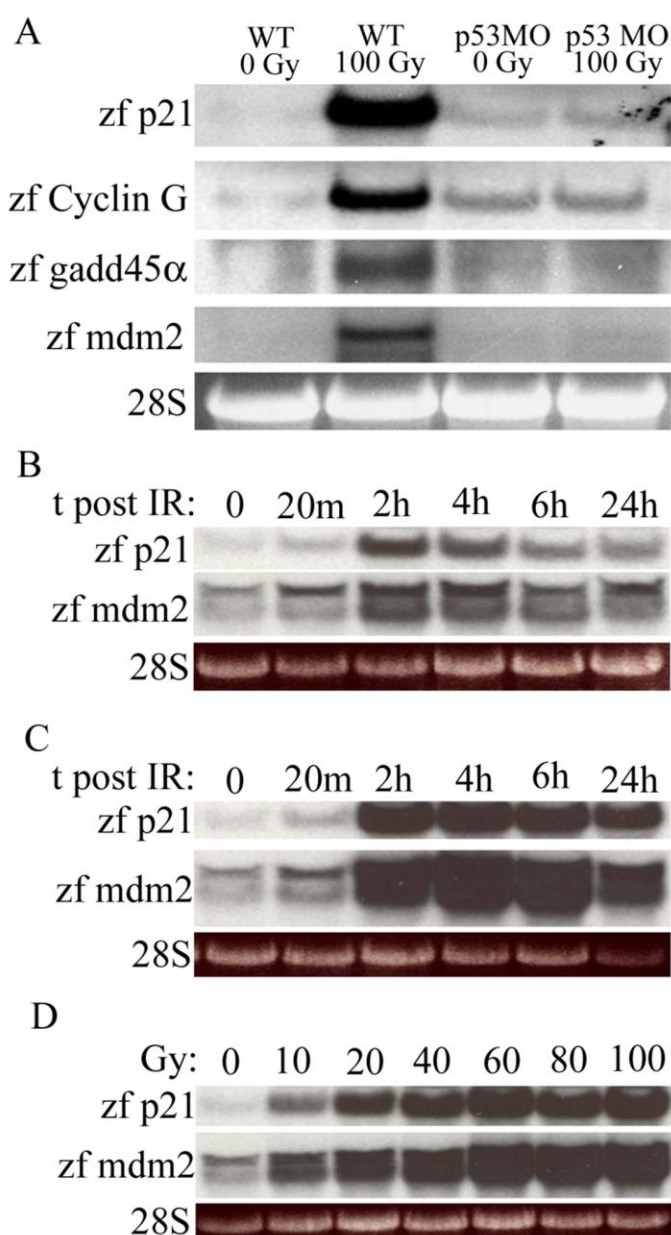
efficiently genotype embryos and adult mutant fish. The PCR is designed to generate a small amplicon (~40bp) surrounding the point mutation. The T to C transition mutation in p53^{L166T} results in a 1-2°C difference in the melting temperature (T_m) of the mutant and WT PCR products that can be resolved by fluorescent melting curve analysis (Figure 2.1D). Importantly, heterozygous fish can also be identified because the products from the two alleles resolve at two peaks (Figure 2.1D). Sequencing confirmed the predicted genotyping in 24 of 24 samples.

Supplemental References

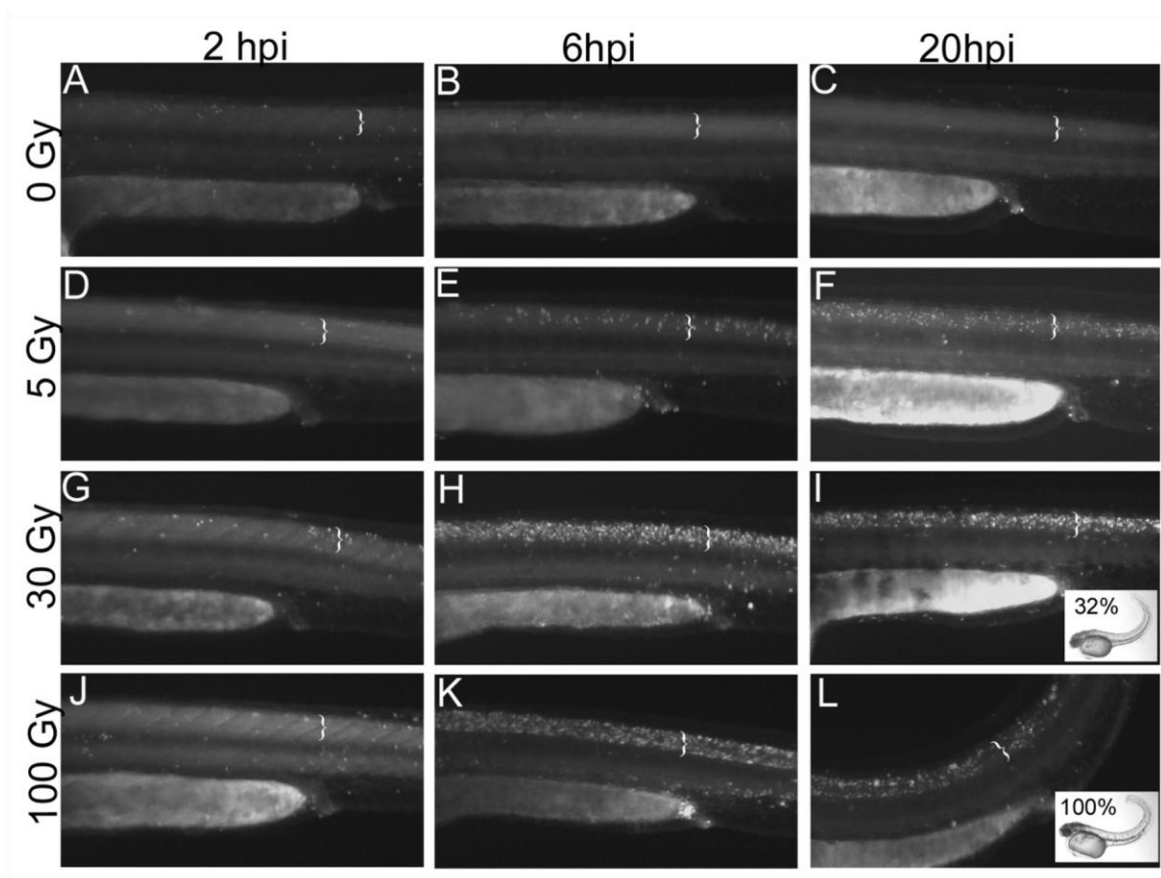
Cadwell, C., and Zambetti, G.P. (2001). The effects of wild-type p53 tumor suppressor activity and mutant p53 gain-of-function on cell growth. *Gene* 277, 15-30.

Lee, Y., Chong, M.J., and McKinnon, P.J. (2001). Ataxia telangiectasia mutated-dependent apoptosis after genotoxic stress in the developing nervous system is determined by cellular differentiation status. *J Neurosci* 21, 6687-6693.

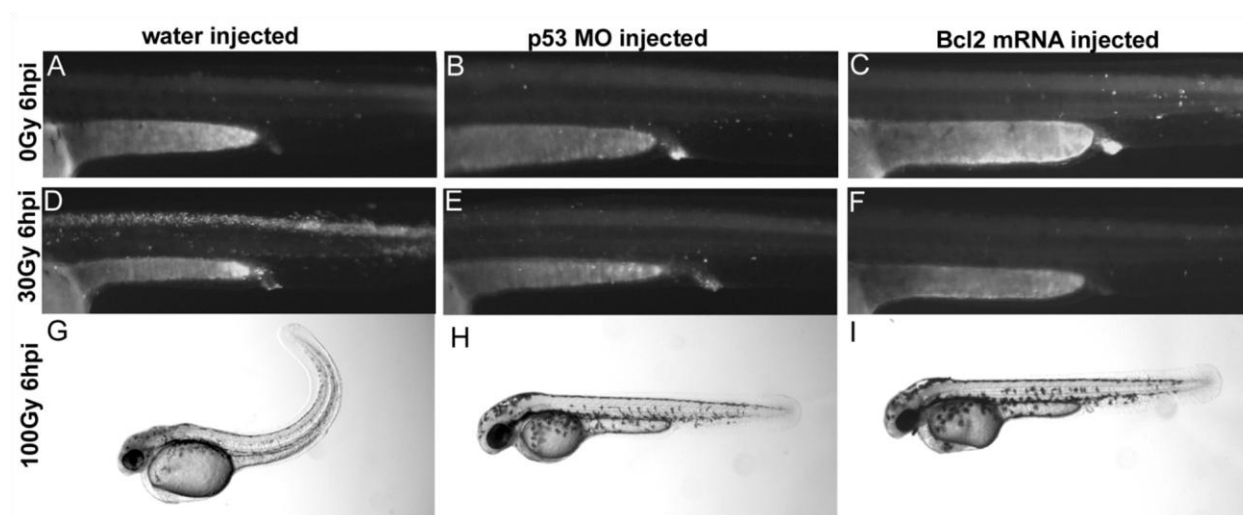
Zhou, L., Wang, L., Palais, R., Pryor, R., and Wittwer, C.T. (2005). High-resolution DNA melting analysis for simultaneous mutation scanning and genotyping in solution. *Clinical chemistry* 51, 1770-1777.



Supplemental Figure 2.1: Induction of p53 target genes. Northern blot of total RNA extracted from either irradiated or unirradiated embryos. 15ug of total RNA was loaded in each case and blots were normalized to 28s band. (A) Irradiated embryos were treated with 100 Gy of gamma irradiation, and total RNA was extracted 6 hours later. To determine whether the inductions are p53 dependent, we injected a p53 morpholino that inhibits p53 production. Unirradiated embryos were collected at the same time as the irradiated. Northern blot were probed with ³²P-labeled cDNA probes to zebrafish p21, zebrafish cyclin G, zebrafish gadd45A, and zebrafish mdm2. (B) Embryos were treated at 30hpf with 0, 10, 20, 40, 60, 80, and 100 Gy gamma irradiation, total RNA was extracted 6 hours later and northern blots were probed with p21, and mdm2 ³²P-labeled probes. Embryos were treated with 10 (C) or 100Gy (D) of gamma irradiation. Embryos were then collected 0, 0.33, 2, 4, 6, and 24 hours postirradiation, processed for total RNA, and northern blots were probed with p21 and mdm2 ³²P-labeled probes.



Supplemental Figure 2.2: IR induced apoptosis in zebrafish embryos. Embryos were treated with 0Gy (A-C), 5Gy (D-F), 30Gy (G-I), or 100Gy (J-L) IR at 30hpf. Embryos were stained with AO and photographed at 2 (A,D,G,J), 6 (B,E,H,K), and 20 (C,F,I,L) hpi. White brackets mark the neural tube. Insets (I,L) show the curled tail phenotype observed at 30Gy and 100Gy at 20hpi.



Supplemental Figure 2.3: rescue of IR induced apoptosis by p53 knockdown or bcl2 overexpression. WT (A,D,G), p53 MO (cccttgcgaaacttacatcaaactct) injected (B,E,H) and Bcl2 mRNA injected (C,F,I) embryos were treated with 0Gy (A,B,C), 30Gy (D,E,F), or 100Gy (G,H,I) IR at 30hpf. 6hpi embryos were stained with AO and photographed (A-F). Transmitted light images were taken of 100Gy-treated embryos 20 hpi (G-I).

CHAPTER 3

A RAPID AND EFFICIENT METHOD OF GENOTYPING ZEBRAFISH MUTANTS

Abstract

In order to facilitate high throughput genotyping of zebrafish, we have developed a novel technique that uses High Resolution Melting Analysis (HRMA) to genotype heterozygous and homozygous mutants. This one hour technique removes the need for restriction enzymes and agarose gels, while maintaining the ability to ensure the PCR reactions amplify the desired products through melting curve profiles. We have been able to reliably genotype a wide variety of mutations including two zebrafish point mutants (APC^{mcr} and $P53^{I166T}$), as well as a small deletion mutant ($BAP28^{y75}$) and a retroviral insertion mutant ($WDR43^{hi821}$). Although we apply this technique to zebrafish mutants, the same technique can be applied other model organisms.

Introduction

Zebrafish as a genetic model organism is coming of age. Considering the relative ease of maintaining large numbers of mutant lines, and large numbers of fish within each mutant line, genotyping on a large scale necessitates the need for efficient and high throughput genotyping techniques. Mutant lines of zebrafish result from multiple types of mutations, increasing the complexity of genotyping. ENU mutagenesis, the predominate mutagen used in zebrafish, most often results in a single base changes, although small deletions and insertions do occur (Noveroske et al., 2000). The second most common approach is insertional mutagenesis, using either retroviral insertions (Golling et al., 2002) or transposable element insertions to disrupt genes (Balciunas and Ekker, 2005).

Therefore development of effective ways of genotyping these mutations is necessary.

Faster, more efficient methods of genotyping are always desirable provided they can maintain 100% accuracy. Therefore techniques/protocols designed in a high-throughput manner where time consuming steps are eliminated, are sought after. With the advent of PCR to amplify genomic DNA, classical genotyping techniques involving Southern blots and radioactivity (RFLP and SSCP) have been phased out. Some PCR-based approaches use the fortuitous creation or elimination of a restriction site by the mutation. Most methods, with the exception of outright sequencing, require PCR products to be run on an agarose gel. When hundreds or thousands of individual genotypes are necessary, this task is time consuming and expensive.

PCR-based RFLP (Restriction Fragment Length Polymorphism) is a useful technique only if a mutation either creates or eliminates a specific restriction site. In this assay, PCR primers are designed so the region of interest is amplified. This product is digested with the appropriate restriction enzyme and the digestions are run on an agarose gel. The genotype is determined to be homozygous mutant, heterozygous, and homozygous wildtype depending on the restriction pattern (Botstein et al., 1980).

dCAPS (derived Cleaved Amplified Polymorphic Sequence) is similar to PCR-based RFLP in that restriction digest patterns are used to determine genotype. The difference is one or more mismatches are also introduced into the PCR primer, so that the additional mismatches, together with the mutation,

creates a specific restriction site in the amplified product. Again, the digested PCR reaction is run on an agarose gel and the genotype is determined based on the corresponding restriction digest patterns (Neff et al., 1998). Unfortunately, these techniques are plagued by incomplete digestion that can result in genotyping errors (i.e., homozygous mutants mislabeled as heterozygous). In addition, the restriction enzymes required are often rare and expensive.

ASA (Allele-Specific Amplification) is another PCR-based method. Two different PCR reactions are performed with two different forward primers, one specific to the wild type allele and the other to the mutant. In this case, the 3' terminal nucleotide of one primer corresponds to the point mutation in the wild type, and in the other the 3' position corresponds to the mutant sequence. Technical details of annealing and amplification of such mismatched sequence determine the specificity of this method (Kwok et al., 1990; Newton et al., 1989). Unfortunately this technique is riddled with false positives due to mispriming during PCR.

Retroviral insertion mutations (or insertions of other exogenous DNA sequences such as transposable elements) are typically genotyped with PCR amplification specific to either the retrovirus insertion site or wild type DNA. These reactions can be performed separately, one for the wild type allele and one for the mutant, or they can be multiplexed. However, multiplexing can be difficult due to allele specific differences in amplification kinetics. In this case, a single forward primer is used. Reverse primers are designed such that one will anneal to the DNA specific to the retrovirus, and another will anneal specifically

to wild type DNA. In the multiplex reaction, primers are designed such that the PCR products of the mutant and wild type allele are distinguishable by size on agarose gels. If the reaction works appropriately, homozygous mutants will have only the mutant product visible on a gel, heterozygous animals will have both products, and homozygous wild type animals will have only the wild type product visible. This technique is very accurate, although time-consuming due to long PCR reactions and the need for agarose or other high resolution gels.

If none of the above techniques apply, sequencing of DNA is always an option to genotype animals. In this case, PCR primers are designed to flank the region of interest, and DNA is amplified. These products can be sequenced to reveal genotypes of individual animals. This genotyping method avoids manual agarose gels. Nevertheless, the time and expense of sequencing is a distinct disadvantage.

High resolution melting analysis (HRMA) is a homogeneous method of PCR product analysis that does not require any processing after PCR. Applications include mutation scanning (Reed and Wittwer, 2004), genotyping (Liew et al., 2004), and sequence matching (Zhou et al., 2004). Primarily applied to humans, these techniques have been recently reviewed (Erali et al., 2008; Farrar JS, 2009; Reed et al., 2007; Wittwer, 2009).

We have developed an efficient and accurate method of genotyping zebrafish that detects multiple types of mutations. We demonstrate genotyping for single base pair substitutions, a deletion, and a retroviral insertion in a fast and efficient manner without the need for agarose DNA gels. This method uses

high resolution melting analysis to determine homozygous mutants, heterozygotes, and homozygous wild type fish.

Results

To overcome the drawbacks of present genotyping techniques three main improvements need to occur: 1) remove the need for inefficient and expensive restriction enzymes; 2) remove the need for agarose gels or other post-PCR steps, while maintaining discrimination of nonspecific products; 3) increase the speed at which genotyping is achieved. The use of High Resolution Melting Analysis (HRMA) achieves these three goals.

The theory behind HRMA is the use of a highly sensitive imaging machine (for our experiments we use the LightScanner[®]) that quantifies double stranded DNA over a range of temperatures. Double stranded DNA quantification is achieved through the use of a DNA dependent fluorescent chemical LCGreen[®] Plus. When bound to double stranded DNA light is emitted. As the samples are heated, fluorescence emission is constantly monitored. Once the melting temperature of a specific duplex is reached, a dramatic decrease in fluorescence is detected. Derivative melting curves are obtained and plotted as the negative change of fluorescence per unit time ($-dF/dT$) on the ordinate (y-axis) for each temperature increment on the abscissa (x-axis). Small changes, even single nucleotide polymorphisms, create changes in the melting temperature of a DNA duplex. Here we apply HRMA to genotype two missense mutations, a small deletion and a viral insertional mutant.

This technique requires no restriction enzymes, no agarose gels, and since the PCR products are less than 60 bp, the entire PCR reaction and melting analysis can be done in less than 1 hour. In addition, the specificity of the PCR product can be determined by the conformity of the melting curves, i.e. if there is a contaminant in the PCR reaction, additional peaks will be identified.

Single Nucleotide Polymorphism (SNP) Detection

ENU is commonly used as a mutagen in forward genetics. The most common mutation caused by ENU is a single base pair change (Noveroske et al., 2000), resulting in a single nucleotide polymorphism (SNP) that distinguishes wildtype and mutant alleles. We have identified a p53 mutant zebrafish line via an ENU induced F3 forward genetics screen (Parant et al., 2009). The mutation is a T→C transition that creates I166T in the DNA binding region of the gene. Because the p53 homozygous mutant line is completely viable and has no morphological differences, molecular genotyping of individual zebrafish is necessary. Initially, direct sequencing of the region including the mutation was the only reliable method to identify genotypes. Therefore, we designed primers flanking the mutation site (Figure 3.1A). The entire PCR product is 39 base pairs. In general, the smaller the PCR products are, the larger the T_m difference will be. The single base difference between wild type and mutant DNA duplexes creates approximately a 1.5°C T_m difference between wild type and mutant alleles. To test this, we acquired 48 DNA samples, each representing one embryo from a heterozygous-heterozygous cross. Upon melting the PCR

products, we observe a difference in the melting curve pattern between homozygous wild type and homozygous mutant embryos (Figure 3.1B). Significantly, the parameters of our protocol also allow us to assess heterozygosity. At the end of the PCR program the samples are heated to 95°C and quickly cooled resulting in heteroduplex formation. Therefore, in addition to having an intermediate T_m (~80°C from the wildtype and mutant homoduplexes), heterozygotes have lower T_m products due to the instability of heteroduplexes.

To test this on another missense allele, we designed primers to flank a T→C missense mutation in APC (Hurlstone et al., 2003). The PCR product produces a 53 base pair product that is predicted to have a 1.5°C T_m difference (Figure 3.1C). Forty-eight DNA samples were analyzed, each from one embryo of a heterozygous-heterozygous cross. Again melting curve analysis produced three distinct melting curves (Figure 3.1D). In this case the mutant allele has the cytosine nucleotide and therefore has the higher T_m while the heterozygous sample produces an intermediate homoduplex peak and a separate heteroduplex peak.

The p53 genotypes (12 wildtype: 24 heterozygous: 12 mutant) and APC genotypes (11 wildtype: 25 heterozygotes: 12 mutants) follow the expected Mendelian ratio of 1:2:1. In addition, sequencing of 24 individual samples from p53 crosses and 24 individual samples from APC crosses indicated that the HRMA results were 100% accurate.

Deletion Detection

In addition to SNP detection we wanted to assess whether HRMA would provide genotyping of small deletions in zebrafish. The BAP28 mutant zebrafish line has a five base pair deletion in exon 2 (Azuma et al., 2006). Primers were designed to immediately flank the deletion, resulting in a 46 bp wild type product and a 41 bp mutant product with a 1.6°C T_m difference (Figure 3.2A). Analysis of 48 DNA samples, each representing one embryo from a heterozygous-heterozygous cross produced three distinct melting curves (Figure 3.2B). In this case the smaller mutant homozygote has the lower T_m and the heterozygote appears as an intermediate T_m product and a heteroduplex product. Like the p53 and APC genotyping, the BAP28 genotypes (12 wildtype: 25 heterozygotes: 11 homozygous mutants) follow a Mendelian ratio of 1:2:1, and all 24 individual genotypes were verified by sequencing.

Retroviral Insertion Detection

Insertional mutagenesis in zebrafish has become a common and efficient method of gene disruption (Balciunas and Ekker, 2005; Golling et al., 2002). We wanted to design a method by which HRMA could be used to genotype specific retroviral insertions in zebrafish. The mutant line hi821 (Amsterdam et al., 2004) has a retroviral insertion within the second intron of the gene *wdr43* (Figure 3.3A). Primers were designed to produce a small product with T_m s that distinguished between wildtype and mutant alleles (Figure 3. 3B). The forward primer (in intron 2, 5' of insertion site) binds both mutant and wild type alleles.

The reverse primers are specific to the allele they are amplifying (i.e one in intron 2, 3' of insertion site, and the other near the 5' end of the LTR of the retrovirus) (Figure 3.3A). Therefore, in the homozygous wild type or mutant fish, only one product was amplified with a unique T_m (Figure 3.3C). Although Primers A and B, or A and C² could theoretically amplify a product from the mutant allele, the large size of the product (7+ KB), along with the short elongation time (4 seconds) selected against amplification of such products. In addition, in cases where larger products might be amplified, the T_m of these products would be high and easy to exclude from analysis. In heterozygotes, both products were amplified. These products had vastly different melting temperatures and the three different genotypes were readily detected (Figure 3.3C). Note that an important step in the analysis of insertional mutants is that the PCR reaction is not heated to 95°C at the end of the PCR program, and an additional 72°C elongation step is added to ensure that only homoduplexes are formed. Genotyping of *wdr43* (12 wildtype: 24 heterozygotes : 12 mutants) followed Mendelian inheritance. All 24 genotypes were individually confirmed using PCR primers that amplify the wild type allele (583 bp) and mutant allele (230 bp), followed by agarose gel separation.

Discussion

Three different types of mutations in zebrafish were easily genotyped by high resolution melting analysis (HRMA). The advantages of this method over other techniques are numerous. The time and processing necessary for PCR

and melting is much less than that of other methods. PCR can be performed rapidly and the melting curve analysis is much quicker than running agarose gels. There is no need to utilize rare and expensive restriction enzymes. The efficacy and specificity of PCR with high resolution melting removes the uncertainties of downstream analysis, such as restriction digestion that is prone to error.

HRMA technology could be easily applied to other genomic samples from zebrafish (such as adult tail-clip DNA), and to genomes of other model organisms. Because the sensitivity of melting curve analysis allows detection of single nucleotide differences, whole genes can be scanned to find where mutations reside. Large human genes such as *BRCA1* (van der Stoep et al., 2009) and *CFTR* (Montgomery et al., 2007) are more efficiently analyzed by scanning rather than sequencing. Human (Liew et al., 2004) and plant (McKinney JT, 2009) genotyping and speciation of microorganisms (Cheng et al., 2006) are common applications.

TILLING is a technique used in zebrafish to identify mutations in a specific gene following ENU mutagenesis (Till et al., 2003). This cumbersome technique involves digestion with a rare, heteroduplex specific enzyme, Cel1, to detect mismatched DNA, followed by gel separation and imaging. The protocols are tedious and required equipment prohibitively expensive. Similar to mutation scanning in humans, genes could be scanned using HRMA to achieve a similar outcome with less expense and time than TILLING.

It is also possible to conduct HRMA on different machines, such as the Roche Lightcycler[®] 480 or the Qiagen Rotor-Gene Q. The sensitivity of these machines may not be as high as the Lightscanner, but if the products have sufficiently large T_m differences, they may be viable options. The range of possibilities for which HRMA can be used continues to increase (Vossen et al., 2009). It has become the most efficient method of genotyping animal models in our lab, and its potential for mutation scanning has made it a very valuable technique.

Experimental Procedures

DNA Extraction

Embryos were placed in 96 well plates, embryo water was removed, and 100 μ L of ELB (10 mM TRIS pH 8.3, 50 mM KCl, 0.3% Tween 20, 0.3% NP40, 1 mg/ml Prot K) was added to each well and then incubated at 55°C for 4 hours. The plates were then heated to 95°C for 15 minutes to inactivate the Proteinase K.

PCR and Melting Curve Analysis

PCR was performed in an MJ Research 96 well PCR machine. All reactions were done in black/white 96 well plates (BioRad cat #HSP9665). PCR reaction protocols for SNP detection and small deletion detection were 95°C for 15 seconds, then 40 cycles of 95°C for 2 seconds, 60°C for 2 seconds, and 72°C for 2 seconds. After PCR, the reaction was heated to 95°C for 10 seconds, cooled to 4°C and stored at 4°C. The PCR reaction protocol to detect retroviral

insertions was 95°C for 15 seconds, 35 cycles of 95°C for 2 seconds, 60°C for 2 seconds, and 72°C for 4 seconds, followed by 72°C for 30 seconds, cooling to 4°C and storage at 4°C. PCR was conducted with the following reagents: 1X ExTAQ PCR buffer, 1X dNTPs (250 µM each), 1X LCGreen Plus, 0.5 µM primers, 1 µl of genomic DNA, and 0.25 U ExTAQ in 10 µl reactions. Following the PCR, samples were analyzed for melting curves on a Lightscanner (Idaho Technology) over a 65-95°C range. The temperature was set to increase at 0.1°C/second.

PCR primers

P53 I166T FWD (F3): GCGCCTGCTGGTCA

P53 I166T REV (F4): CTGATTGCCCTCCACTCTT

APC FWD (F29): CCACTAATAATGTTGCAGCTGA

APC REV (F30): GACTGATGATTGGCTCTCAGA

BAP28 FWD (K73): AAAGAGGTCAACAAGAACTG

BAP28 REV (K74): TGAGGAAGAGAGAAATGCTC

WDR43 FWD (K51): ACAAGATTCTTAAGGGATAAAGT

WDR43 REV (K56): GTAAATCATCATTAACATCTATTACC

VIRUS REV (K53): GAGTGATTGACTACCCGTCAG

WDR43 FWD (SG9): CCATCCTCATCTACAGCACACTGA

WDR43 REV (SG112): GGGTTAATGGGACCAACTGA

VIRUS REV (SG22): GTTCCTTGGGAGGGTCTCCTC

References

- Amsterdam, A., Nissen, R.M., Sun, Z., Swindell, E.C., Farrington, S., and Hopkins, N. (2004). Identification of 315 genes essential for early zebrafish development. *Proc Natl Acad Sci U S A* 101, 12792-12797.
- Azuma, M., Toyama, R., Laver, E., and Dawid, I.B. (2006). Perturbation of rRNA synthesis in the *bap28* mutation leads to apoptosis mediated by p53 in the zebrafish central nervous system. *J Biol Chem* 281, 13309-13316.
- Balciunas, D., and Ekker, S.C. (2005). Trapping fish genes with transposons. *Zebrafish* 1, 335-341.
- Botstein, D., White, R.L., Skolnick, M., and Davis, R.W. (1980). Construction of a genetic linkage map in man using restriction fragment length polymorphisms. *Am J Hum Genet* 32, 314-331.
- Cheng, J.C., Huang, C.L., Lin, C.C., Chen, C.C., Chang, Y.C., Chang, S.S., and Tseng, C.P. (2006). Rapid detection and identification of clinically important bacteria by high-resolution melting analysis after broad-range ribosomal RNA real-time PCR. *Clin Chem* 52, 1997-2004.
- Erali, M., Voelkerding, K.V., and Wittwer, C.T. (2008). High resolution melting applications for clinical laboratory medicine. *Exp Mol Pathol* 85, 50-58.
- Farrar JS, R.G., Wittwer CT (2009). High resolution melting curve analysis for molecular diagnostics. In *Molecular Diagnostics*, 2nd ed, A.W. Patrinos GP, ed. (Oxford, Elsevier Ltd).
- Golling, G., Amsterdam, A., Sun, Z., Antonelli, M., Maldonado, E., Chen, W., Burgess, S., Haldi, M., Artzt, K., Farrington, S., *et al.* (2002). Insertional mutagenesis in zebrafish rapidly identifies genes essential for early vertebrate development. *Nat Genet* 31, 135-140.
- Hurlstone, A.F., Haramis, A.P., Wienholds, E., Begthel, H., Korving, J., Van Eeden, F., Cuppen, E., Zivkovic, D., Plasterk, R.H., and Clevers, H. (2003). The Wnt/beta-catenin pathway regulates cardiac valve formation. *Nature* 425, 633-637.
- Kwok, S., Kellogg, D.E., McKinney, N., Spasic, D., Goda, L., Levenson, C., and Sninsky, J.J. (1990). Effects of primer-template mismatches on the polymerase chain reaction: human immunodeficiency virus type 1 model studies. *Nucleic Acids Res* 18, 999-1005.

Liew, M., Pryor, R., Palais, R., Meadows, C., Erali, M., Lyon, E., and Wittwer, C. (2004). Genotyping of single-nucleotide polymorphisms by high-resolution melting of small amplicons. *Clin Chem* 50, 1156-1164.

McKinney JT, N.L., De Koeyer D, Reed GH, Wall M, Palais RA, Jarret RL, Wittwer CT (2009). Mutation scanning and genotyping in plants by high resolution DNA melting. In *The Handbook of Plant Mutagenesis and Mutant Screening*, K.G. Meksem K, ed. (Weinheim, Wiley-VCH).

Montgomery, J., Wittwer, C.T., Kent, J.O., and Zhou, L. (2007). Scanning the cystic fibrosis transmembrane conductance regulator gene using high-resolution DNA melting analysis. *Clin Chem* 53, 1891-1898.

Neff, M.M., Neff, J.D., Chory, J., and Pepper, A.E. (1998). dCAPS, a simple technique for the genetic analysis of single nucleotide polymorphisms: experimental applications in *Arabidopsis thaliana* genetics. *Plant J* 14, 387-392.

Newton, C.R., Graham, A., Heptinstall, L.E., Powell, S.J., Summers, C., Kalsheker, N., Smith, J.C., and Markham, A.F. (1989). Analysis of any point mutation in DNA. The amplification refractory mutation system (ARMS). *Nucleic Acids Res* 17, 2503-2516.

Noveroske, J.K., Weber, J.S., and Justice, M.J. (2000). The mutagenic action of N-ethyl-N-nitrosourea in the mouse. *Mamm Genome* 11, 478-483.

Parant, J.M., George, S.A., J.A., H., and Yost, H.J. (2009). Genetics Modeling of Li-Fraumeni Syndrome in zebrafish. submitted.

Reed, G.H., Kent, J.O., and Wittwer, C.T. (2007). High-resolution DNA melting analysis for simple and efficient molecular diagnostics. *Pharmacogenomics* 8, 597-608.

Reed, G.H., and Wittwer, C.T. (2004). Sensitivity and specificity of single-nucleotide polymorphism scanning by high-resolution melting analysis. *Clin Chem* 50, 1748-1754.

Till, B.J., Reynolds, S.H., Greene, E.A., Codomo, C.A., Enns, L.C., Johnson, J.E., Burtner, C., Odden, A.R., Young, K., Taylor, N.E., *et al.* (2003). Large-scale discovery of induced point mutations with high-throughput TILLING. *Genome Res* 13, 524-530.

van der Stoep, N., van Paridon, C.D., Janssens, T., Krenkova, P., Stambergova, A., Macek, M., Matthijs, G., and Bakker, E. (2009). Diagnostic guidelines for high-resolution melting curve (HRM) analysis: an interlaboratory validation of BRCA1 mutation scanning using the 96-well LightScanner. *Hum Mutat* 30, 899-909.

Vossen, R.H., Aten, E., Roos, A., and den Dunnen, J.T. (2009). High-resolution melting analysis (HRMA): more than just sequence variant screening. *Hum Mutat* 30, 860-866.

Wittwer, C.T. (2009). High-resolution DNA melting analysis: advancements and limitations. *Hum Mutat* 30, 857-859.

Zhou, L., Vandersteen, J., Wang, L., Fuller, T., Taylor, M., Palais, B., and Wittwer, C.T. (2004). High-resolution DNA melting curve analysis to establish HLA genotypic identity. *Tissue Antigens* 64, 156-164.

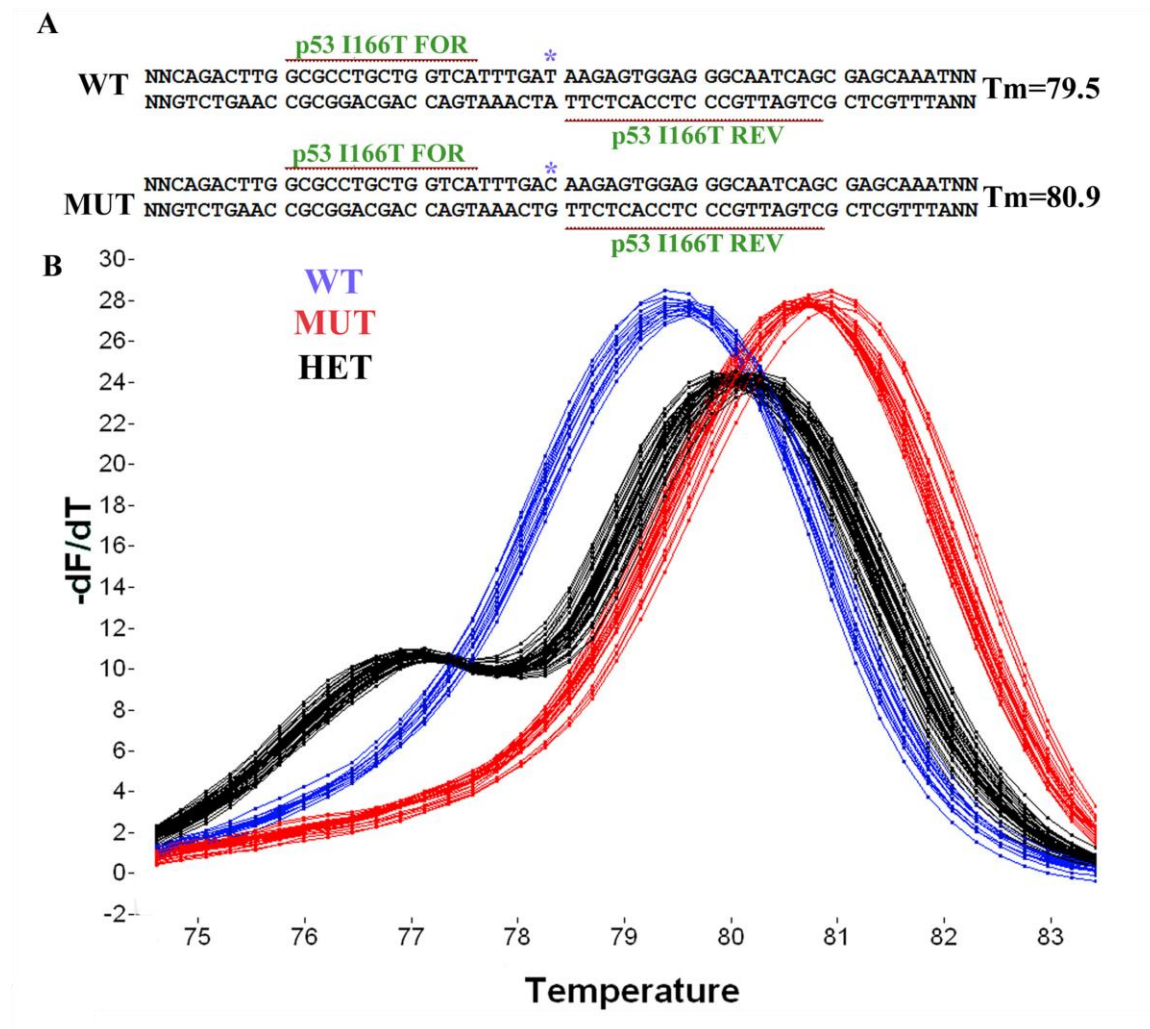


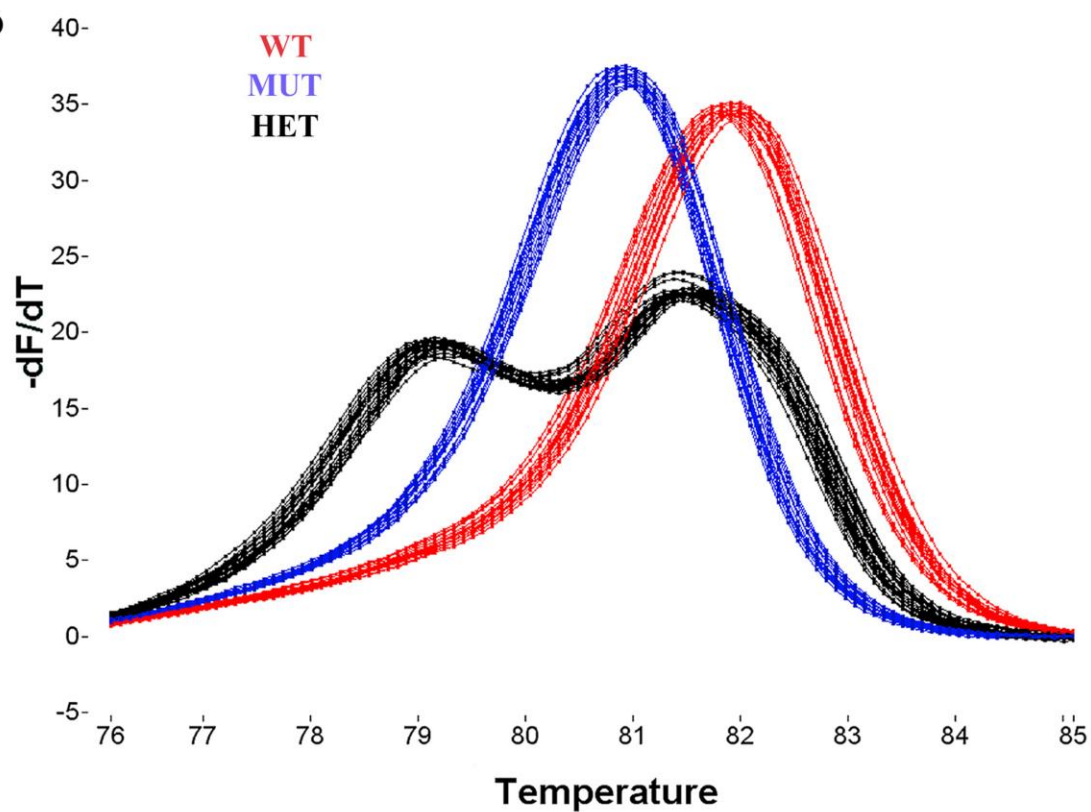
Figure 3.1: Point mutation genotyping of p53^{I166T} and APC^{mcr} by HRMA. (a) The DNA sequence surrounding the p53 I166T missense mutation. Primer sequences are underlined, and the SNP is denoted by an asterisk above the nucleotide. The T_m of the wild type product is 79.5°C and the mutant product, 80.9°C. (b) Melting curves of the PCR products from 48 embryonic DNA samples generated by crossing a p53^{I166T/+} to a p53^{I166T/+} fish. Following clustering analysis the blue curves denote wild type samples, the red curves denote mutant samples, and the black curves denotes heterozygous samples. (c) The DNA sequence surrounding the APC^{mcr} missense mutation. Primer sequences are underlined, and the SNP is denoted by an asterisk above the nucleotide. The T_m of the wild type product is 80.9°C and the mutant product, 82.0°C. (d) Melting curves of the PCR products from 48 embryonic DNA samples generated by crossing a APC^{mcr/+} to a APC^{mcr/+} fish. Following clustering analysis, the red curves denote wild type samples, the blue curves denote mutant samples, and the black curves denote heterozygous samples.

C

WT APC FOR * APC REV **T_m=80.9**
 NNACCACTAA TAATGTTGCA GCTGACCAAC GCACATCTGA GAGCCAATCA TCAGTCCANN
 NNTGGTGATT ATTACAACGT CGACTGGTTG CGTGTAGACT CTCGGTTAGT AGTCAGGTNN

MUT APC FOR * APC REV **T_m=82.0**
 NNTCCACTAA TAATGTTGCA GCTGACTAAC GCACATCTGA GAGCCAATCA TCAGTCCANN
 NNAGGTGATT ATTACAACGT CGACTGATTG CGTGTAGACT CTCGGTTAGT AGTCAGGTNN

D



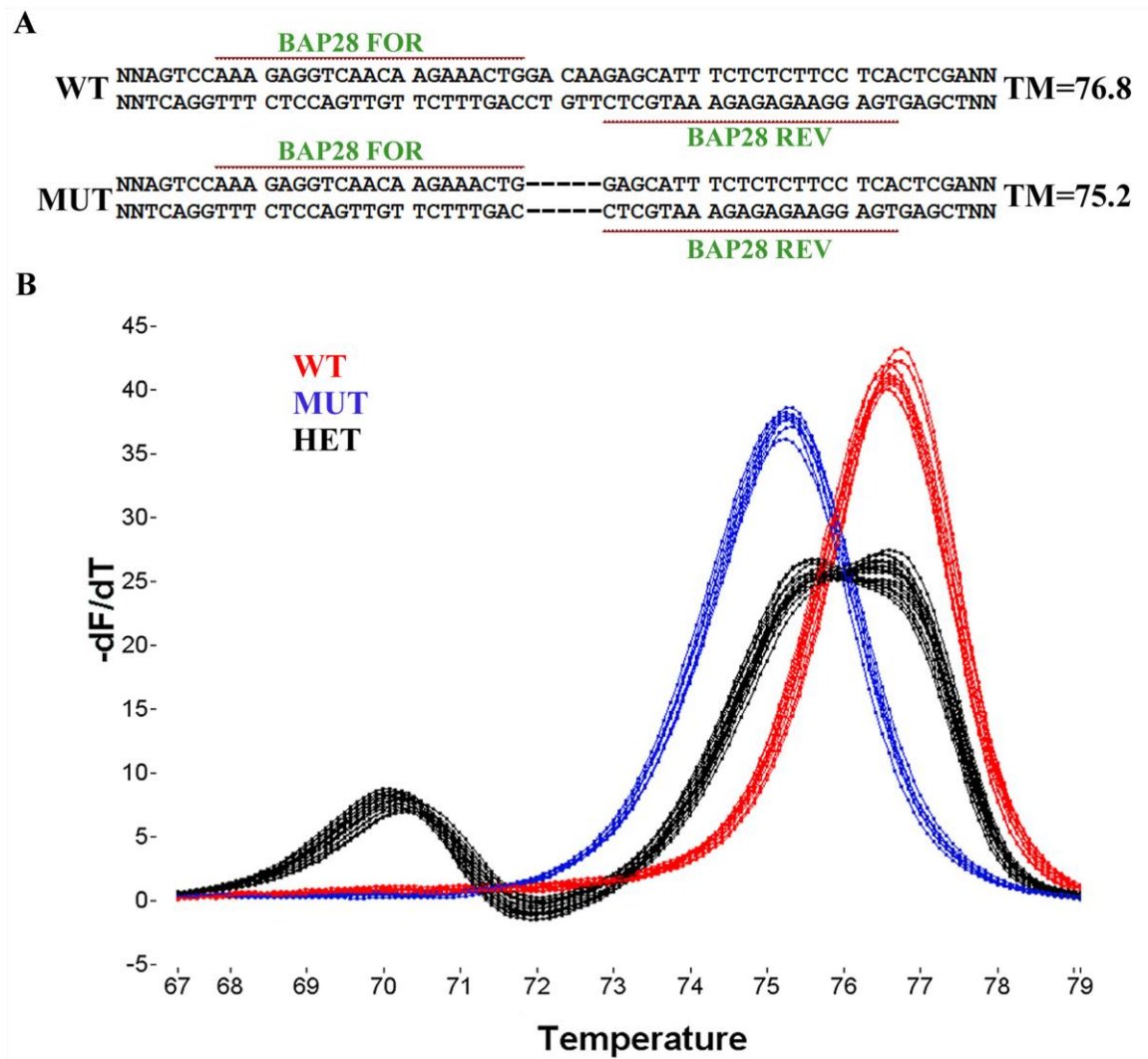


Figure 3.2: Genotyping a small deletion in the BAP28 mutant by melting curve analysis. (a) The DNA sequence surrounding the BAP28 deletion mutation. Primer sequences are underlined, and the deletion is denoted by dashed lines between the nucleotides. The T_m of the wildtype product is 76.8°C and the mutant product is 75.2°C. (b) Melting curves of the PCR products from 48 embryonic DNA samples generated by crossing a BAP28^{y75/+} to a BAP28^{y75/+} fish. Following clustering analysis the red curves denote wildtype samples, the blue curve denotes mutant samples, and the black curve denotes heterozygous samples.

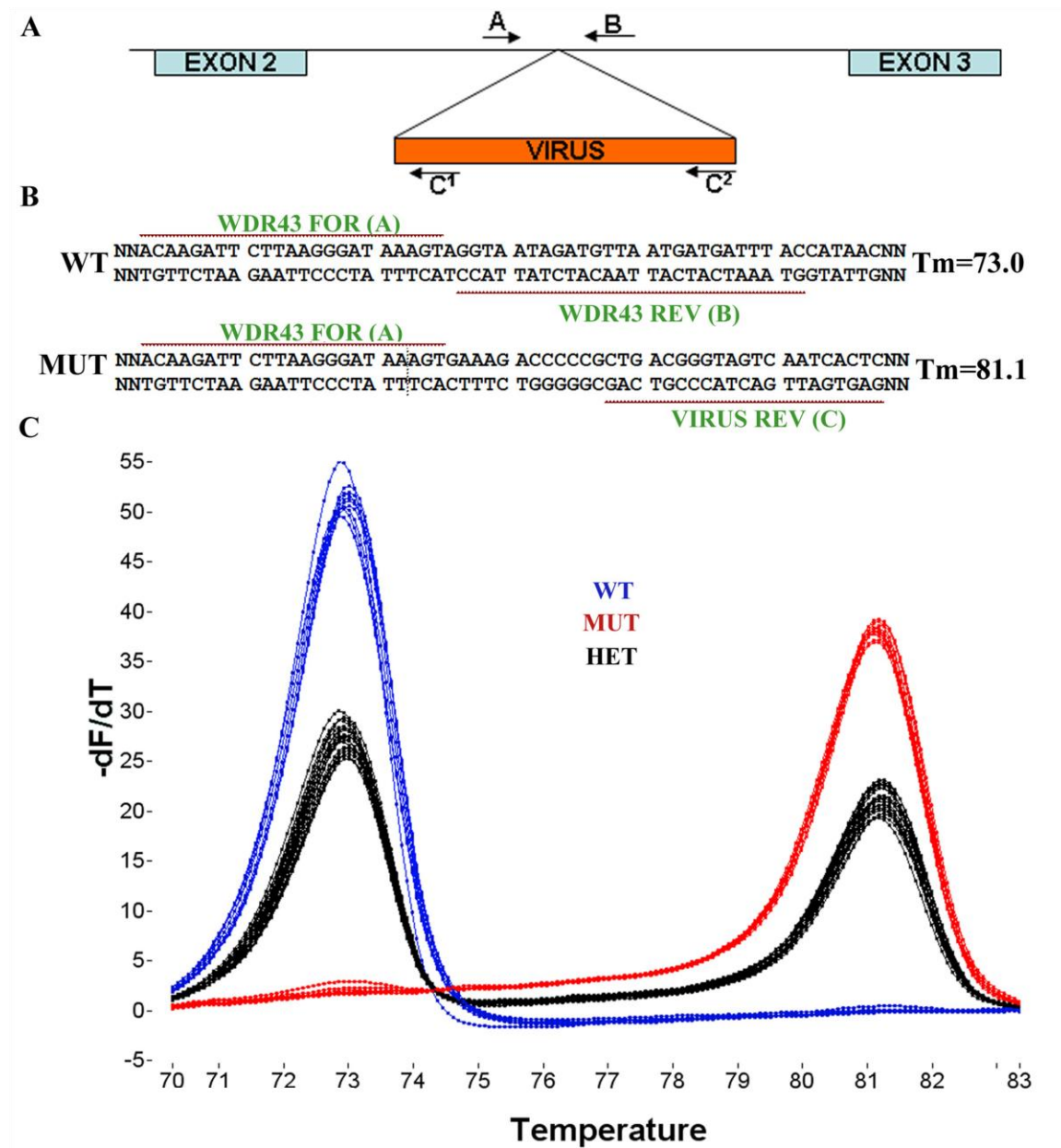


Figure 3.3: Genotyping of the retroviral insertion mutant WDR43 by melting curve analysis. (a) Genomic organization of the WDR43 insertion. (b) The DNA sequence of the wildtype allele and the mutant allele. Primer sequences are underlined. The T_m of the wildtype product is 73.0°C and the mutant product is 81.1°C. (c) Melting curve of the PCR products from 48 embryonic DNA samples generated by crossing a WDR43^{hi821/+} to a WDR43^{hi821/+} fish. Following clustering analysis the blue curves denote wildtype samples, the red curve denotes mutant samples, and the black curve denotes heterozygous samples.

CHAPTER 4

MITOTIC CATASTROPHE AND P53-DEPENDENT APOPTOSIS IN WDR43 MUTANT ZEBRAFISH

Abstract

A novel gene *wdr43* was identified in a zebrafish screen for mutants that have phenotypes indicative of activation of the p53 pathway, and are p53-dependent. *Wdr43* mutants have hyperactivated apoptosis, cell cycle arrest and p53 autoregulatory pathways, and a decrease in S-phase cells within the cell cycle. Strikingly, a subset of cells in *wdr43* mutants undergoes p53-independent mitotic catastrophe, suggesting that chromosomal instability is responsible for the activation of the p53-dependent apoptotic pathway.

Introduction

The power to carry out forward genetics screens in Zebrafish allows rapid identification of novel genes that function in extremely important signal transduction pathways in vertebrates. P53 is a transcription factor whose function is lost in the majority of human cancers. P53 functions as a tumor suppressor and has been touted the “guardian of the genome” for its role in protecting the fidelity of DNA by becoming activated in the presence of DNA damage (Lane, 1992, 1993). Consequently, p53 transcriptionally activates cohorts of genes, whose protein products induce apoptosis and cell cycle arrest in cells in which the genome has been compromised. In addition, a feedback loop in which p53 is post translationally modified also contributes to the activation level of p53, for example phosphorylation by CHK2, or degradation of p53, via ubiquitination by *mdm2* (Castedo et al., 2004; Perona et al., 2008).

DNA damage and the activation of the p53 pathway can be caused by multiple mechanisms, including radiation, genotoxic stresses, errors during DNA

replication and anomalies in mitosis. Each of these leads to different cellular responses in which the damage signal is propagated through different proteins. Maintaining the fidelity of the genome is imperative during each cell cycle of genome replication and during the lifespan of an organism. Failure to do so results in varying degrees of consequences, ranging from unnoticeable silent mutations to fatal disease processes.

Studying the pathways involving DNA damage has revealed a number of genes important to transducing the DNA damage signal. CHK2 is one of the main transducers of the DNA damage signal to p53. It has been shown that CHK2 is capable of phosphorylating p53 in the presence of DNA damage. CHK2 can be activated at multiple points in the cell cycle, G1, S and G2/M, and then is involved in phosphorylating multiple proteins, including p53 that lead to either repair of the damage or apoptosis (Allen et al., 1994; Clarke et al., 1999; Kastan and Bartek, 2004; Weinert et al., 1994).

The extent of DNA damage ranges from small changes in the DNA sequence to large changes to entire chromosomes. The DNA double helix can have one or two strands broken as the result of UV or irradiation. Errors in replication are can be made. If not repaired appropriately, this usually results in changes to the DNA sequence. Large scale changes to chromosomes can be seen when errors in mitosis occur. If the mitotic spindle is not formed correctly, or if checkpoints in mitosis are lost, chromosomal instability can occur. Specific genes in these pathways have been identified and serve as a precedent for finding novel genes that function in similar cellular processes.

ATM (Ataxia-Telangiectasia Mutated) and ATR (Ataxia-Telangiectasia and Rad3 related) are involved in recognizing breaks in the DNA. ATM has specifically been associated with double strand breaks caused by irradiation, for example. Upon recognition of double strand breaks, several proteins are recruited to the foci of damage, including the Mre11/Rad50/Nbs1 complex (Lavin, 2007). Activation of ATM results in the activation of several cell cycle checkpoints. The G1-S and G2-M checkpoints are activated in p53-dependent manner, and results in a decrease of S-phase cells and decreased number of cell entering M-phase, respectively (Kastan and Bartek, 2004; Matsuoka et al., 1998).

Other mechanisms are important to maintaining the fidelity of DNA that are upstream of p53. BRCA1 and DNA ligase IV are two well-studied mutants that are embryonic lethal early, and are rescued, or partially rescued, in a p53 mutant background. BRCA1 is thought to interact indirectly with Rad51 in repairing double strand breaks in the DNA. Deficiency in BRCA1 causes defective DNA repair and defective G2/M cell cycle checkpoints (Deng and Brodie, 2000). Consequently, loss of BRCA1 has been shown to cause increased apoptosis and genomic instability in mice. The degree of rescue is dependent on the mutation in BRCA1 as well as the mutation in p53 (Hakem et al., 1997; McAllister and Wiseman, 2002; Xu et al., 2001). BRCA1 has clearly demonstrated its importance in hereditary breast cancer, as well as ovarian cancer. DNA ligase IV is involved in repairing double strand breaks during the non homologous end joining and homologous recombination. Mice deficient in

DNA Ligase IV exhibit neuronal apoptosis and are also rescued with concurrent deficiency of p53 (Frank et al., 2000; Gao et al., 2000).

The importance of maintaining the fidelity of the DNA throughout mitosis is imperative to cells. Errors in mitosis have been documented ranging from mitotic failure to mitotic catastrophe. The absence of specific genes has been shown to create a DNA damage signal. In fact, the inhibition of genes like ATM, ATR, CHK1, CHK2, Polo like kinase (PLK) 1, PLK2 and PLK3 can induce mitotic catastrophe due to the lack of cell cycle checkpoints (Bunz et al., 1998; Castedo et al., 2004; Chan et al., 1999; Chen et al., 2003). Furthermore, the absence of genes implicated as having a role in the mitotic spindle can lead to mitotic defects. The aurora kinases function in the mitotic spindle and are responsible for phosphorylating specific proteins to initiate phases of mitosis, and are necessary for appropriate spindle formation. In their absence, microtubules do not form appropriately, and chromosomal segregation is impaired. Interestingly, overexpression of both aurora kinases and PLK1 also causes similar mitotic defects, such as tetraploidization and chromosomal aberration. Importantly, this phenotype activates the p53 pathway (Castedo et al., 2004). In a p53 mutant background, this phenotype can persist, suggesting these cells that can continue living with chromosomal instability, and possibly predisposed for tumorigenesis. Evidence that chromosomal instability, due to mutations in mitotic machinery, can lead to tumorigenesis is provided by studies of heterozygous mice deficient in Aurora A, which are predisposed for tumors likely due to high rates of aneuploidy (Cowley et al., 2009; Lu et al., 2008).

Understanding the cell biology of how genome integrity is maintained is imperative to understanding of many disease processes. Because p53 has been touted as such an important player in maintaining genome integrity, we have used it as a center point to search for new genes that, when mutated, cause activation of the p53 pathway and p53-dependent embryonic phenotypes. In this paper, we describe a novel gene which functions in the formation of the mitotic spindle and metaphase plate.

Results

Wdr43 Mutant Recovered from an Embryonic Zebrafish Screen, Rescued by Loss of p53

We conducted a secondary screen on a collection of mutants to find more genes in DNA damage pathways that activate p53. Earlier work in our lab identified p53 dependent phenotypes in zebrafish. These were discovered by inducing DNA damage in fish with gamma-irradiation. Specifically, we saw brain necrosis/apoptosis and a curled tail phenotype. Both of these were rescued with the injection of p53 morpholino (Parant et al., 2009). The Hopkins lab collected approximately 350 embryonic lethal mutant lines (Amsterdam et al., 2004; Golling et al., 2002). Examining the published phenotypes of the mutant collection, we injected a selected number of mutant lines that possibly displayed p53-dependent phenotypes. In a selected number of these mutants, we knocked down p53 via morpholino injection, and scored for rescue of the phenotype (Figure 4.1A). Eleven mutants were recovered from this screen, some of the genes known and well studied. For example, mutants in topoisomerase II and

replication protein A1 genes were rescued by p53 morpholino injection; deficiencies in these genes are known to p53 dependent cell cycle arrest in mammalian studies. These genes provided a proof of principle we were pulling out genes involved in the pathways in which we are interested. This paper will focus on one of the novel genes recovered.

The mutant, *wdr43*, has an embryonic lethal phenotype only as a homozygous mutant. Heterozygous fish show no discernable phenotypes compared to homozygous wild type neither in the embryonic stages nor adulthood. By gross morphology, mutant *wdr43* fish showed brain apoptosis/necrosis visible at 22 to 24 hpf. At 48hpf, mutants were easily discernable from wild type siblings (Figure 4.1B). The head and eyes were smaller, and a tail phenotype was visible at the caudal end. Mutants also have varying degrees of heart edema. To confirm the results of our initial screen, p53 morpholino was injected into *wdr43^{ins/+}* - *wdr43^{ins/+}* crosses. The embryos displayed consistent Mendelian genetics, i.e. 1:2:1, homozygous wild type *wdr43^{+/+}*: heterozygous *wdr43^{ins/+}*: homozygous mutant *wdr43^{ins/ins}*, respectively. P53 morpholino rescued homozygous mutants (N=98/100), with a complete rescue at 48 hpf (Figure 4.1C).

Retroviral insertion could alter not only the function of the gene into which it is inserted, but also alter functions of genes distant from the insertion site. To affirm the fact the phenotypes we have described were due specifically and only to the loss of *wdr43*, we conducted two experiments. First, in order to assess whether other genetic alterations contribute to the mutant phenotype, we tested

whether the mutant phenotype could be rescued by injection of wildtype *wdr43* mRNA. The mutant phenotypes were rescued with the injection of *wdr43* mRNA (Figure 4.1D). Although it was not a complete rescue, the mRNA reduced the curled tail phenotype and brain apoptosis normally visible at 48hpf (Figure 4.1D, N=18/22). Second, to test whether knockdown of *wdr43* conferred the same phenotype as the insertional mutation, we injected morpholino designed to block splicing of *wdr43* transcript. This morpholino was designed so intron 2 would be included in spliced mRNA, introducing a frameshift and a premature stop codon. RT-PCR was conducted on cDNAs from morpholino injected embryos. The wild type product disappeared with increasing amounts of morpholino (Supplemental Figure 4.1). The efficacy of the morpholino was shown by RT-PCR of morphants compared to wild type fish showing the progressive loss of the wild type allele with increasing doses of *wdr43* morpholino (Figure 4.1E).

Because morpholinos sometimes only partially knockdown gene function, we used a genetic approach to confirm whether the *wdr43* phenotype is p53-dependent. A p53 mutant, *p53^{I166T}*, recently derived from a forward genetic screen in our lab, has a mutation in the DNA binding domain of p53, rendering it functionally inactive (Parant et al., 2009). If we injected *wdr43* morpholino into p53 homozygous mutants, we again saw a rescue of the phenotype (Figure 4.1F, N=96/100). Lastly, we bred our *wdr43* mutant into the p53 mutant line, and again, we saw rescue of the phenotype at 48hpf (Figure 4.1G). Although the double mutant rescued many of the early embryonic phenotypes seen in the *wdr43*

mutant, the double mutant was not viable; it died at about 5-6 days post fertilization.

Loss of wdr43 Activates p53 Pathway and Apoptosis

In normal conditions p53 exists at low levels. Insults to the cell that activate the pathway cause p53 transcript levels to increase and a stabilization of the p53 protein. In general, p53 can activate three different pathways: apoptosis, cell cycle arrest, and an autoregulatory loop via mdm2 (Figure 4.2A). As a transcription factor, and in order to activate the three pathways, p53 targets several downstream genes. To assess whether p53 target genes were aberrantly activated in wdr43 mutants, we conducted real time PCR analysis of several downstream genes in the presence and absence of wdr43. The cDNA samples of wild type siblings and mutant were normalized to beta actin. The expression levels in the mutant were divided by those in wild type siblings' samples to give the fold change between the two samples. The apoptotic p53-response genes, bax, puma and noxa, had elevated expression levels of approximately 3- to 6.5-fold. The cell cycle arrest genes, p21 and cyclin G, were upregulated 3- to 4-fold. The p53-regulatory gene mdm2 was up approximately 7.5 fold (Figure 4.2B). Together, these results indicate that wdr43 homozygous mutants have aberrantly activated the expression of cohorts of p53 target genes.

Since the initiation of apoptosis is one of the main roles of p53, we examined apoptosis in developing embryos using a live stain, acridine orange (AO), which differentially stains apoptotic cells with a punctate pattern due to the inability of apoptotic cells to actively pump out the stain. This punctuate pattern

is not to be confused with autofluorescence often visible in an embryo. At 24hpf, an increased level of apoptosis was quite evident in mutant embryos (Figure 4.2C, D, N=100). Apoptosis appeared to be increased throughout the embryo, but is particularly evident throughout the neural tube. The levels of apoptosis in p53;wdr43 double homozygotes were comparable to wildtype levels (Figure 4.2E), indicating that the increased levels of apoptosis seen in wdr43 mutants was p53 dependent.

Genetic Modulation of the p53 Pathway by bcl2 mRNA and CHK2

Morpholino Partially Rescued wdr43 Homozygous Mutants

The results described above provide genetic evidence the wdr43 mutant phenotype is p53-dependent and the p53-dependent pathways were activated in the wdr43 mutant. However, these results do not reveal where wdr43 intersects the p53 pathway. To test whether the wdr43 mutant activates the p53 pathway by activating the arm between p53 and apoptosis, we explored whether the p53 pathway remained responsive to bcl2 mediated inhibition of apoptosis in wdr43 mutants. Bcl2 is a known anti-apoptotic gene capable of intervening in the steps between p53 activation and apoptosis by inhibiting the p53 downstream apoptotic response. Bcl2 was overexpressed by mRNA injection into clutches of embryos from wdr43 heterozygous crosses. Bcl2 mRNA at least partially rescued the mutant phenotype at 48hpf (Figure 4.3 A, B, C, D; N=25/30). The tail of the mutant embryo with bcl2 mRNA did not exhibit the same phenotype as an uninjected mutant. Also, there appeared to be less apoptosis in the head of the mutant embryo. These results indicate that in wdr43 mutants the pathway

between p53 activation and apoptosis is intact and responsive to bcl2 regulation. This suggests that the wdr43-dependent activation of the p53 pathway occurs upstream of the bcl2 modulated step.

In contrast to bcl2, which functions downstream of p53 to modulate apoptosis, CHK2 functions upstream of p53, by phosphorylating p53 in response to DNA damage signals, leading to p53 protein stabilization and activation (Matsuoka et al., 1998; Perona et al., 2008). To test whether CHK2 functions in the same genetic pathway as wdr43, we injected CHK2 morpholino into embryos from wdr43 heterozygote crosses, and examined wdr43 mutant embryo phenotypes. Knockdown of CHK2 partially rescued the wdr43 mutant phenotypes (Figure 4.3 E, F). The mutant tail phenotype was less prominent and there was less apoptosis visible in the neural tissues. These results indicate that wdr43 mutant phenotype is at least partially dependent on the function of CHK2, implicating wdr43 in the transmission of signals for genome instability or DNA damage.

Cell Cycle Analysis Shows Decrease of Cells in S phase in Mutant Embryos

Considering CHK2 can be activated by defects in all parts of the cell cycle, we examined the cell cycle in wdr43 mutants versus wild type siblings. Embryos were homogenized into cell suspensions, stained with propidium iodide and processed in a FACScan machine. Cell cycle was analyzed at the developmental stage at which brain necrosis was grossly visible, at approximately 24hpf, allowing segregation of mutants from siblings (Figure 4.4 A, B). The major

difference in the cell cycle was the amount of cells in S-phase, or during the process of DNA replication, when the cell has between $2n$ and $4n$ DNA content. The mutants had a statistically significant lower number of cells in S-phase. Interpreting cell cycle analysis in whole zebrafish embryos poses a problem. Because whole embryos are homogenized, many cell types are present in the suspension. Therefore, there is a variety of cell sizes present, and perfect peaks in cell cycle, particularly at a young age, are difficult to obtain. Nonetheless, even with the variable background of cells derived from whole embryos in which cell cycles are not synchronized, these data indicate mutants have fewer cells that are resident in S-phase at this stage of development, suggesting the possibility that *wdr43* mutants have a defect in mitosis.

wdr43 Mutants Have Mitotic Spindle Defect

In order to assess whether *wdr43* mutants have a cell cycle defect in mitosis (M-phase) fixed whole embryos in mutants and wild type siblings were stained with an antibody to alpha-tubulin, to reveal microtubules, and with an antibody to phosphorylated histone H3 (pH3). Histone H3 is phosphorylated only during mitosis, and serves as a useful chromatin stain that is indicative of a cell in mitosis. In wild type sibling embryos, normal mitosis generates a well-organized metaphase plate stained with anti-pH3 and a spindle apparatus of microtubules, with two poles (Figure 4.5A; 100%, $N=100/100$). In contrast, *wd43* mutants have defective mitotic figures in approximately 23% of cells stained with pH3 at 24hpf (Figure 4.5B, $N= 46/200$). In these defective mitotic cells, microtubules do not line up as a bipolar metaphase structure and appear to be in extreme disarray.

Similarly, the chromatin in defective cells was not lined up in an orderly metaphase plate. This suggests that wdr43 is involved in ensuring normal mitosis and segregation of replicated DNA. Every mutant embryo examined (N=30) displayed metaphase plate defects; however, as noted, not every mitotic figure appeared to be abnormal at this level of resolution.

If the wdr43-dependent metaphase plate defect is an upstream component of p53 activation in the wdr43 mutant, then it would be predicted to be independent of p53 function. To test this possibility, wdr43; p53 double homozygous mutant embryos were examined, and found to have defective metaphase plates (Figure 4.5C, N= 18/100) similar to those seen in wdr43 mutants.

wdr43 Protein Localizes Around the Mitotic Spindle

In order to further assess the roles of wdr43 in mitosis, we generated a C terminal His-tagged wdr43 protein (His-wdr43). His-Wdr43 mRNA was injected into wild type embryos at the single cell stage. Embryos were collected at 24 hpf and immunohistochemistry was performed to detect microtubule arrays (anti-alpha-tubulin) and the epitope-tagged wdr43 protein (anti-6X-His). Although the staining patterns were sporadic as expected for an ectopic protein expressed by mRNA injection, one reproducible hallmark was the localization of wdr43 near microtubule spindle apparatus in metaphase stage cells (Figure 4.6 A). Uninjected embryos were used as controls for background levels of anti-6X-His antibody immunostaining (Figure 4.6 B). In interphase cells, His-wdr43 appeared to localize to the nucleus of the cell, although the staining pattern was faint (Figure

4.6 C, D). Thus, the wdr43 protein appears to accumulate in cells undergoing mitosis, consistent with the mitotic phenotype seen in wdr43 mutants.

Discussion

Here we describe a zebrafish secondary mutant screen that has uncovered mutants with embryonic lethal phenotypes that are dependent on the p53 pathway. A novel gene, wdr43, is required for normal formation of the mitotic spindle and metaphase chromatin plate. In the absence of wdr43, a subset of cells undergo mitotic catastrophe, and the p53-dependent pathway is activated, resulting in apoptosis and embryonic lethality (Figure 4.7). Partial rescue with the CHK2 morpholino suggests the signal is transduced to p53 via CHK2. Strikingly, mitotic catastrophe in wdr43 mutants is not dependent on the p53-dependent pathway, suggesting mitotic catastrophe is upstream of p53-dependent apoptosis. This explains the reason that p53 morpholino, or a functionally deficient p53 mutant background, rescued the wdr43 mutant phenotype. Also, it explains why wdr43 mutants still die. Mutant p53 does not allow mitotically defective cells to initiate the apoptotic response, explaining why double homozygous mutants live longer and early embryos (24hpf-48hpf) look phenotypically normal.

The p53 pathway can be activated as a result of many cellular mechanisms. The study of DNA damage, mitosis, and autoregulation of p53 has revealed many genes important to the activation and regulation of the pathway. Designing a screen using p53 allows us a unique opportunity to find genes that function in all of these branches of the pathway. Wdr43 appears to function in

the mitotic spindle in dividing cells. In the absence of wdr43, mitotic spindle aberrations occur, and this signal appears to be transduced to p53. This activation of p53 results in large scale apoptosis in the developing embryo.

An interesting trait of this wdr43 mutant is the partial penetrance of the mitotic spindle defect. Although mitotic spindle defects appear in 100% of mutant embryos, only 23% of mitotic cells at 24hpf had spindle aberrations. There are at least three possible explanations for this incomplete penetrance. First, it is striking that wdr43 mutant embryos develop fairly normally during the first days postfertilization, implying that most mitoses must have occurred normally, or at least sufficiently enough to not induce widespread developmental arrest and/or apoptosis. Mutant embryos are derived from crosses of heterozygotes, so it is possible that heterozygous females produce eggs that contain sufficient maternally provided wdr43 mRNA and/or protein to carry homozygous mutant embryos through early development. Thus, the onset of apoptosis at 22-24hpf, particularly in rapidly dividing cells of the developing nervous system, might reflect the stage at which maternal stores of wdr43 mRNA and protein are depleted. However, without a specific anti-wdr43 antibody it is not possible to measure maternal stores of the protein. Second, it is possible that the wdr43 insertional mutant is a hypomorph, not a complete null. Thus, there might be sufficient residual wdr43 protein to provide normal mitosis in most cell cycle. However, our morpholino, which appears to knockdown all of the wild type transcript by RT-PCR, yields the same result. Third, it is possible that wdr43 is necessary for normal spindle formation, only for a subset of cell divisions. For

example, cell contacts with neighbors, the duration of cell cycle, or specific spindle orientations, might make a dividing cell hypersensitive to deficiencies in *wdr43*. In light of these considerations, further studies of *wdr43* and the potential mechanisms by which a mutant generates a small number of metaphase catastrophes and chromosomal aberrations will have interesting disease implications. If these mitotic catastrophes do lead to chromosomal instability, even a small number over a lifetime would increase the propensity for tumorigenesis (Jallepalli and Lengauer, 2001).

Together, these data point to a cellular mechanism that leads to an embryonic lethal phenotype in *wdr43* mutant embryos. Abnormal mitoses are present in mutant embryos. DNA is improperly segregated, leading to a mitotic catastrophe. This DNA damage signals to activate the p53 pathway, which then initiates an aberrant apoptotic response leading to embryonic death.

Wdr43 is upstream of p53 activation. Other genes upstream of p53 have significant roles in cancer. For example, loss of *BRCA1* activates p53, and in mice, loss of *BRCA1* can be rescued in a p53 deficient background. Without *BRCA1*, cells lose the ability to respond appropriately to DNA damage, particularly double strand breaks. Understanding the role of *BRCA1* in hereditary breast cancer has led to prophylactic treatments and improved management of individuals carrying a mutation in this gene.

Genes that function in mitotic spindle formation have also been shown to be important in the study of cancer. Aurora A is localized to the centrosome and Aurora B is localized to the spindle midzone. Together they are responsible to

phosphorylating multiple factors necessary for spindle formation and proceeding through mitosis. Strikingly, Aurora A deficient mice have a mitotic catastrophe that is similar to the wdr43 mutant phenotype that we have described in zebrafish embryos. Aurora A has already been shown to be overexpressed in many cancers. The importance of this regulation suggests that either an overexpression or a deficiency can lead to a tumorigenic state. Further studies are necessary to assess whether the mitotic spindle defect in wdr43 mutants contributes to cancer.

Materials and Methods

Zebrafish Maintenance

Zebrafish (*Danio rerio*) were maintained on an Aquatic Habitat system (Florida, USA). Embryos were collected from natural matings and raised as described (westerfeld, 1995). The AB wildtype strain was used for morpholino oligonucleotides (MO) and mRNA injections.

Injection

Morpholino antisense oligonucleotides (Gene Tools, Oregon) and mRNA synthesized with a mMessage machine SP6 transcription kit (Ambion) were injected into the yolk just under the nuclei of 1- to 2-cell stage embryos in a volume of 0.5 nl. p53 splice-blocking morpholino (p53 MO) overlaps to splice donor site of exon 2 and intron 2 effectively preventing splicing out of intron 2, (5'-cccttgcgaaacttacatcaaattct -3'); Working concentrations of p53 MO was 0.5mM. wdr43 MO overlaps the splice donor site of exon 2 and intron 2, preventing

splicing out of intron 2, (5'- gatttctcaccaatgtacaatgcag-3'). 0.5nL was injected of 2mM stock solution. Capped RNAs were synthesized from these pCR II plasmids using the mMessage machine SP6 transcription kit (Ambion). The working mRNA concentration for Bcl2 was 300 ng/μl, and wdr43 was 200 ng/μl.

Acridine Orange

Apoptosis was assayed by soaking embryos in 50 μg/ml Acridine Orange (Sigma) for 45 min and subsequently destained for 15 minutes. Photographs were taken using a FITC filter.

Light Cycle PCR

Real time RT-PCR was performed on a light cycler PCR machine (Roche). The following primer sets were used: p21 (SG1:tgacatcagcgggttacag and i102:ttctgctgctttcctgaca), Cyclin G (C11:ccaccatgattgaccaggtgacc and C15:agcagcacagaccacac), mdm2 (SG76:ctcgggtgctgttcttgag and SG77:cactgcttctcctcctctg), Bax (SG66:acagggatgctgaagtgacc and SG67:gaaaagcgccacaactcttc), Puma (i97:acgctgtcttccttcagagg and i98:cctgcagaaaattcccagag), Noxa (i91:atggcgaagaaagagcaaac and i92:cgctcccctccattgtat), p53 (SG72:accccggatggagataactt and SG73:cccagcaactgaccttcctgag), and β-actin (SG86:ggatgggacagaaagacag and SG87:agagtccatcacgataccag). Experiments were done in triplicate and normalized to β-actin.

Cell Cycle Analysis

24hpf embryos were homogenized in an eppendorf tube. Cells were washed three times in PBST, and pelleted at 1500 x g for 30 seconds at 4°C. Cells were fixed in 1% paraformaldehyde, washed three more times in PBST and repelleted. -20°C Ethanol was added dropwise to cells, while vortexing, to resuspend, and stored overnight at 4°C. Cells were pelleted, and resuspended in solution of propidium iodide (20µg/ml in PBST).

Immunohistochemistry and Fluorescence Microscopy

For zebrafish immunohistochemistry of the mitotic spindle, embryos were fixed in microtubule stabilization buffer (1X PBS, 3.7% formaldehyde, .25% glutaraldehyde, 1mM MgCl₂, 5mM EGTA, 0.2% Triton X-100) for three hours at room temperature. Embryos were washed in PBST, then dechorionated, and subsequently blocked for 1 hour in PBS containing 10% sheep serum, 1% DMSO. Embryos were incubated in primary antibody including mouse anti-alpha- Tubulin (1:200), rabbit anti-phospho Histone H3 (Santa Cruz, 1:200), and rabbit polyclonal anti-6 His (Covance, 1:100). After washes block solution, embryos were incubated in secondary antibodies, including goat anti-rabbit Alexa Fluor 647 and donkey anti-mouse Alexa Fluor 488. Embryos were cleared and mounted in Slow Fade Reagent (Molecular Probes). Images were acquired using an Olympus Fluoview FV300 laser scanning confocal microscope and assembled using ImageJ (NIH) and Photoshop (Adobe).

References

- Allen, J.B., Zhou, Z., Siede, W., Friedberg, E.C., and Elledge, S.J. (1994). The SAD1/RAD53 protein kinase controls multiple checkpoints and DNA damage-induced transcription in yeast. *Genes Dev* 8, 2401-2415.
- Amsterdam, A., Nissen, R.M., Sun, Z., Swindell, E.C., Farrington, S., and Hopkins, N. (2004). Identification of 315 genes essential for early zebrafish development. *Proc Natl Acad Sci U S A* 101, 12792-12797.
- Bunz, F., Dutriaux, A., Lengauer, C., Waldman, T., Zhou, S., Brown, J.P., Sedivy, J.M., Kinzler, K.W., and Vogelstein, B. (1998). Requirement for p53 and p21 to sustain G2 arrest after DNA damage. *Science* 282, 1497-1501.
- Castedo, M., Perfettini, J.L., Roumier, T., Andreau, K., Medema, R., and Kroemer, G. (2004). Cell death by mitotic catastrophe: a molecular definition. *Oncogene* 23, 2825-2837.
- Chan, T.A., Hermeking, H., Lengauer, C., Kinzler, K.W., and Vogelstein, B. (1999). 14-3-3Sigma is required to prevent mitotic catastrophe after DNA damage. *Nature* 401, 616-620.
- Chen, Z., Xiao, Z., Chen, J., Ng, S.C., Sowin, T., Sham, H., Rosenberg, S., Fesik, S., and Zhang, H. (2003). Human Chk1 expression is dispensable for somatic cell death and critical for sustaining G2 DNA damage checkpoint. *Mol Cancer Ther* 2, 543-548.
- Clarke, D.J., Segal, M., Mondesert, G., and Reed, S.I. (1999). The Pds1 anaphase inhibitor and Mec1 kinase define distinct checkpoints coupling S phase with mitosis in budding yeast. *Curr Biol* 9, 365-368.
- Cowley, D.O., Rivera-Perez, J.A., Schliekelman, M., He, Y.J., Oliver, T.G., Lu, L., O'Quinn, R., Salmon, E.D., Magnuson, T., and Van Dyke, T. (2009). Aurora-A kinase is essential for bipolar spindle formation and early development. *Mol Cell Biol* 29, 1059-1071.
- Deng, C.X., and Brodie, S.G. (2000). Roles of BRCA1 and its interacting proteins. *Bioessays* 22, 728-737.
- Frank, K.M., Sharpless, N.E., Gao, Y., Sekiguchi, J.M., Ferguson, D.O., Zhu, C., Manis, J.P., Horner, J., DePinho, R.A., and Alt, F.W. (2000). DNA ligase IV deficiency in mice leads to defective neurogenesis and embryonic lethality via the p53 pathway. *Mol Cell* 5, 993-1002.
- Gao, Y., Ferguson, D.O., Xie, W., Manis, J.P., Sekiguchi, J., Frank, K.M., Chaudhuri, J., Horner, J., DePinho, R.A., and Alt, F.W. (2000). Interplay of p53

and DNA-repair protein XRCC4 in tumorigenesis, genomic stability and development. *Nature* **404**, 897-900.

Golling, G., Amsterdam, A., Sun, Z., Antonelli, M., Maldonado, E., Chen, W., Burgess, S., Haldi, M., Artzt, K., Farrington, S., *et al.* (2002). Insertional mutagenesis in zebrafish rapidly identifies genes essential for early vertebrate development. *Nat Genet* **31**, 135-140.

Hakem, R., de la Pompa, J.L., Elia, A., Potter, J., and Mak, T.W. (1997). Partial rescue of Brca1 (5-6) early embryonic lethality by p53 or p21 null mutation. *Nat Genet* **16**, 298-302.

Jallepalli, P.V., and Lengauer, C. (2001). Chromosome segregation and cancer: cutting through the mystery. *Nat Rev Cancer* **1**, 109-117.

Kastan, M.B., and Bartek, J. (2004). Cell-cycle checkpoints and cancer. *Nature* **432**, 316-323.

Lane, D.P. (1992). Cancer. p53, guardian of the genome. *Nature* **358**, 15-16.

Lane, D.P. (1993). Cancer. A death in the life of p53. *Nature* **362**, 786-787.

Lavin, M.F. (2007). ATM and the Mre11 complex combine to recognize and signal DNA double-strand breaks. *Oncogene* **26**, 7749-7758.

Lu, L.Y., Wood, J.L., Ye, L., Minter-Dykhouse, K., Saunders, T.L., Yu, X., and Chen, J. (2008). Aurora A is essential for early embryonic development and tumor suppression. *J Biol Chem* **283**, 31785-31790.

Matsuoka, S., Huang, M., and Elledge, S.J. (1998). Linkage of ATM to cell cycle regulation by the Chk2 protein kinase. *Science* **282**, 1893-1897.

McAllister, K.A., and Wiseman, R.W. (2002). Are Trp53 rescue of Brca1 embryonic lethality and Trp53/Brca1 breast cancer association related? *Breast Cancer Res* **4**, 54-57.

Parant, J.M., George, S.A., J.A., H., and Yost, H.J. (2009). Genetics Modeling of Li-Fraumeni Syndrome in zebrafish. submitted.

Perona, R., Moncho-Amor, V., Machado-Pinilla, R., Belda-Iniesta, C., and Sanchez Perez, I. (2008). Role of CHK2 in cancer development. *Clin Transl Oncol* **10**, 538-542.

Weinert, T.A., Kiser, G.L., and Hartwell, L.H. (1994). Mitotic checkpoint genes in budding yeast and the dependence of mitosis on DNA replication and repair. *Genes Dev* **8**, 652-665.

Xu, X., Qiao, W., Linke, S.P., Cao, L., Li, W.M., Furth, P.A., Harris, C.C., and Deng, C.X. (2001). Genetic interactions between tumor suppressors Brca1 and p53 in apoptosis, cell cycle and tumorigenesis. *Nat Genet* 28, 266-271.

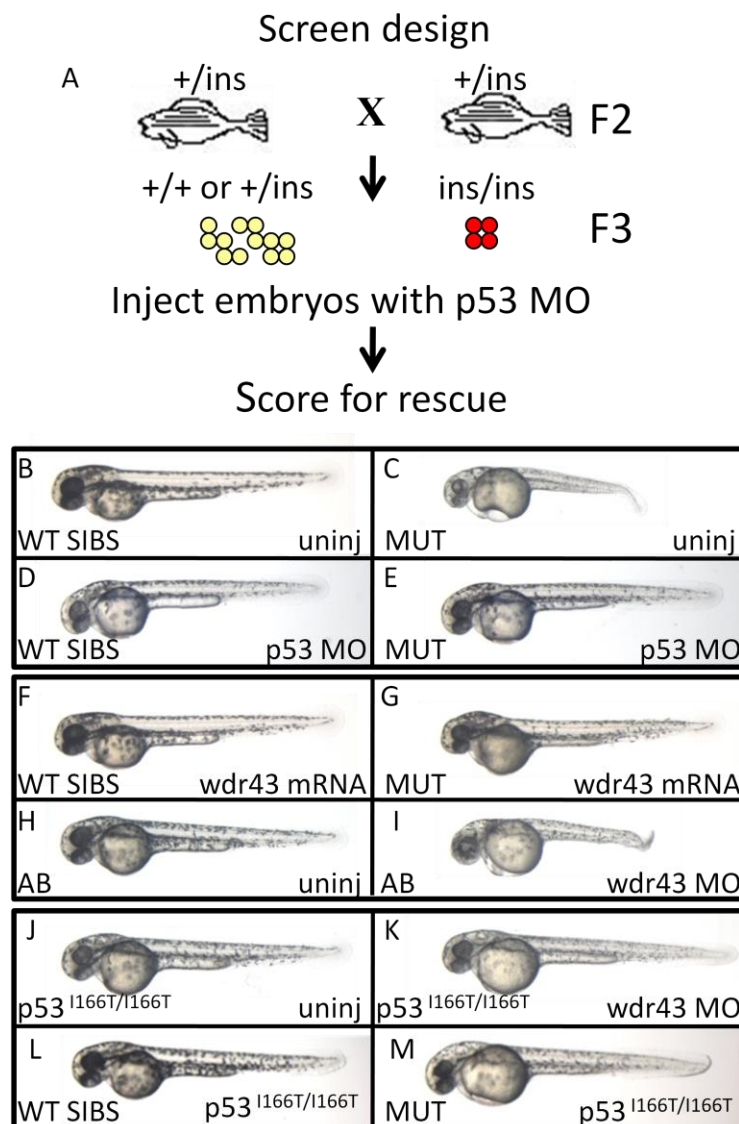


Figure 4.1: Identification of novel gene *wdr43* in zebrafish screen. (A) describes screen design. Adult fish heterozygous for insertion ($+/ins$) were crossed. Three quarters of resulting embryos were wild type siblings ($+/+$ or $+/ins$), one quarter were homozygous for insertion (ins/ins). B and C show uninjected wild type siblings and *wdr43* mutant embryos. D and E show wild type siblings and *wdr43* mutants injected with p53 morpholino (MO). F and G show wild type siblings and *wdr43* mutants injected with *wdr43* mRNA. I shows wild type embryos (AB) injected with *wdr43* morpholino compared to uninjected control (H). K shows *wdr43* MO injected into p53 homozygous mutant ($p53^{I166T/I166T}$) compared to uninjected control (J). L and M show *wdr43* wild type sibling and *wdr43* mutants in a p53 mutant background.

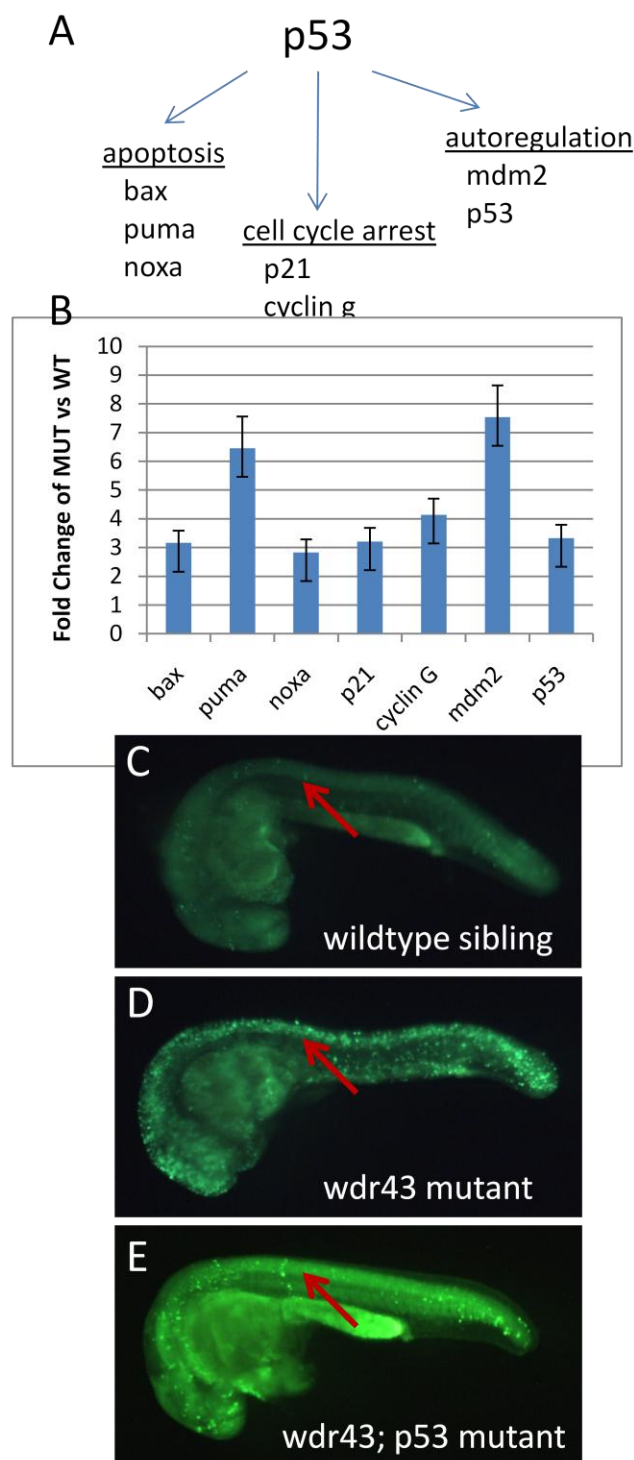


Figure 4.2: Loss of *wdr43* activates *p53* target genes and apoptosis. (A) Model of *p53* target genes. (B) Real-time quantitative PCR analysis showing fold change of mutant expression compared to wild type siblings. Samples normalized to *beta-actin*, tested in triplicate, error bars represent standard deviation. C, D and E show acridine orange stain of embryos at 24hpf. The arrows point to the neural tube, where the majority of apoptotic cells are visible.

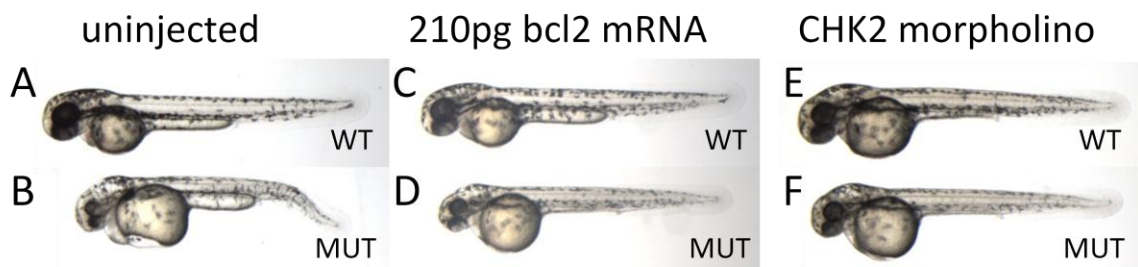


Figure 4.3: *wdr43* Mutant embryos are partially rescued by *bcl2* mRNA and CHK2 morpholino injection at 48hpf. WT denotes wild type siblings, and MUT denotes *wdr43* homozygous mutant embryos.

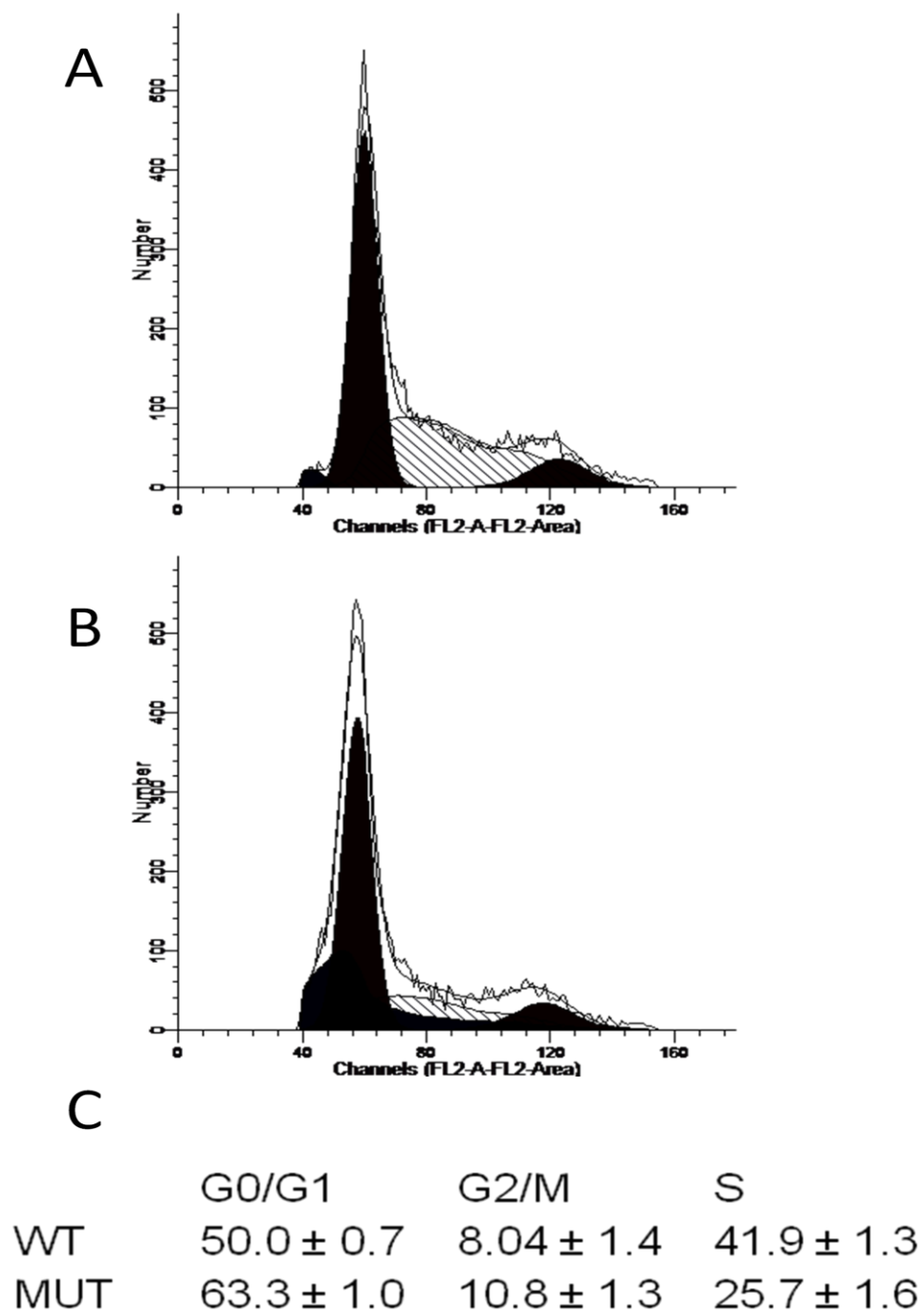


Figure 4.4: Cell cycle analysis showed decrease of S-phase cell in *wdr43* mutant at 24hpf. Wild type (A) and mutant (B) cells were plotted with number of cells on the y-axis and the effective DNA content on the x-axis. Experiments were done in triplicate, each counting > 10,000 events. In the table (C), numbers are percentage of cells ± standard deviation.

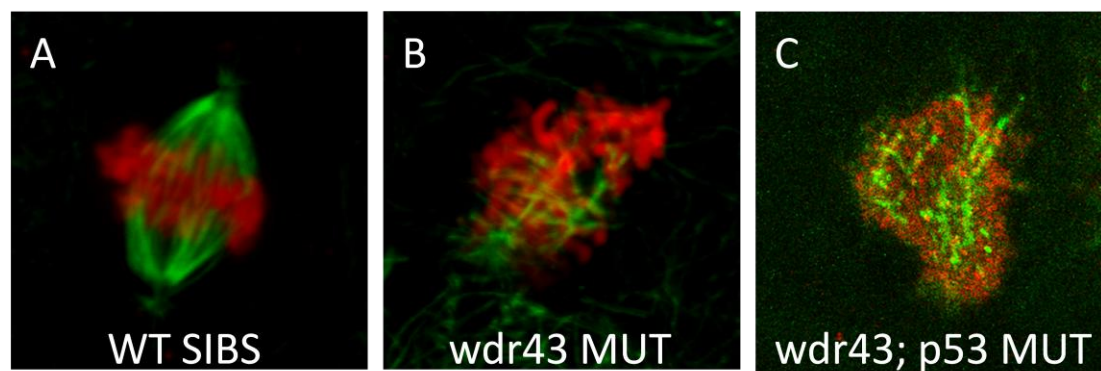


Figure 4.5: Immunohistochemistry shows mitotic spindle at 24hpf in *wdr43* mutant and *wdr43*; *p53* double mutant embryos. Microtubules were stained in green with anti-alpha tubulin. M-phase chromatin was stained in red with anti-phospho histone H3. Spindle defects were visible in *wdr43* MUT (N=46/200) and *wdr43*; *p53* double mutant (N=18/100). No defects were visible in wild type cells (N=100).

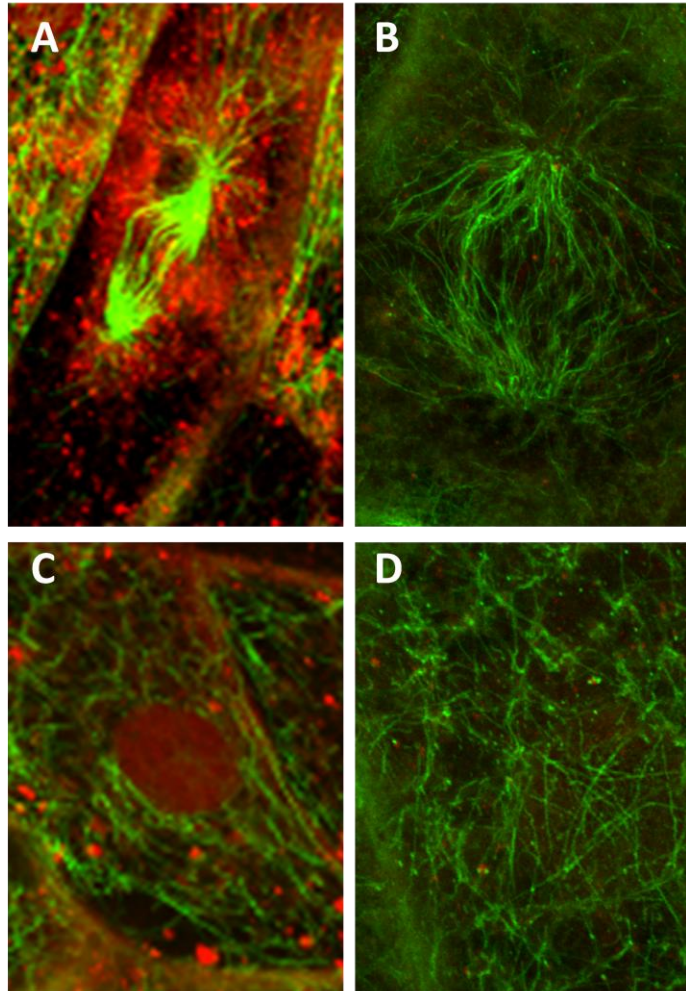


Figure 4.6: Localization of His-wdr43. Microtubules were stained in green with an anti-alpha-tubulin, anti-6X-His was stained red. A and B were M-phase cells, C and D were interphase cells. A and C were injected with 200pg His-wdr43 mRNA, B and D were uninjected controls.

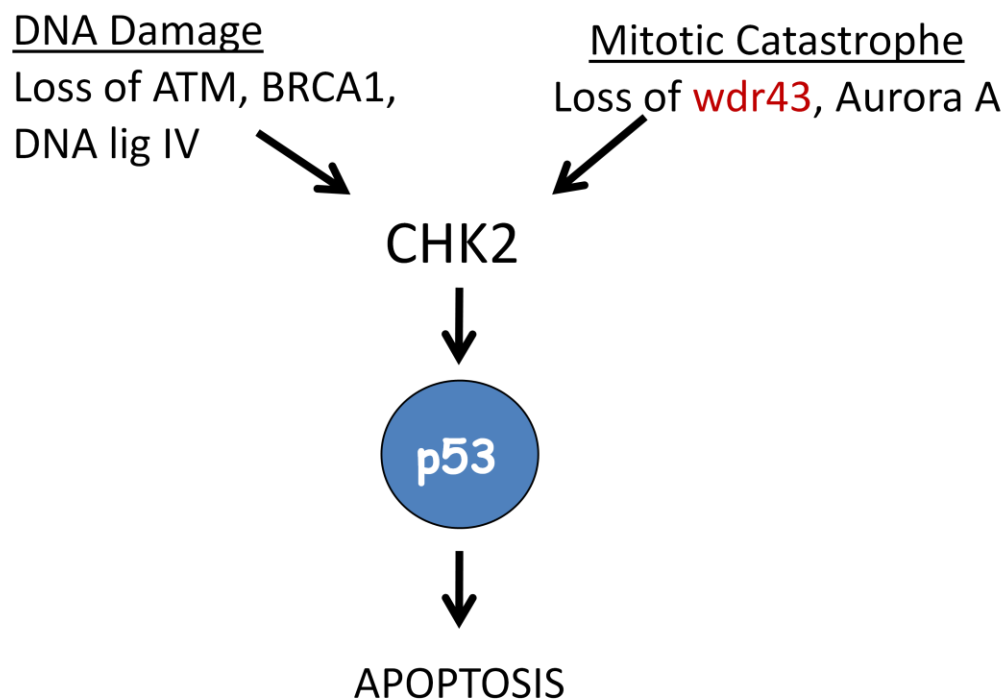
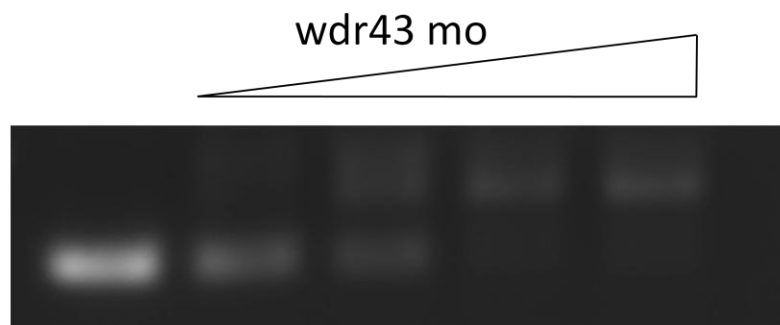


Figure 4.7: Activation of the p53 pathway. P53 is activated via CHK2 after loss of DNA Damage genes or loss of genes resulting in mitotic catastrophe. This results in apoptosis.



Supplemental Figure 4.1: RT-PCR of zebrafish embryos injected with a gradient of wdr43 morpholino. Lower band indicates wild type splicing. Upper band indicates alternate splicing due to morpholino. From left to right, concentrations of morpholino were, 0pg, 0.25pg, 0.5pg, 1pg, 2pg. Working concentration for experiments was 1pg.

CHAPTER 5

P53 INDEPENDENT ROLE OF WDR43 IN DEVELOPMENT

The *wdr43* mutant fish was originally recovered due to its embryonic lethal phenotype. Although we saw rescue of early p53 dependent phenotypes, the mutant fish still died. Furthermore, we noticed developmental abnormalities not rescued in the p53 mutant background. Specifically, the gut and eyes did not seem to develop normally. This observation led to a marker analysis in order to better understand the developmental phenotypes due to the loss of *wdr43*.

The expression of *wdr43* is ubiquitous in the early zebrafish embryo, until 12hpf (Figure 5.1 A, B) and then it localizes to specific tissues, visible by 26hpf. At 26hpf, expression of *wdr43* exists in the neural regions of the embryo, including the eye, as well as in the tail, exactly where the phenotypes are visible (Figure 5.1 C). By 48hpf, expression is only visible in a small region of the neural tissue (Figure 5.1 D). Interestingly at 72hpf, we see expression of *wdr43* arise in specific organs. Expression exists in the developing gut, as well as the otic vesicle (Figure 5.1 E). By 96hpf, *wdr43* expression is visible only in the gut.

At 96hpf (4dpf), the gut in a wild type embryo is visible extending through the yolk. This structure is not present in either the *wdr43* mutant or *wdr43*; p53 double mutant (Figure 5.2 A-C). To examine whether a primitive gut tube forms, we used an early gut marker, FKD2 (or FoxA3), a marker of endoderm. At 48hpf, wild type, mutant and double mutant guts were indistinguishable by FKD2 in situ hybridization (Figure 5.3 A-C). The first evidence that the gut in the mutant develops abnormally comes from looking at FKD2 expression at 72hpf. The wild type staining pattern was much more diffuse than mutants. Furthermore, it

appeared that single and double mutant guts are stalled and look similar to 48hpf staining patterns (Figure 5.3 D-F).

To see if the mutant gut was able to differentiate, intestinal fatty acid binding protein (iFABP) was used as a marker at 96hpf. Normally, this marker is visible starting at approximately 72hpf in wild type gut and is a marker of differentiated enterocytes. Wild type, single and double mutant embryos were collected at 96hpf and underwent in situ hybridization for iFABP. This marker was clearly visible in the wild type gut, but not in either the single or double mutant gut (Figure 5.3 G-I). The combination of FKD2 and iFABP staining showed that mutants were able to form a primitive gut but not differentiate, and this phenotype was independent of p53.

This finding was verified in plastic sections of the three different guts at 96hpf. The wild type gut exhibited architecture indicative of a gut developing normally. The cells were well organized and the columnar epithelium was visible. The beginning of crypt formation was also evident (Figure 5.3 J). The guts of *wdr43* mutants and *wdr43*; p53 double mutants did not have the same appearance. The cells were not well organized, and they did not appear to be columnar epithelium. The cells were more cuboidal in structure with larger nuclei. Crypt formation was not evident in either the single or double mutant (Figure 5.3 K, L). In essence the mutant and double mutant guts looked like more primitive guts, approximately that of a 48hpf wild type embryo.

Eye morphology was also affected in both *wdr43* morphants and *wdr43* morphants in a p53 mutant background. By 72hpf, the eyes were much smaller

and the cells did not appear to be as well organized as in wild type embryos. Similar to the gut, it appeared the eyes were able to begin development normally. We have verified that early development of the eye proceeds appropriately with several early eye markers, including *bmp4*, *rx3*, and *tbx5* (Figure 5.5). Later eye markers are necessary to determine if they do not develop past a certain point.

Because there appeared to be issues with gut and eye differentiation, we looked to see if this issue was global or specific. In this case we looked at heart differentiation. We sought a marker for a gene that would not arise until after we see defects in the other organs, approximately 3dpf. Tropoelastin is a marker of the outflow tract of the heart. This marker is present at 3-4dpf in wild type embryos, and seemed to be the perfect candidate to test against our mutants. At 4dpf, tropoelastin was visible in wild type, mutant and double mutant embryos. This implied other organs in the embryo were able to differentiate, even at this later timepoint, implying the specificity of the gene in organ development

The gut and eye were not the only visible p53 independent phenotypes in the embryos. The pectoral fin also did not develop appropriately. The combination of these three developmental phenotypes, inability for gut to differentiate, inability for eye to develop, and inability for the pectoral fin to develop are very reminiscent of phenotypes seen in fish deficient in APC or Retinoic Acid pathway components. In APC morphant embryos, we saw a misregulation of *wdr43* at 72hpf, although this finding needs to be verified. In situ hybridization showed *wdr43* expression in through the head region, yet not in the developing gut. In wild type embryos at 72hpf, expression of *wdr43* was very

constricted to the developing gut. Although this piece of data is intriguing, more experiments are necessary to link wdr43 to this pathway.

These data provide evidence that wdr43 functions in development in a p53 independent manner. We have shown some data that suggest wdr43 is necessary for gut development, specifically the differentiation that occurs around 72hpf in the zebrafish. Many similar phenotypes exist between the wdr43 mutant embryos and phenotypes indicative of the APC/RA pathway; however, more data is necessary to establish this link.

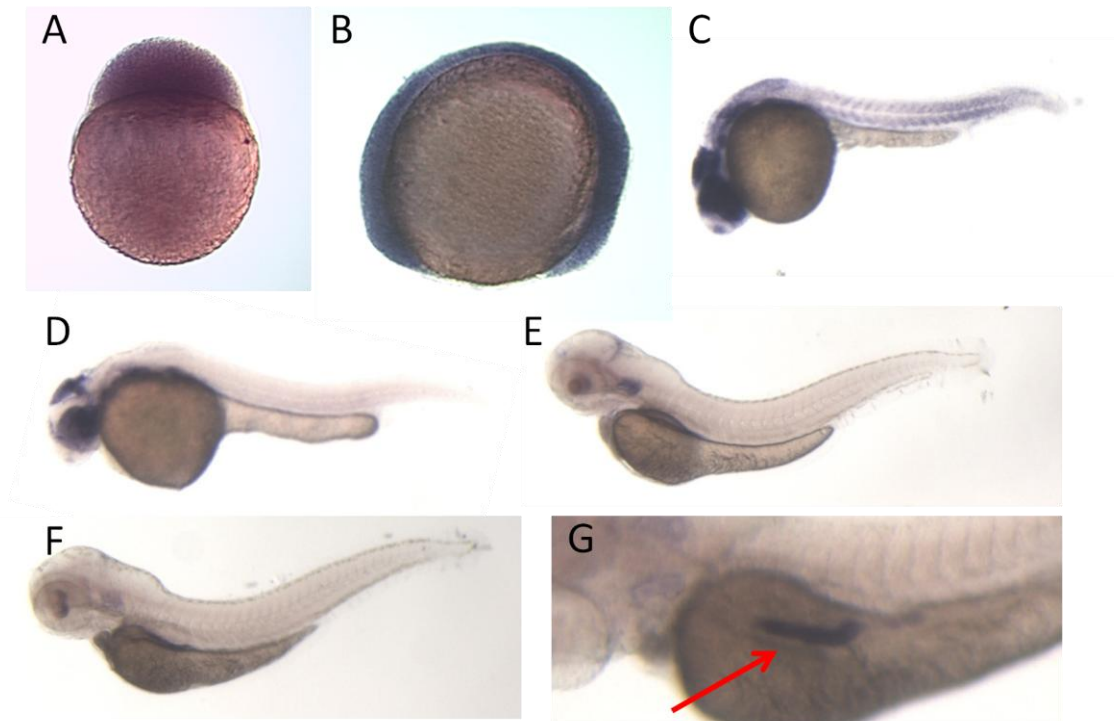


Figure 5.1: Expression pattern of *wdr43* is ubiquitous in the early zebrafish embryo, and narrows to specific tissues at later stages. (A) 4hpf. (B) 12hpf. (C) 26hpf. (D) 48hpf. (E) 72hpf. (F) 96hpf. (G) 96hpf zoomed in with arrow pointing to gut tube.

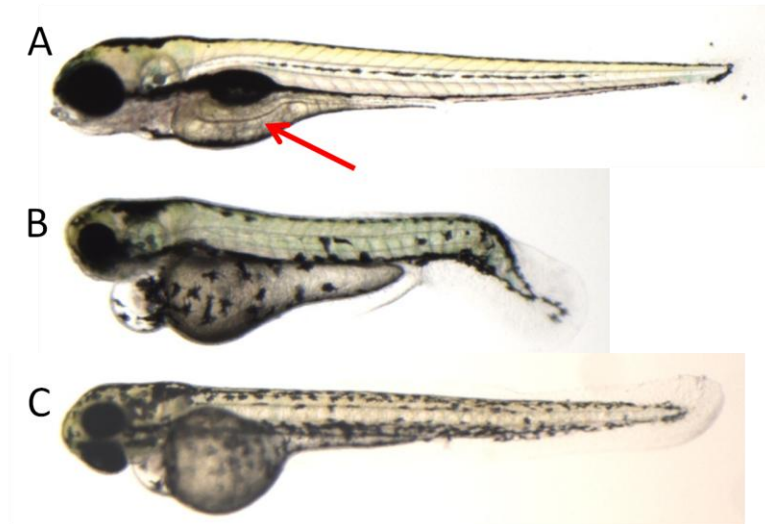


Figure 5.2: Gross morphology of wild type (A), wdr43 homozygous mutant (B), and wdr43; p53 double homozygous mutant zebrafish embryos at 4dpf. The arrow in A points to the gut tube visible in wild type embryos, but not in either wdr43 mutants, or wdr43; p53 double mutants.

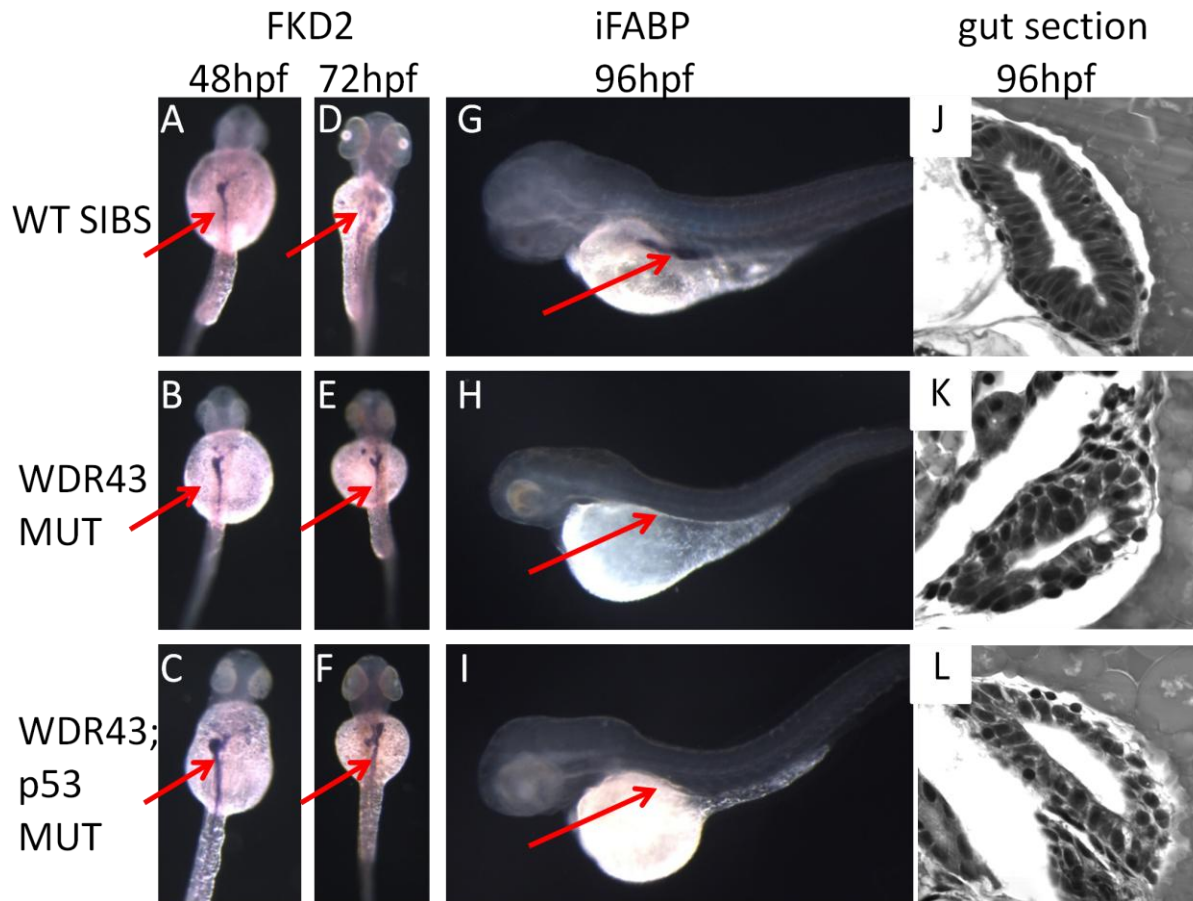


Figure 5.3: Gut in *wdr43* mutant and *wdr43*; *p53* double mutant unable to differentiate. FKD2 in situ hybridization of primitive gut at 48hpf (A-C) and 72hpf (D-F) embryos. iFABP in situ hybridization of differentiated enterocytes in 96hpf embryos. (J-L) Histology of gut at 96hpf. A, D, G, J are wild type siblings. B, E, H, K are *wdr43* homozygous mutants. C, F, I, L are *wdr43*; *p53* double homozygous mutants.

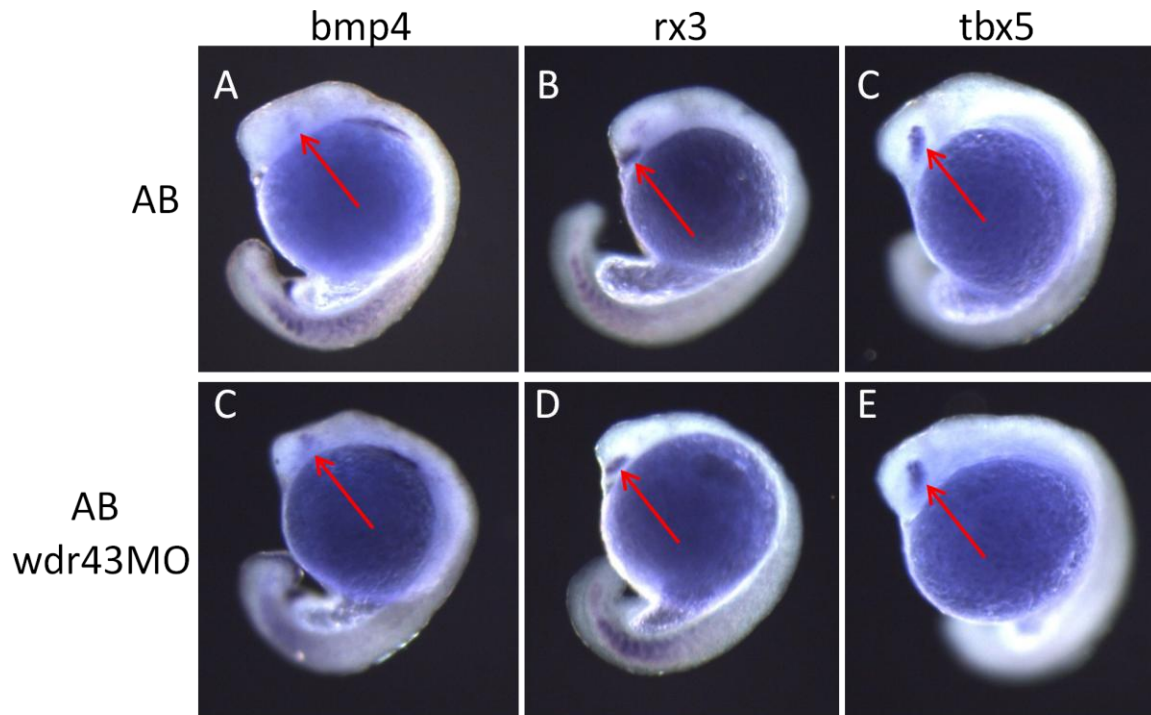


Figure 5.4: Expression of early eye markers was normal in wdr43 morphant embryos. Wild type (A-C) and morphant (C-E) embryos were collected and fixed at 20hpf. In situ hybridization with *bmp4* (A,C), *rx3* (B,D), and *tbx5* (C,E) was performed. N>10 embryos per experiment.



Figure 5.5: In situ hybridization of tropoelastin reveals ability of mutants to differentiate heart outflow tract at 96hpf. A is a wild type sibling, B is a *wdr43* homozygous mutant, C is *wdr43*; *p53* double homozygous mutant

CHAPTER 6

CONCLUSIONS AND FUTURE DIRECTIONS

Overview

Zebrafish offer very unique attributes to study the genetics of human disease. Its attributes as a model organism make it well poised to offer insight into the genetics pathways involved in disease and the discovery of novel genes implicated. The work presented in this thesis describes the use of zebrafish to develop a new model of the genetic syndrome Li-Fraumeni. We describe a p53 mutant in zebrafish and its propensity toward tumor development. Next, a novel method of genotyping various zebrafish mutants is described. High Resolution Melting Analysis (HRMA) has the sensitivity to differentiate melting points of DNA duplexes representing wild type and mutant alleles. Finally, the novel gene *wdr43*, is identified in another forward genetics screen. The p53 dependent characterization of this gene reveals a role in the mitotic spindle. P53 independent observations indicate *wdr43* has a role in specific tissue development in zebrafish.

Li-Fraumeni Model

A forward genetics screen recovered a zebrafish line with a mutation in the DNA binding region of p53. The I166T amino acid change rendered the gene not functional in the sense that although the p53 is stabilized following DNA damage, it does not transactivate downstream target genes. This model not only exhibited p53 pathway phenotypes at the embryonic level, but adult fish developed tumors with 100% penetrance. Furthermore, this was the first indication of Loss of Heterozygosity in zebrafish, offering more validation of using zebrafish to model human cancer. We were able to show this mutation causes a

loss of function allele and can rescue mdm2 lethality. This p53 mutant provided more than a Li-Fraumeni model; it provided a key tool to use in genetics assay to find more about cellular and disease mechanisms involving p53.

This forward genetics screen, based on an apoptosis assay, will continue to find additional mutants that show no, or less, apoptosis following irradiation. The identification of the p53 mutant provided a proof of principle that screen will reveal genes of interest. Ideally, we will recover novel genes that function in this pathway, either upstream or downstream of p53. Precedents exist for both of these possibilities. An upstream gene would not transduce a DNA damage signal to p53. An example of a known gene would include ATM, a gene that recognizes double strand breaks in DNA. A downstream gene would not be able to transduce the p53 initiated apoptotic signal. The caspases involved in the apoptotic pathway are examples of downstream genes. To date, we are far from saturation in this screen, so the possibility of recovering more mutants as a result of screening more genomes is likely.

Also, a modifier screen is currently underway. This screen was devised by ENU mutagenesis of p53 mutants to create G0 fish. A dominant screen at the F1 generation can be carried out to find modifiers of p53 that enable the fish to get tumors earlier than a normal p53 mutant cohort. Activating mutations in oncogenes would be examples of genes expected to be recovered. A recessive screen at the F3 generation is also possible. In this case, tumor suppressors would be expected. If p53 and another tumor suppressor that acts in a different

pathway are both mutated, the propensity for tumors would be greater than in the p53 mutant alone.

Complementation screens will be conducted to find other alleles of p53. This screen is designed such that screened fish are heterozygous for p53 and mutagenized fish are heterozygous for another allele of p53. When crossed, if both alleles are inherited, and complementary, mutants will not have a functional p53. This screen will also pick up nonallelic noncomplementation mutants. This would describe two genes, p53 and another gene, that when both are heterozygous, cause a phenotype similar to homozygous p53 mutants.

Zebrafish are ideal model organism for drug screening. Because they are a vertebrate organism capable of producing many offspring, drug screening of thousands of small molecules is possible. A screen currently underway is a synthetic lethal drug screen. The goal of this screen is to find small molecules which kill only p53 homozygous mutants and not wild type embryos. This is analogous to the tumor environment in humans. Because the majority of tumors have a mutated p53, while the rest of the affected individual has wild type p53, a drug that kills only mutated p53 cells could be a very effective therapeutic.

High Resolution Melting Analysis to Genotype Animal Models

The discovery of this mutant, as well as the establishment of many other mutant lines, has necessitated the need for efficient and accurate methods of genotyping in zebrafish. High resolution melting analysis (HRMA) describes a PCR based technique that is able to genotype based on differences in melting curve. The technique utilizes a rapid cycle protocol for PCR, amplifying very

small products and the use of a DNA stain, LC Green plus. This stain emits fluorescence when DNA duplexes are bound, but not when the duplex is separated after the melting temperature was reached. Small changes, even from a single point mutation, can be detected in PCR products. We showed the efficacy of this technique in multiple types of mutations, including point mutations, a small deletion, and a retroviral insertion. The usefulness of this tool to genotype is clear; however, additional uses for HRMA such as mutation scanning are a distinct possibility and could dramatically improve on existing tools available in zebrafish. HRMA is already used for mutation scanning for genes in humans. A likely future possibility for using HRMA is for TILLING. Currently, TILLING requires a cumbersome protocol to discover new mutations in genes of interest, including a specific, rare enzyme, Cel1, and a Li-Cor machine. Using HRMA to detect mutations in genes of interest may be an efficient way to scan genes of interest for new mutations.

Identification of Novel Gene wdr43

A different type of forward genetics screen recovered novel gene wdr43. This screen highlights the advantage of zebrafish to use morpholino technology, targeted knock down of a specific gene, to conduct a screen for other genes with genetic linkage to p53. Data show that loss of wdr43 activates the p53 pathway. Immunohistochemistry indicate 23% mitotic figures cannot properly form the spindle or metaphase plate. This disorganized array of microtubules likely leads to chromosomal instability, or mitotic catastrophe, activating the p53 pathway. P53 dependent apoptotic pathways are activated due to the irreversibly damaged

DNA, and cell death is inevitable. This chapter highlights the possibility of discovering novel genes that play a role in very important pathways.

The next step of this project is to determine whether or not this gene has a causative role in tumor development. Currently, we have set up cohorts of wdr43 heterozygous and wild type fish to see if tumors develop in mutants. These cohorts are set with and without the p53 mutant background. In normal circumstances, zebrafish do not develop tumors. Comparing fish in a wild type p53 background will tell us if heterozygotes have a propensity towards tumorigenesis. In the p53 mutant background, we can see if wdr43 heterozygosity decreases the time for fish to develop tumors. Depending on the results of these tumor cohorts, wdr43 may establish itself as a gene important to tumor formation. We have some preliminary data that suggest an upregulation of wdr43 in human tumors. These data could imply a fine tuned regulation of wdr43 is necessary, similar to regulation of Aurora A. Depending on the results of these studies, inhibition or activation of wdr43 may or may not be beneficial to tumor therapy. Preliminary studies of specific inhibitors of Aurora A have entered drug trials, yet it is debatable whether or not they will be efficacious, based on the evidence that heterozygous mice deficient in Aurora A have a propensity for tumors.

P53 Independent Role of wdr43 in Development

The p53 independent role of wdr43 in development was also examined. The concurrent loss of p53 was not enough to completely rescue the phenotype of wdr43, suggesting that wdr43 has additional roles outside of the p53 pathway.

Specifically, the gut, the eye and pectoral fin were developmentally delayed or stalled in the *wdr43*; *p53* double homozygous mutant. Marker and histological analysis of the gut show a primitive gut tube is formed, but it does not have the ability to differentiate. The eye has a similar phenotype- it begins development normally, but stalls at some timepoint. This phenotype appears to be specific to these organs, because other organs, like the heart, do have the ability to differentiate at a similar timepoint. It is possible that *wdr43* is regulated by the APC/RA pathway, although further experiments are necessary to make this conclusion.

Further experiments are necessary to definitively place *wdr43* in or out of the APC/RA pathway. Misregulation of *wdr43* in mutant/morphants in downstream components of the APC/RA pathway could help to pinpoint the regulation of *wdr43*. Epigenetics experiments with these genes could help to understand the function of *wdr43*.